

BLDSC no: D003235

LOUGHBOROUGH
UNIVERSITY OF TECHNOLOGY
LIBRARY

AUTHOR ~~DE~~ SILVA, S R

COPY NO. 025900/02

VOL NO. CLASS MARK

ARCHIVED COPY
FOR REFERENCE ONLY

TRANSMISSION OF FORCE THROUGH PARTICULATE SYSTEMS

WITH RESTRICTED GEOMETRY

BY

S.R. DE SILVA

SUBMITTED FOR THE DEGREE OF DOCTOR OF PHILOSOPHY OF

THE LOUGHBOROUGH UNIVERSITY OF TECHNOLOGY

DEPARTMENT OF CHEMICAL ENGINEERING

JULY 1972

DIRECTOR OF RESEARCH

PROFESSOR D.C. FRESHWATER

SUPERVISORS

P.J. LLOYD



by S.R. de Silva

Loughborough University Of Technology Library	
Date	Dec 72
Class	
Acc. No.	025900/02

This thesis is dedicated to my daughter Tania, whose efforts at locomotion provided me with the perfect example of the random walk

I wish to express my gratitude to the following.

Mr P.J.Lloyd and Mr B.Scarlett, my Supervisors, for encouragement, guidance and help.

Professor D.C.Freshwater, for the excellent research facilities

Mr R.H. Beresford and Mr A.Fairlie, for valuable discussion

Mr J.I.T Stenhouse for a great deal of help in running the programs while I was in Germany

Professor K.Leschonski for encouragement and financial assistance for travel between Germany and England

My numerous friends and colleagues for much criticism and witticism so essential to the writing of a thesis

B.S.A Metal Powders Ltd. and Mr J.Brackpool of that company for the many free samples

McKechnie Ltd, also for many free samples

The SRC for an equipment grant to Mr. Lloyd

The University for a research scholarship and generous help

And last, but by no means least, the laboratory and workshop staff for toleration and patience.

SUMMARY

Particle systems may be characterised by a knowledge of the dimensions of the individual particles. By using the Feret's diameter distribution and the random filament distribution of an iron powder, the characterisation of a system of the powder particles, constrained in a cylindrical die, has been achieved. The Monte Carlo method has been used to simulate the transmission of force through the model created by this characterisation. The results of 500 Monte Carlo simulations have been used to produce a description of the force due to one surface particle at various points in the system. Using this diagram together with a knowledge of the spatial distribution of the surface particles and the dimensions of the die it was possible to produce

- 1) Curves of side wall pressure vs. depth in the die for various loads
- 2) Curves of applied to transmitted pressure for various height:diameter ratios
- 3) Curves of friction loss at the walls vs. depth for different height:diameter ratios

The differences between the experimentally determined values and the values predicted on the basis of the model have been explained in terms of the assumptions made, and suggestions made as to how these may be eliminated.

CONTENTS

Acknowledgements

Summary

1. Introduction	1
2. Literature Survey	3
3. Theory	47
4. Apparatus and Experimental Method	73
5. Results	79
6. Discussion of Results and Comparison with Theory	99
7. Conclusions and Suggestions for Further Work	103

Appendices

Nomenclature

Bibliography

List of figures

Section 2

2.1	Velocity-Friction curves at various loads	9
2.2	Density-Lubricant curves for 1.25 g. compacts	11
2.3	Density-Lubricant curves for 7.50 g. compacts	12
2.4	Specific gravity and Brinell hardness distributions in, (a) 3kg. and 1kg. copper compacts of mixed powder size (b) 3kg. and 1kg. copper compacts of fine powder size (c) 3kg. and 1kg. iron compacts	16
2.5	The effect of applied pressure on Brinell hardness and specific gravity of 22mm diameter and 2mm thick compacts	17
2.6	The effect of applied pressure on the variations of density	19
2.7	The effect of compact height on the variations of density	19
2.8	The effect of lubrication on the variations of density	20
2.9	The split die assembly used by Train	21
2.10	Density distributions in 160g. compacts pressed at 671kg/sq.cm ,lubricated and unlubricated.	23
2.11	Density distributions in 160g. compacts pressed at 2040kg/sq.cm ,lubricated and unlubricated.	24
2.12	The apparatus used by Duwez and Zwell	25
2.13	Variation of side wall pressure with compacting pressure for compacts of varying thickness	26
2.14	Ratio of average pressure on fixed piston to pressure applied Vs. (a) Ratio of thickness to diameter of compact (b) Ratio of depth to diameter	27
2.15	Radial segregation effects	32
2.16	Axial segregation effects	32
2.17	Effect of particle mixtures on segregation	33
2.18	(a) Feret's statistical diameter (b) Martin's statistical diameter	35
2.19	Determination of perimeter using Feret's diameter	35
2.20	(a) The probability of sectioning a sphere of diameter, $2x$, to obtain a circle of diameter, $2y$ (b) The probability of a chord, length $2z$, in a circle of diameter, $2y$	37
2.21	The random selection of values from a cumulative undersize curve	42

2.22	The hours of life of a component-represented by a number-frequency curve	43
2.23	Cumulative under-size curves	44

Section 3

3.1	Representation of a force by three components	49
3.2	The probability of a contact on the surface of a sphere	50
3.3	(a) Feret's diameter	52
	(b) Random filaments	
	(c) Sectioned random filaments	53
	(d) α, l from particle characteristics	
3.4	Coordinates of a point	54
3.5	Rotation of axes	55
3.6	The transmission of force in a particulate system	56
3.7	Transmitting and non-transmitting contacts on a sphere	59
3.8	Rotation of axes	62
3.9	Rotation of axes	63
3.10	A random walk	67
3.11	Representation of a random walk on a two-dimensional grid	67
3.12	Sub-division of a large system by grid lines	69
3.13	A cylindrical system of particles	72
3.14	Particles on a surface	72

Section 4

4.1	The measurement of random filaments	74
4.2	The die Assembly	75
4.3	The press	76

Section 5

5.1	Calibration of the pressure gauge	83
5.2	Calibration of the load cell	84
5.3	Feret's diameter distribution	85
5.4	Random filament distribution	86
5.5	Experimental side wall pressure curves	87
5.6	Experimental side wall pressure curves	88
5.7	A force diagram	89
5.8	Percentage of applied force transmitted vs. compact depth for various height:diameter ratios.	90
5.9	Friction losses at the wall as a function of compact height for various height:diameter ratios	91
5.10	Comparison of side wall pressure vs. depth curves, Experimental and predicted	92

List of Tables

2.1	Areas of contact between two metal plates	5
2.2	Frictional behaviour of junctions	6
2.3	Values of the coefficient of friction with different junctions and different lubricants	6
2.4	The effect of normal load and velocity on the coefficient of friction	7
2.5	Lubricants for various metal powders	10
2.6	The effect of lubrication on the die wall pressure	14
2.7	The effect of mixing different sizes on the packing density of spheres	29
2.8	The effect of mixing different sizes on the packing density of irregular particles	29
2.9	The effect of the method of filling on the fill volume of a die	30
2.10	The effect of funnel orifice diameter and die diameter on segregation	34
5.1	Voidage of the compact as a function of applied load and compact height	80
5.2	A random walk	93

SECTION 1

INTRODUCTION

1

For many years, the compaction of powders has been used in industry, in the manufacture of a wide range of products, such as, tablets in the pharmaceutical industry, bricks in the ceramic industry and sintered metal parts in the metallurgical industry. Although it has such a wide use, the mechanics of the compaction process are inadequately understood, and consequently a large number of experimental determinations have had to be made in order to gauge the importance of the various parameters influencing the process.

Compaction is generally the first step of a two step operation, in the production of a compact. With the exception of the pharmaceutical industry, compacts are normally finished off by a process called sintering, where further cohesion between the powder particles is obtained by raising the temperature of the compact and thus promoting the formation of metallic and other bonds.

The final strength of the compact obtained, however, depends on the density achieved in the first (compaction) stage of its manufacture, and it is with this process that this research is concerned. Although there is such an abundance of experimental results, there is as yet, no general theory which can be used in an attempt to optimise the process. The presently available theory views the process macroscopically and all the predictions deal with the macro-properties of the system, such as average density, average volume etc.

Unfortunately, there is no direct relationship between the macroscopic properties and such important parameters as the strength of compacts, which still have to be determined experimentally. It is unlikely that any macroscopic approach could, in fact, predict such parameters, which are to a large extent dependant on local variations and local properties.

The theory presented in this thesis is, therefore, an attempt to extend the presently available theory, using it as a starting point to analyse the system, and using a particulate approach with a view to obtaining those parameters which cannot be obtained now without experimentation.

A theory such as the one proposed would be invaluable to industry in the saving of much time and money, and would also be widely used in research, not merely in the field of compaction but in a number of other fields, where similar problems are encountered.

Since the complexity of particulate systems makes the use of ordinary mathematical analysis impractical, it was decided to use a statistical approach and bring to bear on the problem, the latest advances in particle characterisation. In order to do this, it was necessary to build a stochastic model of the system on which a simulation of the force transmission could be performed.

A search of the literature indicated that the Monte Carlo method (formerly called the method of random walks), which had been used with varying degrees of success by Scheidegger(89) and Eastham(71) could probably be used with success in the simulation of the force transmission, and that the method of sizing particles by regarding an assembly of particles as a series of filaments(35), (70) could be used, together with the more conventional Feret's statistical diameter, in the building of the type of model required.

The systems which were considered, were of cylindrical shape (which possess axial rotational symmetry) and were enclosed by a rigid die. One of the plane surfaces was then subject to an applied pressure. The transmission of the force, from the surface through the system was then simulated, using the Monte Carlo method and a stochastic model of the system. Using the results from these runs it was possible to build up a force diagram for every point in the system, which could then be compared with experimental data.

SECTION 2

LITERATURE SURVEY

- 2.1 Introduction to literature survey
- 2.2 Friction and lubrication in powder compaction
- 2.3 Theoretical and experimental evaluations
of density variations in powder compaction
- 2.4 Particle packing
- 2.5 Particle statistics
- 2.6 Monte Carlo methods
- 2.7 Deformation and crushing of particles
- 2.8 Conclusion

2.1 Literature survey.....Introduction

This thesis is concerned with developing a theory which would enable the prediction of pressures at various points within a confined system of particles which is subjected to an external force. It is agreed by all workers in the field, that friction between the powder and the walls of the retaining vessel is the most important factor in the non uniform transmission of stress through such a system. This friction, which is considerable in magnitude, causes a variation in the axial stress throughout the system (or compact): as a result of this variation in stress there arise variations in the consolidation of the powder at different points within the system. These variations have been widely investigated experimentally.

The literature survey presented in the following pages thus highlights the various factors influencing the value of the coefficient of friction and then goes on to describe how friction can be minimised by the use of lubricants. In the building of the model, it was necessary to use some of the information given here, relating to friction and lubrication but the importance of some of the facts presented has not always been understood and suggestions in the past by such eminent workers : as Unckel (30) have been found to be incorrect. Thus the inclusion of the information here is not merely a justification of the assumptions used in the building of the present model, but also an introduction to that part of the literature dealing with density variations in powder compacts.

The information required to simulate the system under analysis, is found in parts 2.4 and 2.5, where the most recent advances in particle characterisation and the information available on particle packing are recounted. The inclusion of the information available on the effects of die filling and segregation was considered valid and necessary as a lack of attention to these details leads very often to non-reproducibility of results. It is particularly important to control such procedures carefully, especially since models, such as this one, assume random packing arrangements. To conclude this section, a description is given of Monte Carlo methods, which have been used in the simulation techniques, and of the future possibilities of incorporating the deformation of particles into the model.

2.2 Friction and lubrication in powder compaction

In the introduction to this section the importance of friction in the analysis of density variations occurring in powder compacts was stressed. Recounted below are some of the suggested relationships between applied and transmitted pressure and the coefficient of friction between the powder and the wall of the die. Unckel (30) and Duffield (10,24) use the relationship,

$$\frac{P_t}{P_b} = e^{+4\mu\beta L/D} \quad \text{-----2.1}$$

Where, L = Compact height

D = Compact diameter

μ = Coefficient of friction between powder and wall

β = Ratio of axial to radial stress

to evaluate the pressure on the bottom platten during a uni-directional pressing operation.

Train (7) modified this to

$$\frac{P_t}{P_b} = \frac{V_{rt}}{V_{rb}} e^{+4\mu\beta L/D} \quad \text{-----2.2}$$

Where V_r is the relative volume and t and b refer to top and bottom of the die.

β has been obtained by Unckel (See Appendix 2.1) as,

$$\beta = \frac{1 + \mu_i + \sqrt{\mu_i^2 - (1 + \mu_i)^2 \mu^2}}{1 + \mu_i - \sqrt{\mu_i^2 - (1 + \mu_i)^2 \mu^2}} \quad \text{-----2.3}$$

Where μ_i is the coefficient of internal friction.

The importance of the variation of both μ and β has not been sufficiently well investigated, but it is proposed to deal with some papers that have been published in recent years.

Bowden and Tabor and their co-workers have performed a large number of experiments to clarify the laws relating to friction. Amonton's laws state a) friction is independent of the area of contact between the solids, b) it is proportional to the load between the surfaces and c) it is independent of the speed of sliding. The theory developed by Bowden and Tabor is based upon the hypothesis that there is the formation of junctions at all points of contact between the two surfaces, and that the frictional force observed is due to the resistance of these junctions to shear. It is well established now that solids have only a small proportion of their surface actually in contact with one another. In fact (Table 2.1) the actual areas of contact may be as low as 1/100000th the apparent contact area.

TABLE 2.1
Areas of contact between two metal plates (39)

Load, Kg	True area of contact	Fraction of macro. area
500	.05	1/400
100	.01	1/2000
5	.005	1/40,000
2	.002	1/100,000

The theory states that as the load on the points of contact is high, there is cold welding at these points and consequently there is a resistance to movement. Experiments have shown hot spots can actually be measured on the surfaces of sliding metals, and that their temperatures often exceeded the melting point of the metal. The temperatures generated depend on the conductivity of the metals and the solids of low conductivity show greater increases of temperature at contact points (40). Johnson and Adams (41) have investigated the effects of melting point, density, surface condition and temperature on friction. Green (42) has investigated the variation of friction with surface conditions. Three types of friction were found.

(a) Seizure or very high friction. At slow speeds this occurs only with out-gassed surfaces of extreme cleanliness and is achieved by

- heating in vacuo. The coefficient of friction varies between 3 and 10.
- (b) Strong adhesion between clean metals in air. Moderate friction coefficient (Approximately 1)
- (c) Weak adhesion between clean metals in air

Under static loading, the mean pressure is about six times the yield stress in shear, whereas in steady sliding it is only of the same order as the yield stress, since the area of contact increases as soon as sliding commences. The yield stress in shear varies with the type of sliding obtained, and the nature of the junctions formed also affects the coefficient of friction. Thus ductile metals have higher coefficients of friction than brittle ones. Greenwood and Tabor (43) demonstrate this. Table 2.2 shows the values of μ under different conditions.

TABLE 2.2

Frictional behaviour of junctions (42)

Type of junction	Material	Surface condition	μ_s	μ_k
One piece	Any	Perfect adhesion	3	-
Two piece	Indium	Strong adhesion	2.5	2
Two piece	Aluminium	Weak adhesion	1	1
Two piece	Aluminium	Lubricated	0.15	0.05

Table 2.3 shows the effect of lubricating films on friction

TABLE 2.3

Values of μ for different junctions with different lubricants

α_j	Ideal single piece junction	Oxide	Two piece junctions with films of				
			Lead	Tin	Indium	Soap	PTFE
14	2	1	0.6	0.4	0.26	0.22	0.23
7	3	1	0.24	-	0.15	0.09	0.19
3.5	5-6	1	0.17	-	0.10	0.05	0.10

where α_j is the angle of the leading edge of the junction.

Surface roughness had a small effect on the coefficient, amounting to about 10% for a variation in the angle between 30 and 60 degrees.

Dokos (47) investigated the effect of sliding and load on the coefficient of friction and found that it was dependant on both. Table 2.4 shows the results he obtained.

TABLE 2.4

The effect of normal load and velocity on the coefficient of friction

Velocity of disc i.p.s	Normal load Kg.	Coeff. of friction
1.6×10^{-4}	50	0.56
	100	0.55
	150	0.49
	200	0.515
1.44×10^{-3}	50	0.43
	100	0.47, 0.43
	150	0.49
	200	0.465
	250	0.62
1.18×10^{-2}	50	0.34
	100	0.30
	150	0.43
	200	0.45
	250	0.66
9.6×10^{-2}	50	0.26
	100	0.32
	150	0.28, 0.31
	200	0.375
5.76×10^{-1}	50	0.24
	150	0.27
2.31	50	0.22
	150	0.20
20.4	50	0.20
	100	0.185

Contd.

TABLE 2.4 (Contd.)

20.4	150	0.175
	200	0.17
54.0	50	0.20
	200	0.15

His conclusions, which are interesting, are

- a) For clean contact surfaces, the coefficient of friction greatly increases with decreasing velocity. (See Figure 2.1)
- b) There is a critical velocity above which stick-slip friction is not observed.
- c) There are three velocity ranges.

In the upper and lower ranges the coefficient decreases with load and in the middle range the opposite occurs.

The papers reviewed above contain most of the material relating to friction and the coefficient of friction. From the conclusions of the many authors, it is quite clear that the frictional behaviour of metals is not described by Amonton's Laws, that it is very complex and that to say with any degree of certainty that one can completely allow for it in any theory would be too optimistic. The effect of friction can however be greatly minimised by lubrication and the following paragraphs describe some of the more common methods employed in lubricating powders before compaction.

2.2.2 Lubrication of powder compacts.

Lubricants, binders and additives are used in almost all applications of the compaction process. Lubrication has a two fold effect on the powder compact, first by its effect on the frictional forces i.e the sliding forces between surfaces, it allows more uniform transmission of stress within the compact and thereby reduces the variations in density. Since, however, the lubricants form an adsorbed layer on the surfaces of the individual particles, they decrease the coherence of the compact.

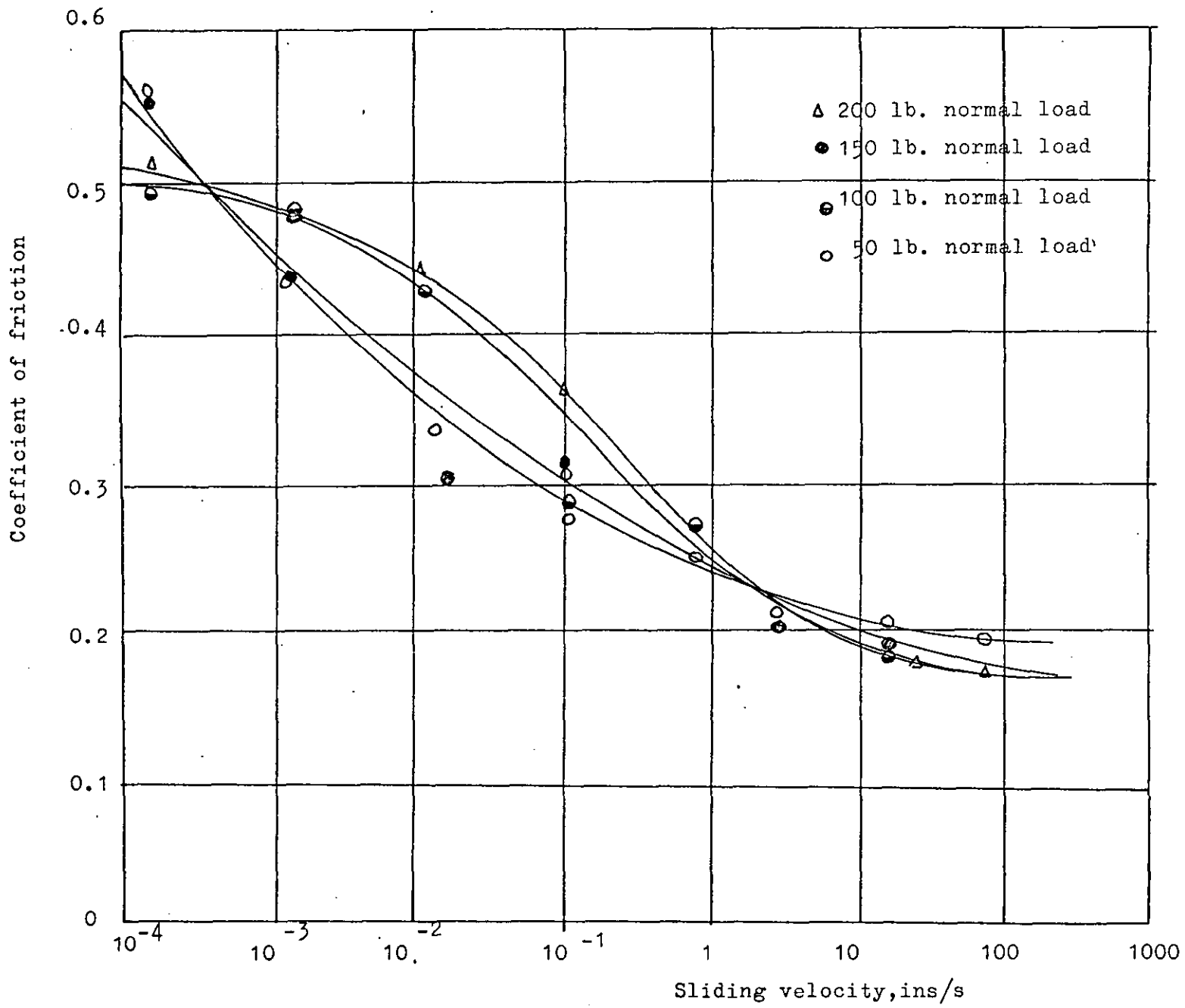


FIGURE 2.1 Velocity-Friction curves at varying loads (47)

In the ceramic industry, in the manufacture of refractories, water is largely used, as also are water soluble organic materials or additives, which react with the material of the compact giving rise to chemical bonds. The compounds in the first group are the lignin-sulphonic acids and the sodium, ammonium and the calcium ligno-sulphates. Sulphuric and phosphoric acids and aluminium phosphates belong to the second group. Other compounds used include polyvinyl alcohols, urea, stearine and cellulose derivatives.

Those lubricants used with metals, which are, incidentally, more relevant to the model presented in this thesis, are generally the metal salts of stearic acid or stearic acid itself. Leopold and Nelson (49,50) investigated the effects of lubrication on the die wall (51,52). Many workers have indicated that the lubrication of the powder mass does not produce any change in the nature of the compact as opposed to lubrication of the wall alone. Leopold and Nelson carried out a series of experiments to determine the effects of both admixed and wall lubrication. At higher pressures wall lubrication proved superior to admixed lubrication whereas at lower pressures the reverse was true, although the difference in the latter case was minimal. Specific applications for the commonly used lubricants are given in Table 2.5

TABLE 2.5

Lubricants for various metal powders.

Metal	Lubricant / s
Iron	Zinc Stearate
Copper	Lithium-Zinc or Cadmium-Zinc
Aluminium	Zinc or Cadmium Stearate
Brass	Lithium Stearate
Stainless	
Steel	Lithium or Nickel Stearate

The results obtained by Leopold and Nelson are shown in Figures 2.2 and 2.3. Further observations are that for small compacts, the effects of lubrication are smaller than for large ones.

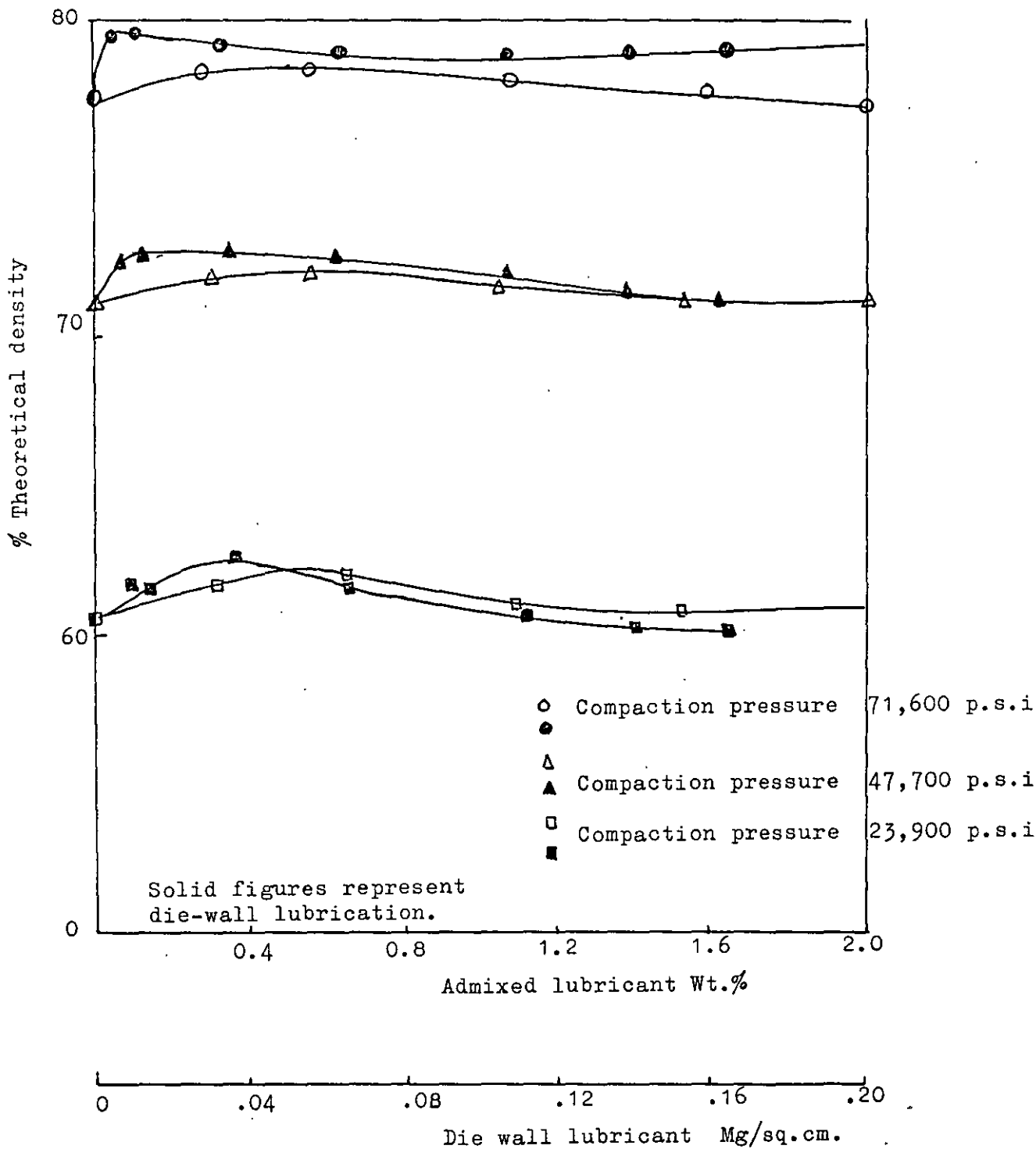


FIGURE 2.2

Density-lubricant curves for 1.25 g. compact

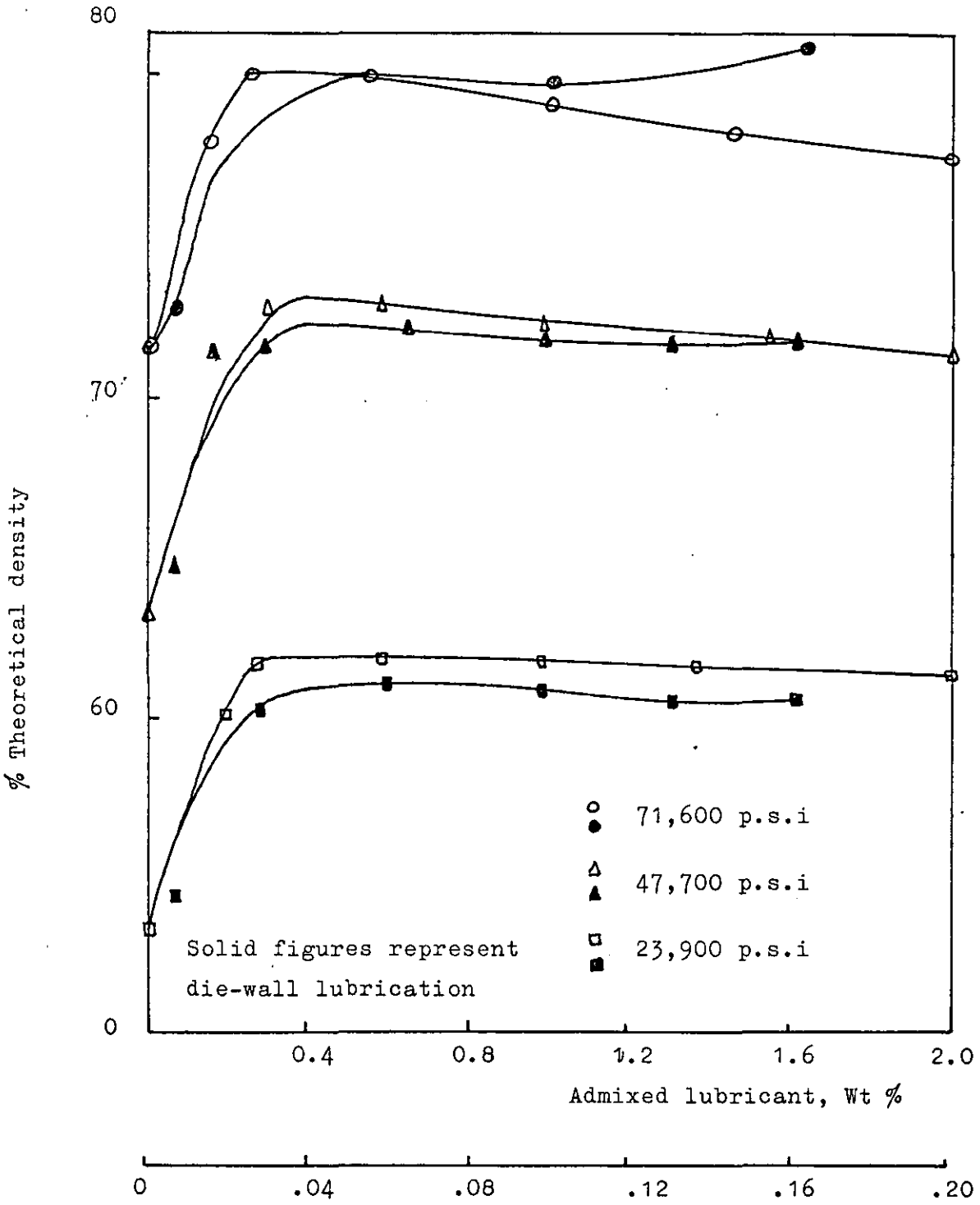


FIGURE 2.3
Density-lubricant curves for 7.50 g. compact

Hausner (90) and Burr (72) have also investigated the effects of lubricants in powder compaction. Although there are some differences in their conclusions as compared with those of Leopold and Nelson there is substantial agreement on the fundamental question as to whether the lubrication of the powder mass has any advantage over the lubrication of the wall alone. There is unanimous agreement that lubrication of the wall provides all the lubrication necessary and that in lubricating the powder mass the disadvantages introduced by the reduction in coherence of the compact are encountered.

An important conclusion that may be drawn from these observations is that the transmission of force through the system is only minimally affected by inter particle friction whereas the wall friction is an important factor that must be considered in any calculations undertaken. It would thus appear that since inter particle friction plays an insignificant role in the compaction process that there is little inter particle movement within the die during compaction. This assumption is further borne out by the fact that there is a noticeable difference in the effect of admixed lubrication at the lower pressures when it would be expected that ^{there} would be inter particle movement and consequent particle friction effects.

2.2.3 Conclusions

To conclude the review of literature on friction and lubrication it is useful to summarise the important facts to emerge from the literature.

- a) The coefficient of friction varies with surface and other conditions .
- b) Friction can be drastically reduced by the addition of lubricants.
- c) Elimination of wall friction is desirable and, to a large extent, possible, by lubrication at the wall, but elimination of the interparticle friction is irrelevant and probably undesirable.
- d) It is possible to evaluate the coefficient of friction at the wall if the angle of internal friction were known.

2.3 Theoretical and experimental evaluation of density variations in powder compaction

2.3.1 Unckel's evaluation of stress in dies

Unckel (30) was the first to attempt to evaluate, mathematically, the experimental observations of pressing powders in dies. His experimental method consisted of making compacts of various diameters and heights, and taking specific gravity and hardness measurements along the length of the compacts, as well as in the centre, by cutting the compacts into discs. As others after him have done, Unckel, using unidirectional pressing techniques, found a low density zone near the bottom outer edge of the die. He also noticed that in compacts with high length to diameter ratios that the bottom centre pressure is less than at the top centre, but that with low ratios the reverse was the case. Subject to the effects of work hardening, the hardness values gave the same results. Figures 2.4 and 2.5 show some of his results. Unckel also made the observation that the density at a particular depth was greater in shorter than in longer compacts. He did not, however notice the high density region near the centre, which has been noted later by Train (7) and others.

His experiments on the friction at the wall yielded the conclusion that three quarters of the applied force is lost at the wall in unlubricated dies, but that this could be reduced by two-thirds by lubrication. Table 2.6 shows the results he quotes to justify his views. Another interesting observation made by Unckel relates to his attempt to press a hollow compact with a flange at the bottom. He noted that the powder in the flange part remained uncompacted at the end of the pressing operation with the exception of a slight bulge at the sides. This seems to indicate that there is little force transmitted outside the area covered by the punch surface.

TABLE 2.6

The effect of lubrication on die wall pressure.

Powder	Total punching force, Kg.				Ejection force, Kg.
	2000	4000	8000	12000	
100gCopper (Mixed size)	1600	2700	4300		5800

TABLE 2.6 (Contd.)

120gCopper (Fine size)	1500	3170	5600	7600	7350
As above (Lubricated)	900	1550	2150	2250	2300
100gIron	1400	2480		6920	7760
50gIron				2310	2700
100gIron (With 3% Graphite)		2610	6140		4675

Unckel tried to interpret his observations, mathematically. This treatment is recounted in Appendix 2.1. His work was performed in 1945 and was the first of a series of attempts to obtain information relating to the process of compaction. His experimental techniques have been improved upon but there has been no comparable mathematical treatment in the papers reviewed for this thesis. Most of the current work has been concerned with relationships between macro properties of the system such as pressure-volume curves, and information concerning a particulate approach has been sparse.

2.3.2 Early investigations

Much of the early work on density distributions was performed by a group at the Massachusetts Institute of Technology. This group included Seelig, Wulff, Kamm and Steinberg (1)(2)(3). Some work had also been done by Balshin (31) and Rokowski (29). Kamm et al used an embedded lead grid to study the transmission of the force within the die. This was done by radiographing the die assembly after compaction and calculating back from the deformations observed on the grid. The axial strain measurements so obtained were used to calculate the density distributions. They reached more specific but similar conclusions to those of Unckel. These were

- a) For varying height to diameter ratios, lower pressures gave more uniform density distributions.
- b) For the same diameter, an increase in pressure or height increases the density variations.
- c) Upto a height to diameter ratio of 2:1 the density at the centre of the base exceeds that at the centre of the top, but if this ratio is exceeded the reverse becomes the case.

Specific gravity			Brinell hardness				
			54	54	79	89	
8.03	7.50	7.26	48	55	73	85	86
7.72	7.54	7.25	48	54	60	79	79
7.40	7.50	7.35	43	47	51	55	65
7.50	7.54	7.03	39	46	51	46	54
6.56	6.32	6.53	37	38	37	36	38
5.56	6.17	6.73	30	37	30	24	29
5.27	5.53	6.03	27	27	26	19	27
			27	26	19	15	16
			27	24	21	16	
			60	62	85	100	
7.5	7.22	7.11	54	60	67	87	93
7.40	7.54	7.65	54	58	58	60	79
6.78	7.20	7.50	60	59	55	44	62
			71	65	65	54	

(a) Copper mixed sizes

Specific gravity			Brinell hardness				
			54	67	73	94	
7.53	7.08	6.85	68	70	73	85	93
7.05	7.06	5.80	65	70	74	82	85
6.71	6.95	6.74	60	65	67	70	78
6.48	6.64	6.74	62	52	54	65	54
6.06	6.47	6.32	54	54	43	47	37
5.77	6.26	6.53	55	51	45	44	30
			51	47	39	30	22
			39	37	25	19	
			55	65	70	97	
7.32	7.00	6.94	54	58	65	92	97
6.08	7.02	6.99	60	62	65	73	82
7.16	7.01	7.06	65	65	54	40	40
			65	62	50	35	

(b) Copper, fine size

FIGURE 2.4

Specific gravity			Brinell hardness				
			55	63	73	100	
6.76	5.84	5.80	54	62	79	93	91
5.28	5.58	5.53	55	54	58	70	86
5.28	5.39	4.98	48	55	53	54	79
4.84	4.60	4.91	51	56	47	39	73
4.66	4.73	4.87	41	40	37	36	55
4.23	4.55	4.77	34	34	36	27	39
			30	30	27	23	32
			34	34	30	24	
			65	67	70	86	
6.40	6.26	5.70	54	62	65	90	73
5.47	5.75	5.60	65	65	63	67	54
4.95	5.35	5.26	73	62	54	39	40
			73	67	65	65	

(c) Iron powder

3Kg. and 1Kg. (lower row) compacts. Longitudonal sections at 6000Kg pressure.

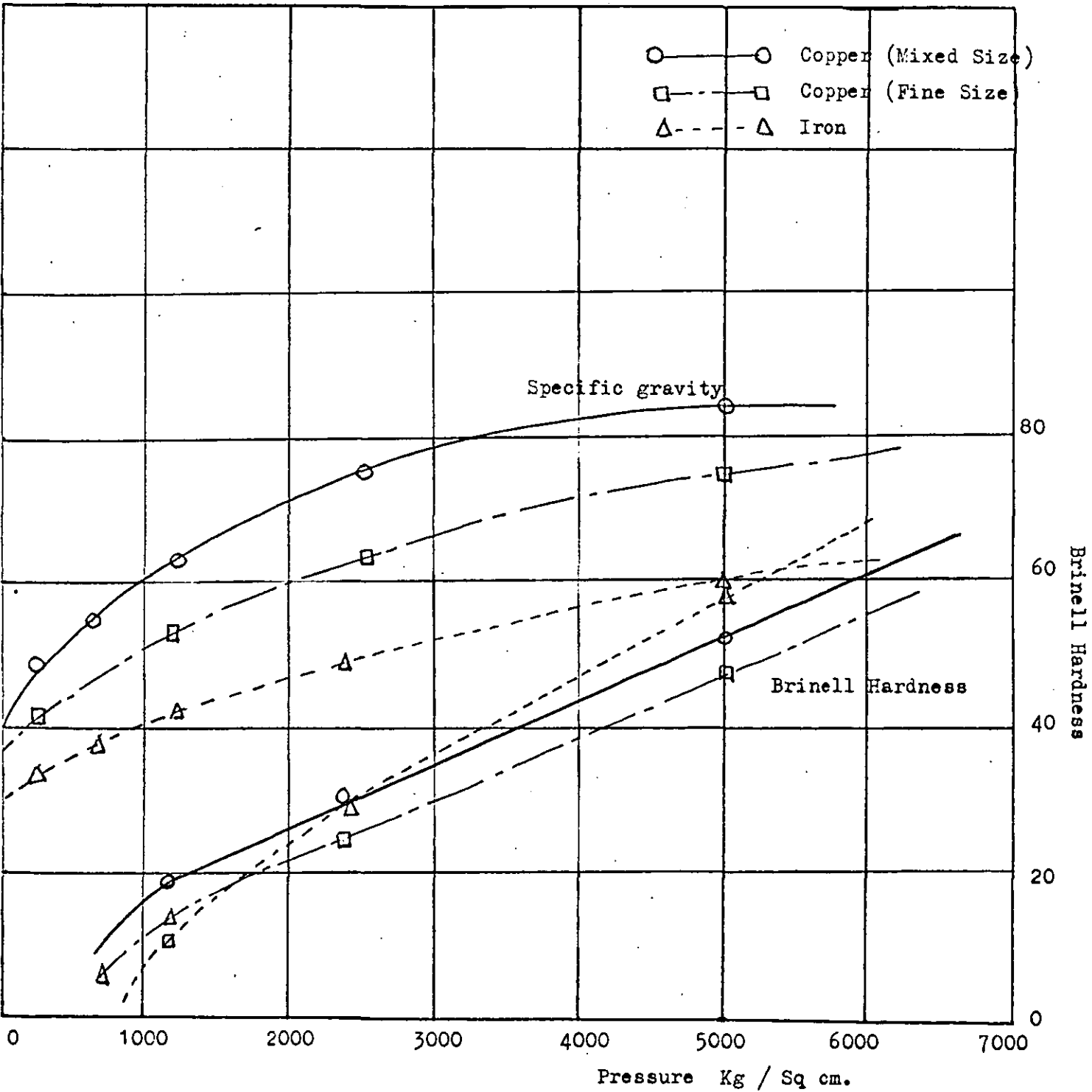


FIGURE 2.5

The effect of pressure on Brinell Hardness and specific gravity of compacts 22 mm diameter ,2mm thick specimens

- d) For the same height to diameter ratios, larger diameters reduced the variations in density.
- e) Increased diameters lessened wall friction.
- f) The lubrication of the wall had a significant effect on the density variations whereas the lubrication of the particles did not.

These experiments were performed with carbonyl iron powder and later repeated with coarse electrolytic, coarse reduced and fine iron powder. The above conclusions remained unaffected. Some of the results are shown in graphical form in Figures 2.6 - 2.8. Unfortunately, the lines represent points at identical depths on the undistorted grid and cannot be given an exact physical location in the system on the basis of the information obtainable from their papers. They also studied the effect of varying the rate of application of pressure and of de-gassing on the density distributions but these results have little relevance to this research.

2.3.3 Recent investigations

Train working in the field of pharmaceuticals, has also performed extensive investigations into density variations in die compaction. His use of a split die (Figure 2.9) enabled him to make direct determinations of density. He used colloidal graphite as a wall lubricant and also investigated unlubricated dies. His conclusions are also similar to those of Kamm, Unckel et al, but because of his use of layers of alternately coloured and white powder, he noted that there was a greater displacement at the top and that this displacement was reduced by lubrication. He also noted, and gave explanations for cracks which appear on the ejection of the compacts from the die

In lubricated dies the cracks appear to be concave upwards whereas in the unlubricated case there were also some which were concave downwards. The explanation he gave for the formation of these cracks is based on the phenomenon known as elastic relaxation. As the compact is extruded from the die there is a peripheral relaxation of the elastic strain which induces a longitudinal strain in the top centre region, where the material is less dense and therefore probably weaker. Thus any additional strain such as that introduced by handling etc. causes cracks to appear. In the case of harder metals particularly, Bowden and Rowe (38) have shown

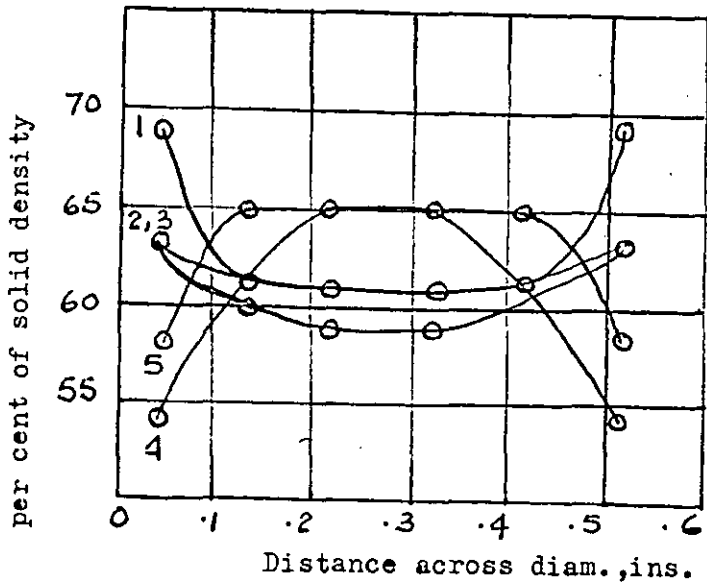
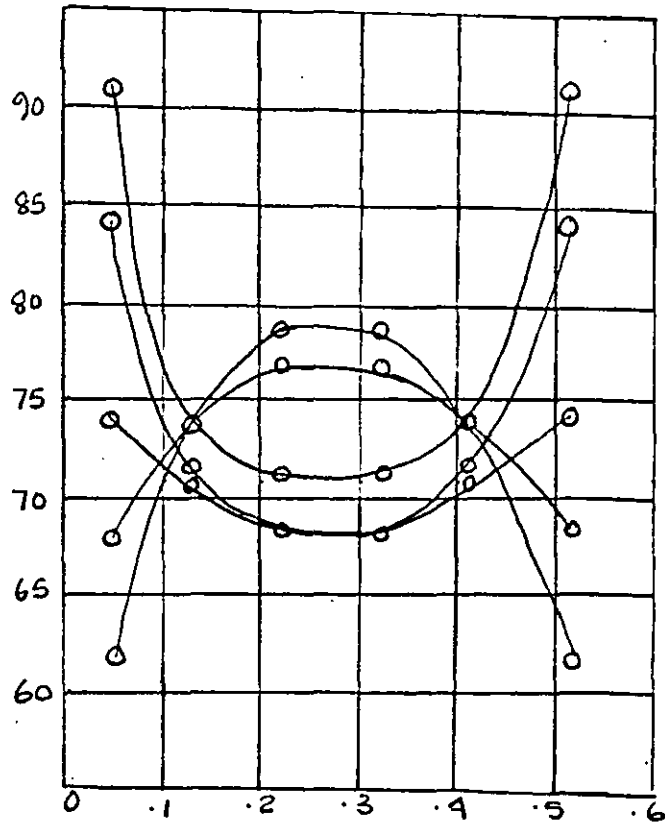


FIGURE 2.6 Applied pressure 16 t.s.i

The effect of applied pressure on the variations of density (lines are streamlines-see text)



Applied pressure 32 t.s.i.

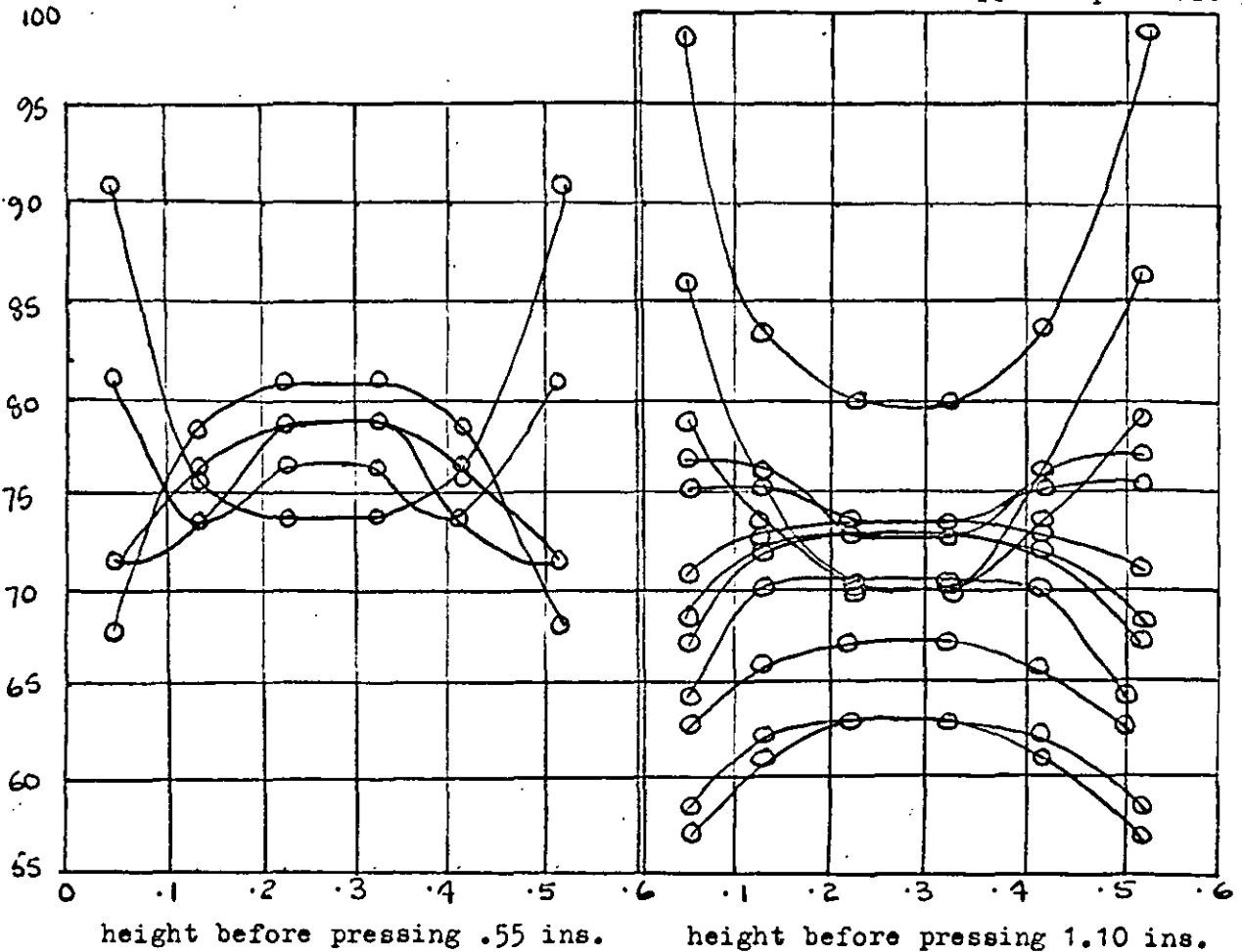


FIGURE 2.7

The effect of height on the variations of density

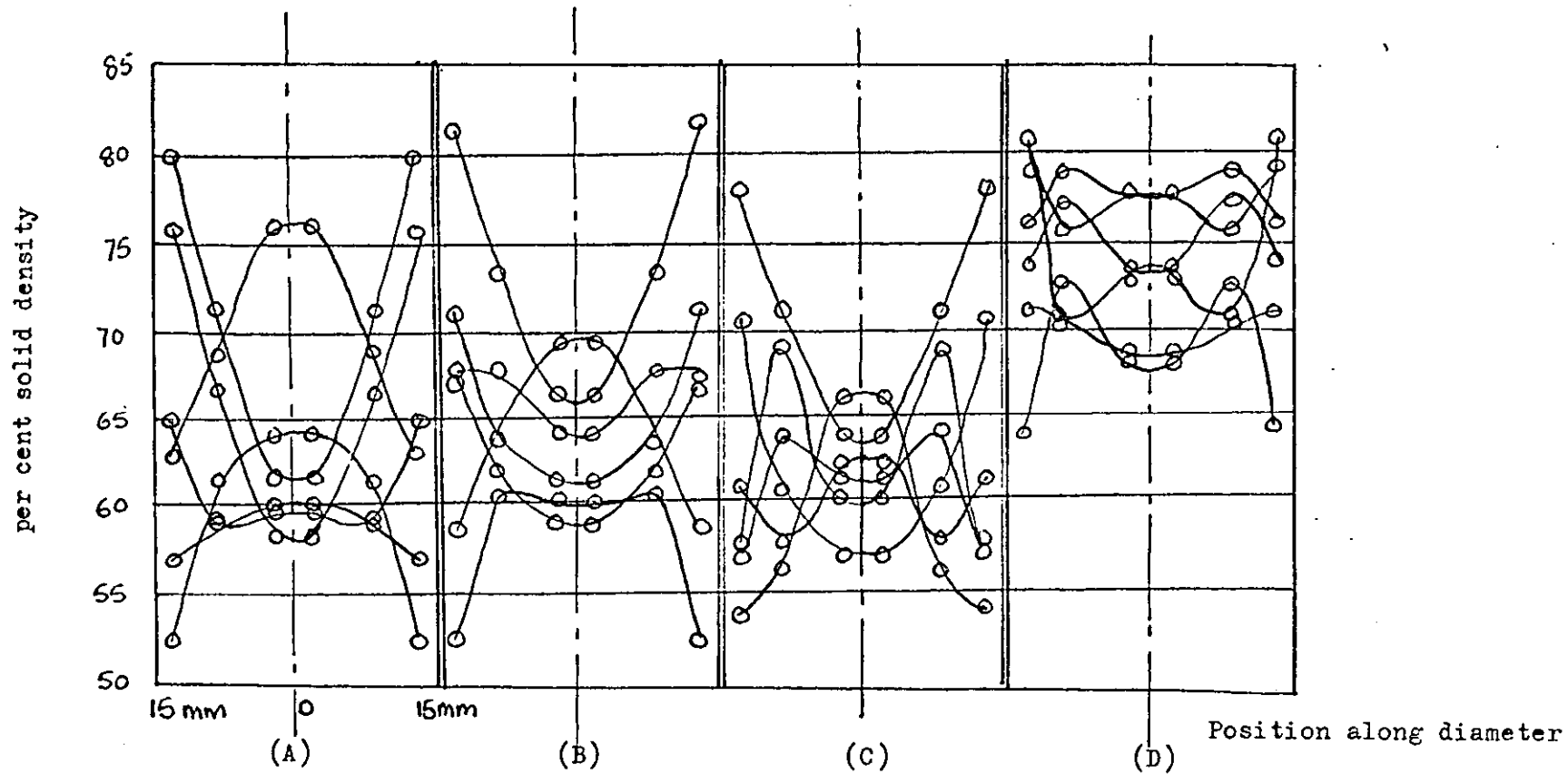


FIGURE 2.8

The effect of lubrication on the variations of density

- (A) -300 mesh Nickel -no lubricant
- (B) -300 mesh Nickel -graphite flake, internal lubricant
- (C) -300 mesh Nickel -0.18 % stearic acid in powder only
- (D) -300 mesh Nickel -0.05 g. stearic acid on die walls only

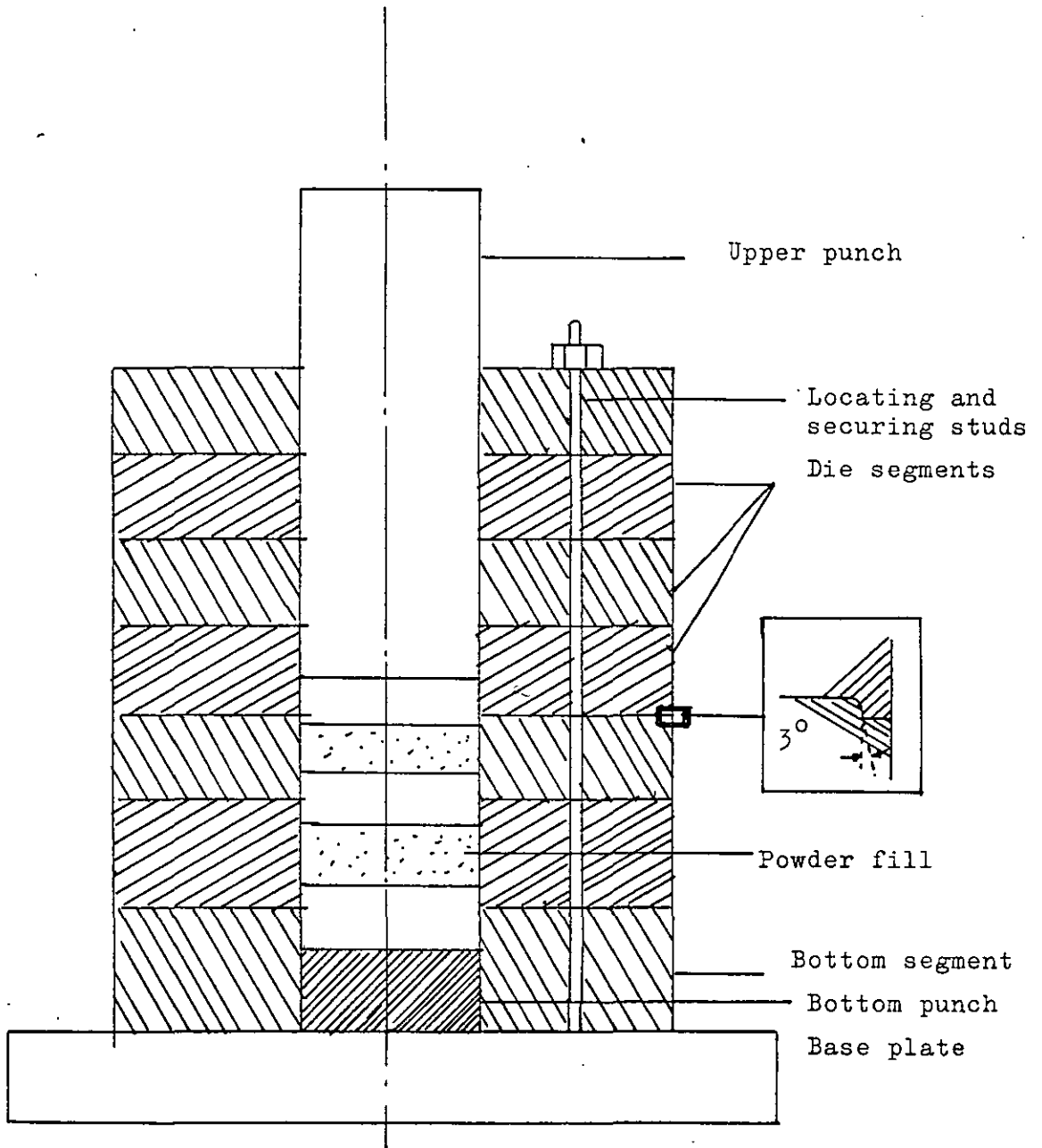


FIGURE 2.9
Split die assembly used by Train (7)

that these elastic stresses cause the snapping of brittle junctions formed when the metals are pressed together. The cracks often appear only after complete extrusion, this being due to the partial bonding of the surfaces with brittle bonds which are easily ruptured by such phenomena as the expansion of entrapped air. The absence of the second type of crack in the lubricated die is probably due to the greater uniformity of density, and hence strength, in these compacts. The cracks appearing in the lubricated compacts tend to confirm that the additional stress which caused the crack was sufficient to break all the bonds in the plane whereas in the unlubricated case local failure may occur. Some of Train's results are shown in Figures 2.10 and 2.11.

2.3.4 Side wall pressures

The only work in metal powder compaction which concerned itself with side wall pressures is that due to Duwez and Zwell (6). They used the apparatus shown in Figure 2.12, to measure the side wall pressure at different points on the die wall for a given applied pressure. (Pressure of course being applied axially). Some of their results are shown in Figures 2.13 and 2.14. These results confirm what has been said by Train and others but provide more qualitative information which can be used in evaluating the performance of a model. The results also show that, regardless of applied pressure, the pressure on the bottom is only a function of compact thickness, and also that, regardless of thickness, this pressure is a function of the height to diameter ratio. These conclusions are contrary to the results of Unckel and the others.

Reviewed above are all the papers of significance to this work. There are, of course, many, many others but it has been neither possible nor desirable to refer to all these. However, those that might be of interest are due to Huffine and Bonilla(9), Duffield(10), Train and Hersey(11,12), Bockstiegel(13) and Long(14). To summarise, therefore, the papers reviewed above, it is possible to say that density distributions are caused by the non uniform stress distribution in the die which in turn is caused by wall friction. According to Unckel there is a zone at which the pressure is independent of the

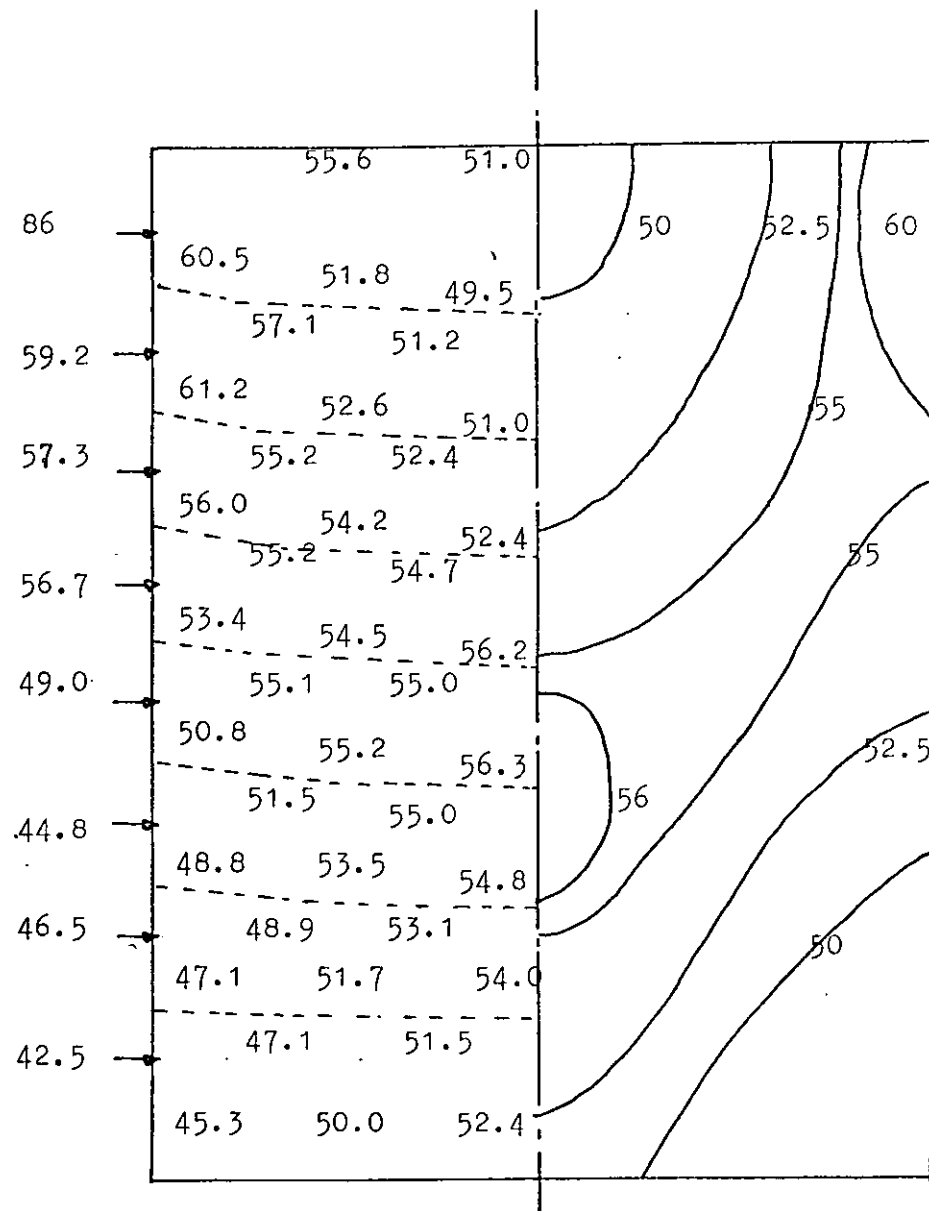
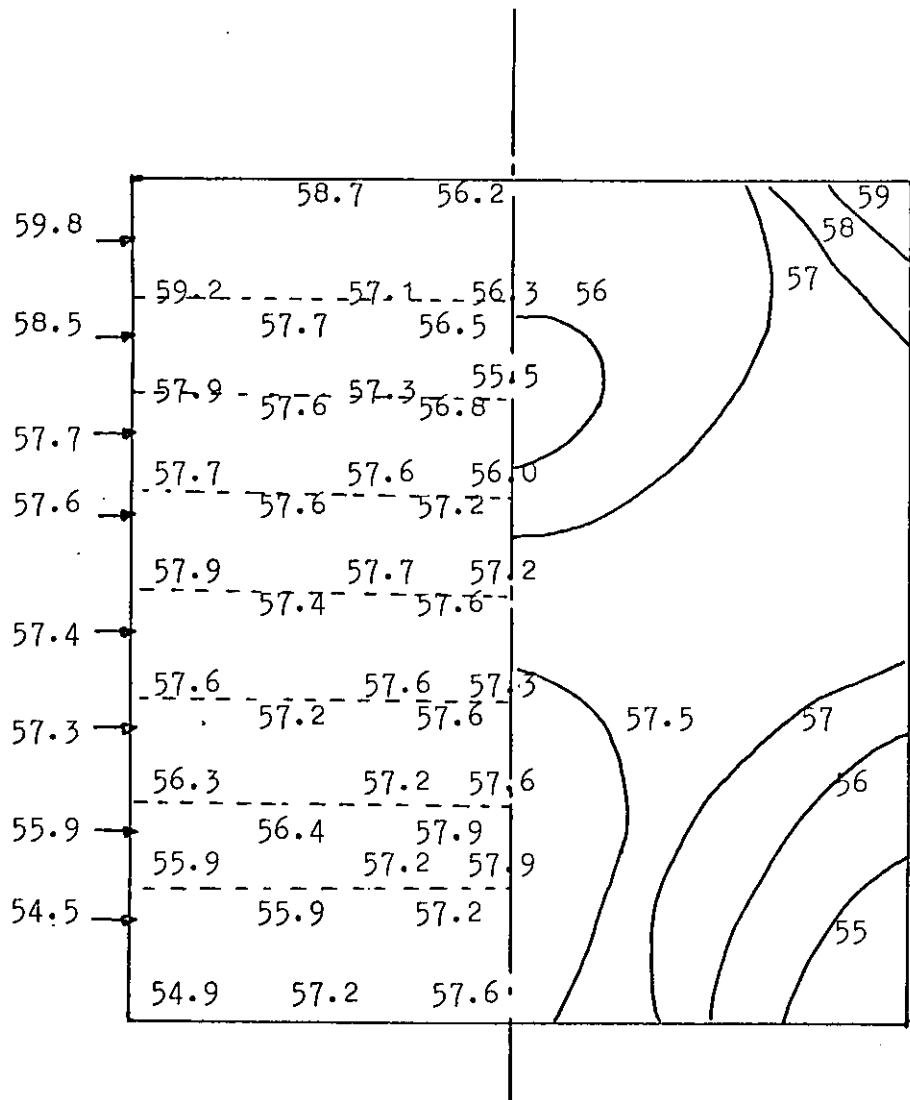


FIGURE 2.10

Density distributions, expressed as per cent solids present, 160 g. compacts made at 671 Kg/sq.cm. (7)

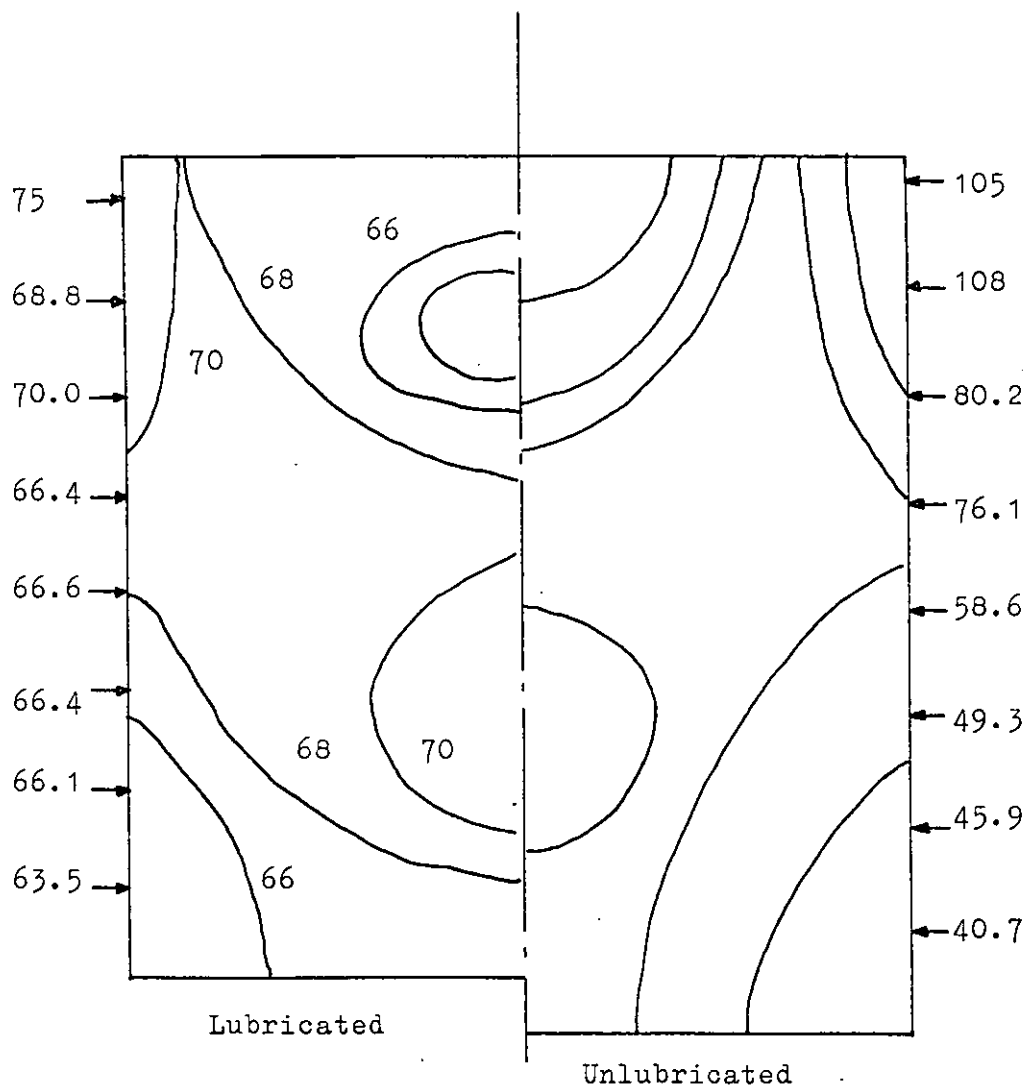


FIGURE 2.11

Density distributions, expressed as per cent solids present, 160 g. compacts made at 2040 Kg/sq.cm. (7)

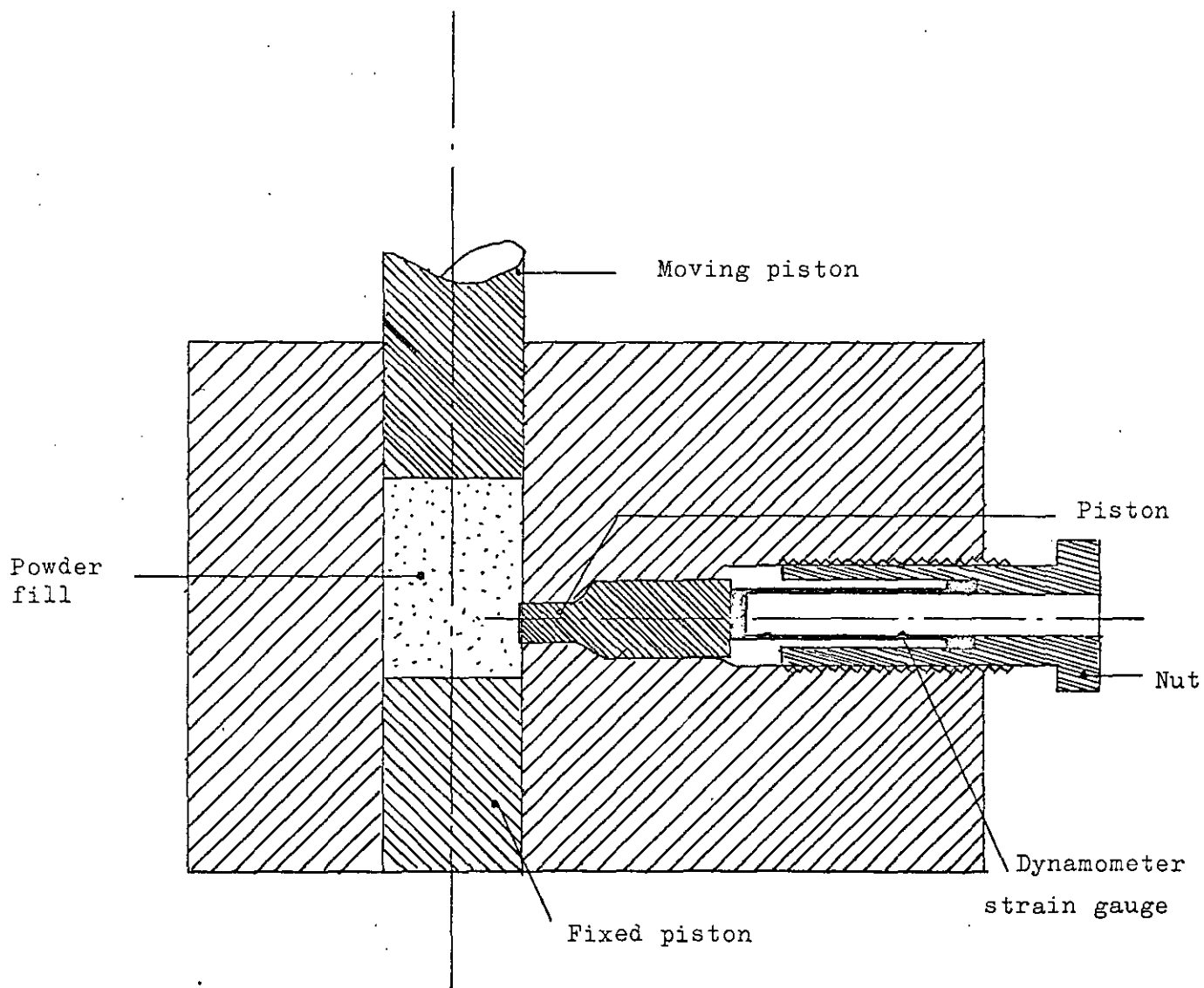
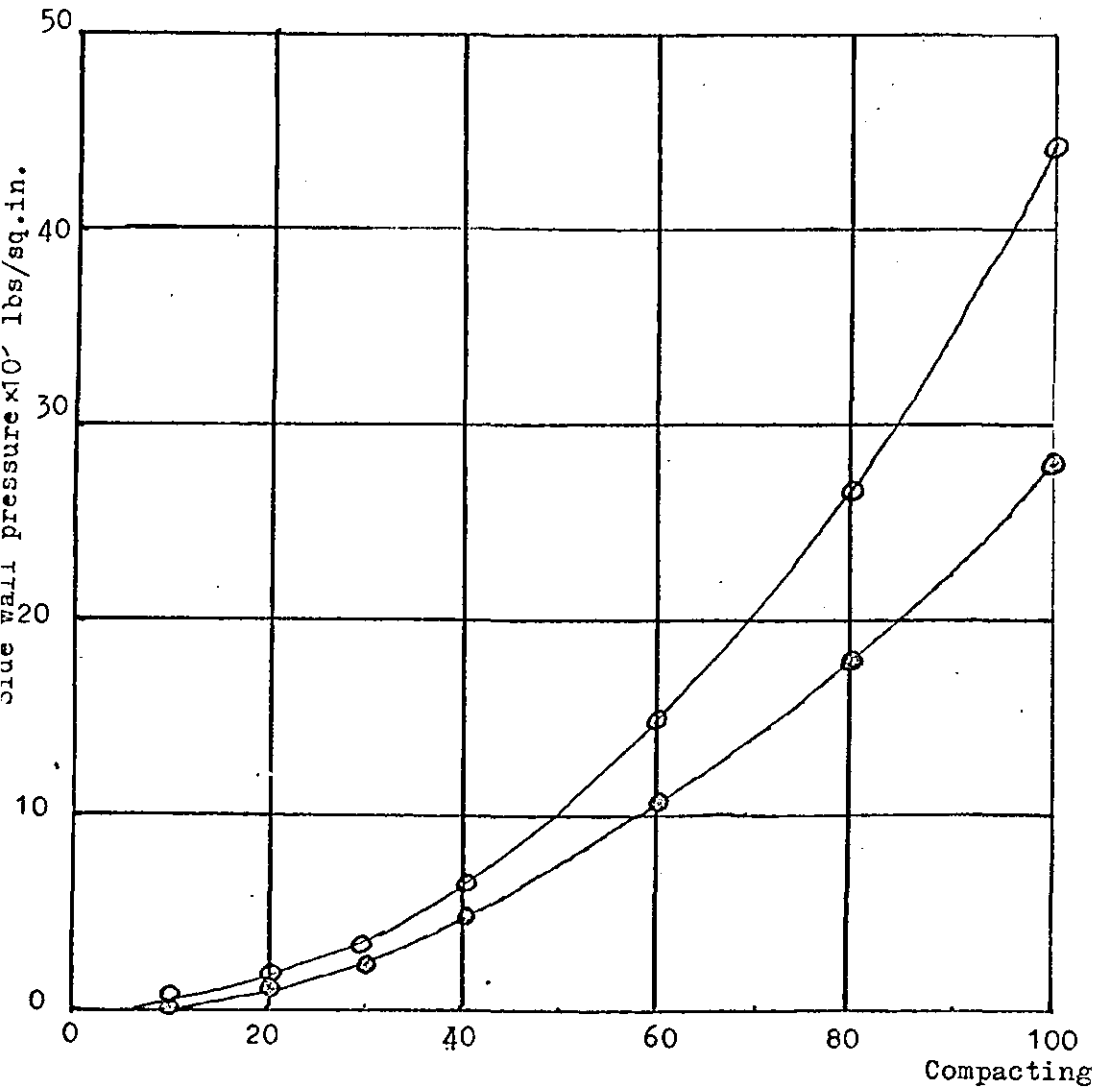
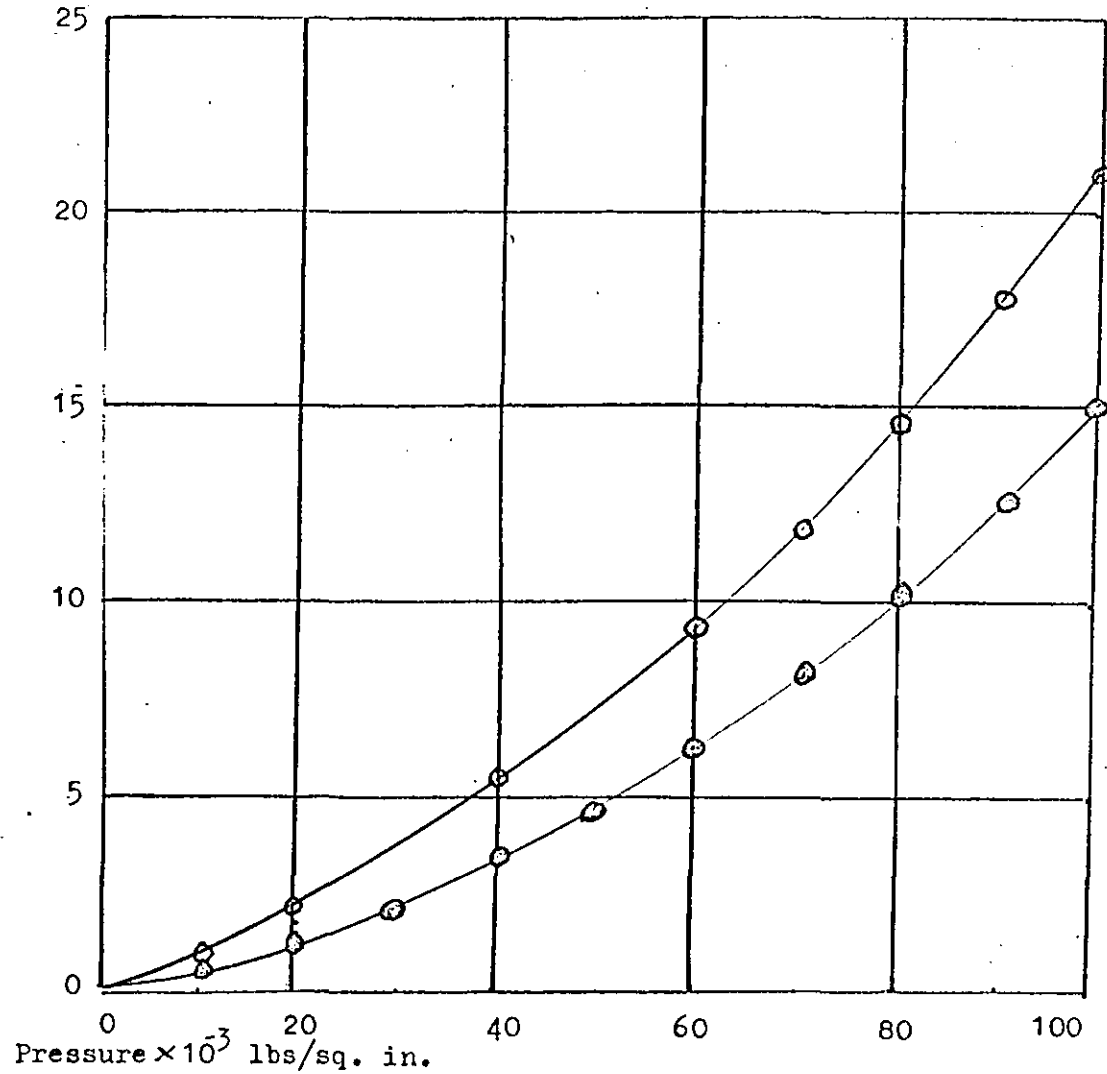


FIGURE 2.12

Apparatus used by Duwez and Zwell for measuring side wall pressures (6)



(a) compact thickness 1.15 ins.



(b) compact thickness 1.27 ins.

- .10 from fixed piston
- ⊙ .15 from fixed piston

FIGURE 2.13

Variation of side wall pressure with compacting pressure for compacts of different thickness

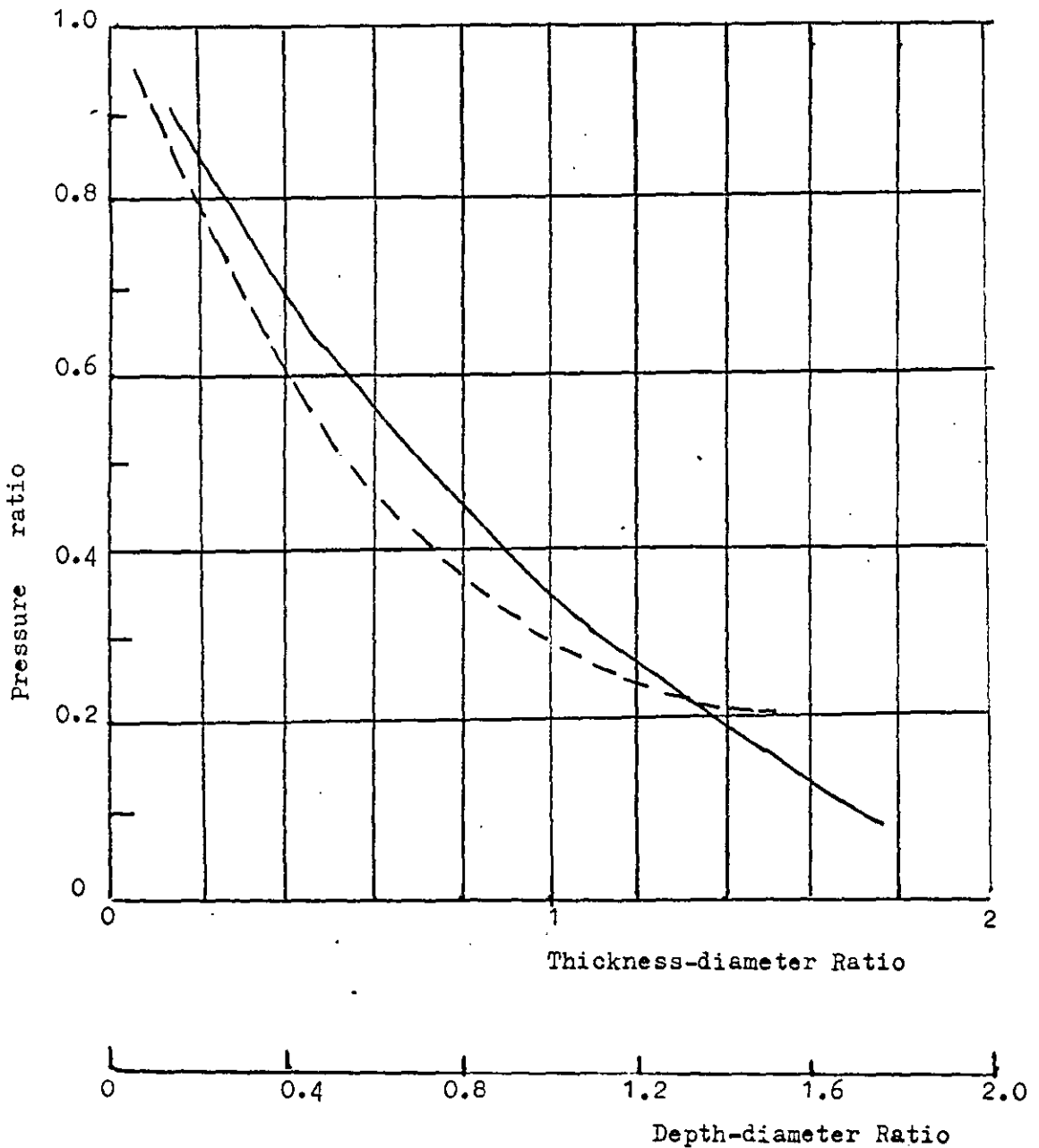


FIGURE 2.14

Ratio of average pressure on fixed piston to applied pressure vs.

(a) Thickness - Diameter ratio for copper compacts

(b) Depth - Diameter ratio for copper compacts

distance of the zone from the centre axis of the die. The formation of these zones can be explained by the lack of shearing forces and a consequent lack of cold welding. Thus if both the theories of elastic relaxation and no cold welding are taken together, the cause of the appearance of cracks becomes clear. Unckels observation that the angles made by these zones is the same is noteworthy although his assumption of a constant coefficient of friction and of a constant stress ratio are fallacious. Both Train and Zwell have remarked on the variation of the stress ratio along the length of the compact and Kamm et al found a variation of the coefficient of friction from .07 at the bottom to .625 near the top of the die, whereas Unckel assumed a constant coefficient of .15. For the purposes of this work, however, it is proposed to use a ~~first order relationship between the~~ ^{constant} coefficient of friction and ~~depth~~, since there is an absence of any usable information in the literature.

2.4 The packing of particles

In any theory, which considers individual particles, the packing arrangements occurring in particle systems must be considered. Duffield(24) has shown that, in die compaction, the initial density of the die fill has an effect on the pressure-volume relationship. Hausner(27) has demonstrated the effects of size on the properties of compacts. Although there is no conclusive evidence to show that the effects on compact properties of size is through its effects on the packing arrangements possible, it seems likely that this is so. Any development of this model must, therefore, consider packing and size aspects, especially at higher pressures when deformation of particles is likely to depend on both particle size and particle packing.

A number of papers have been written on the packing of spherical particles (53-59) and on the packing of irregular particles (60-66). The essential information available about spheres and mixtures of spheres is summarised in Table 2.7. Obviously, the packing of spheres is of greater academic than industrial interest but it is believed that with the approach used here, it may be possible to use information obtained on models based on spheres to solve problems associated with the more difficult irregular shapes.

TABLE 2.7 (Reference 55)

Number of components	Max. density	% vol. of each compont.	Ratio of dias.	Relative Part. size
1	62-64	100	-	-
2	86	75	10	1.00
		25	1	0.10
3	90	66	77	1.00
		25	7	0.091
		9	1	0.012
4	95	60.7	316	1.00
		23.0	38	0.12
		10.2	7	0.022
		6.1	1	0.003

TABLE 2.8 (Reference 61)

Adwick and Warmers results with irregular particles

Material	Individual fraction density			% Vol. of each comp. for max.density.	Max. density
	<6 >44	<44 >300	<300		
Coral	63	63	60	28 25 47	82
Alumino silicate	25	27	31	39 21 41	41
Uranium dioxide	57	54	49	42 20 38	71
Dense spheres	62 to 64			66 25 9	90

From the above results it seems reasonable to conclude that proportions of smaller sizes must be used to obtain decreases in porosity. It is of interest that the 66:25:9 ratio for spheres is replaced by a 40:20:40 ratio for irregular particles by Adwick and Warner and by a 45:10:45 ratio by Hugill and Rees (60). With greater irregularity of shape or with particles with surfaces of an open nature, the quantity of fines required increases due to the lodging of the fines in the surface pores.

Although the results described above are interesting, it is difficult to relate them to die compaction. They would, however, be important when it becomes necessary to consider the deformation of particles, which is the next step in the logical development of this model. A factor influencing the packing of material in dies is undoubtedly the method of deposition. McCrae (63) investigated the effects of density, height of discharge tube from top of packing, surface condition etc. on packing densities. He found that with higher velocities of impact the porosity increased, especially for particles with large coefficients of restitution. Duffield (24, 10) had found that the method of pouring was vital as far as correlation between the results of separate runs was concerned. Table 2.9 shows the effect on the packing density, of the method of filling the die.

TABLE 2.9
Filling volumes (10)

Pouring through funnel	Pouring from nozzle	Pouring from stationary nozzle	Inverting test-tube
1.661	1.695	1.699	1.680
1.673	1.687	1.694	1.690
1.675	1.691	1.705	1.689
	1.674	1.696	1.682
Mean	1.682	1.702	1.656
1.675	1.651	1.707	1.681
Std.	1.662	1.719	1.679
Deviation	1.651	1.685	1.687
0.011	1.686	1.692	1.680
	1.695	1.694	1.653
	1.677	1.699	1.651
	Mean	Mean	Mean
	1.677	1.699	1.675
	Std.	Std.	Std.
	Deviation	Deviation	Deviation
	0.016	0.009	0.014

Atmospheric conditions were found to affect the results, but the degree of oxidation and the depth of fill did not. The error of about 2.5 % could not be improved upon by simple means.

Another important aspect of die filling, is segregation of sizes on pouring into the die. This is the main reason why high densities, such as those obtained by Hugill and Rees and Adwick and Warmer, are not obtained in practice. When compaction is used on an industrial scale, it is not economical to have sophisticated and time consuming filling equipment. The effects of segregation have been described by Lawrence (69). He reaches the following conclusions, after having examined segregation in iron-lead mixtures.

- a) During the filling of the die with a two-component mixture, segregation occurs by the fines, d , filtering down through the moving powder mass. This effect builds up an inner mound of fines rich material at the bottom of the die. (See Figure 2.15)
- b) As a result of filtering out of the fines, an excess of coarse particles, D , is flowed to the outer layers of powder in the die. This is termed normal segregation. (See Figure 2.16)
- c) In a powder system in which D is kept constant, increasing the $D:d$ ratio increases segregation upto a relative size difference of $(D-d)/d$ of approximately 0.6 to 0.8. As the fines are reduced further in size, the filtering becomes more difficult and hence segregation decreases or even stops. (See Figure 2.17)
- d) In coarse particle systems (D large), inverse segregation occurs. This occurs in high percentage fines mixtures where there are less coarse particles in the outer layers than in the original mixture. This effect is ascribed to there being limited coarse particles in the system, with resultant burial of the incoming coarse particles in the fill thus hindering their travel to the die wall. In similar mixtures but containing less than 60% fines normal segregation occurs once more.
- e) Particle shape and density have little effect on segregation.
- f) In general, increasing the height of drop caused a drop in segregation, presumably due to increased mixing caused by bouncing. In fine particle mixtures, the coefficient of restitution is low and hence little bouncing occurs thus segregation in these systems is independant of the height of drop.

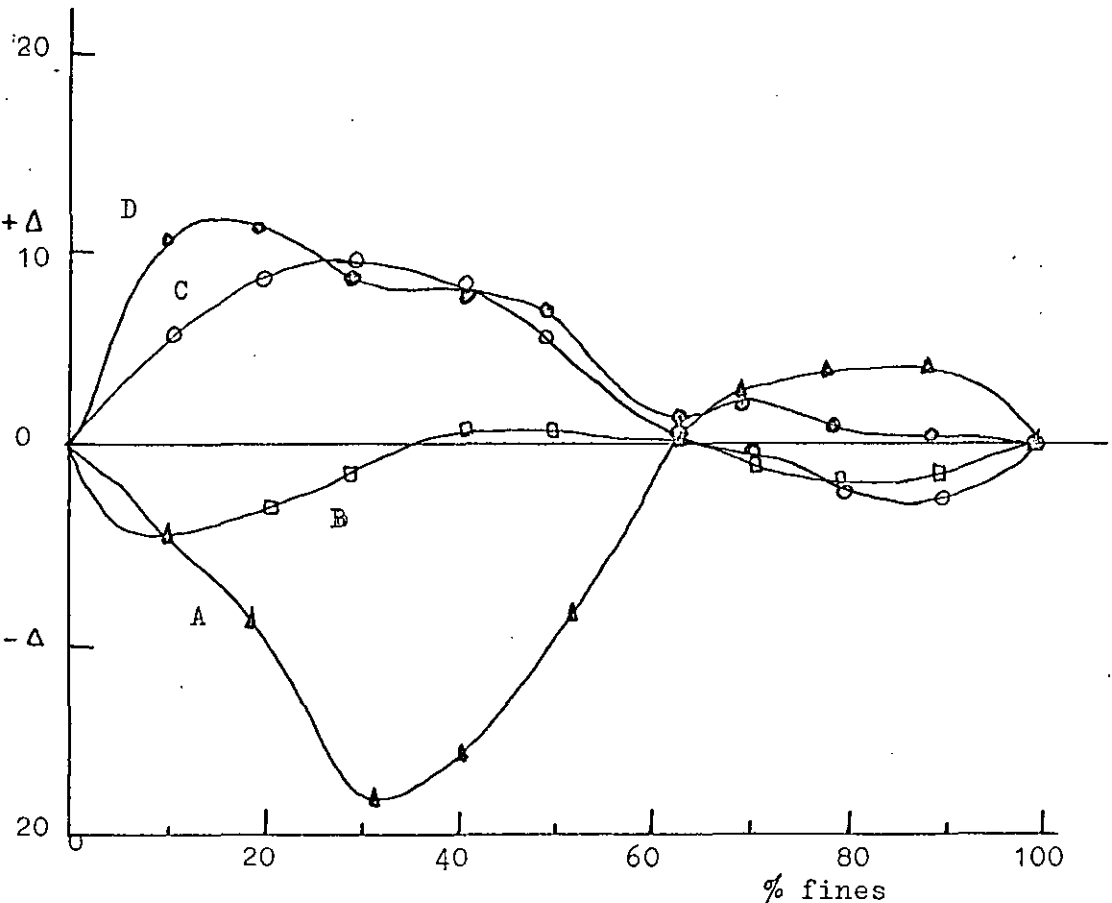


FIGURE 2.15
 A indicates the outer most annulus
 D is the centre of the die
 Radial Effects

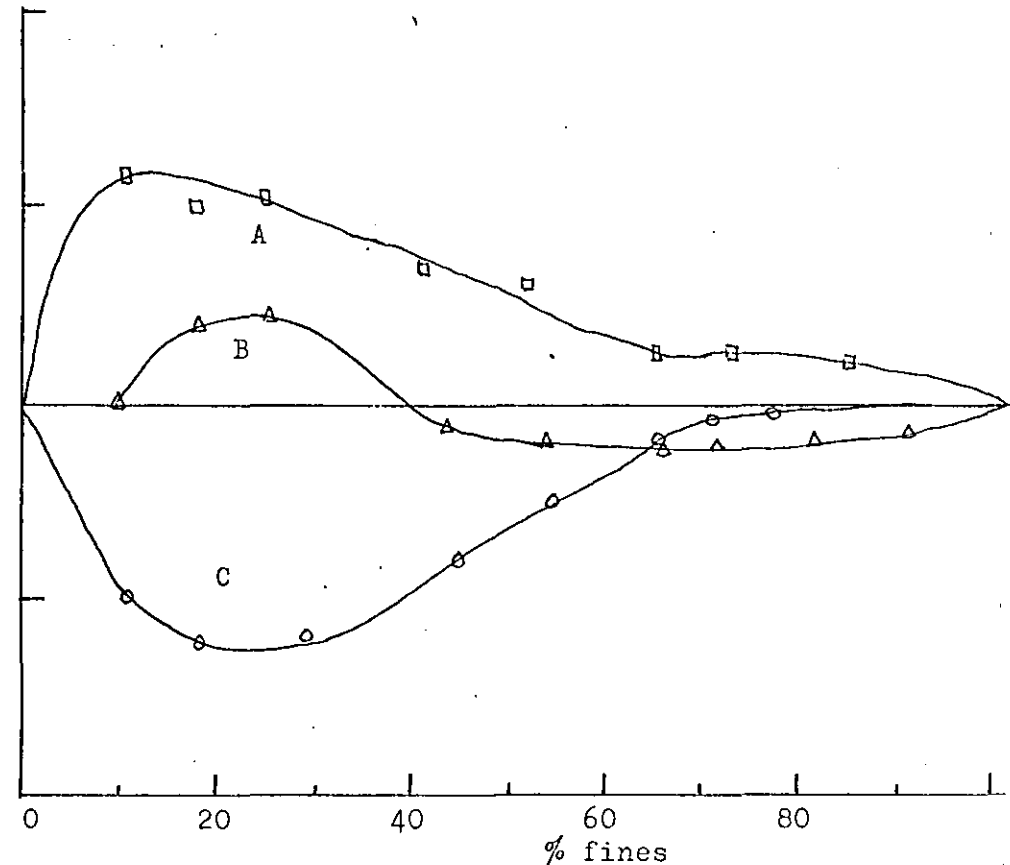
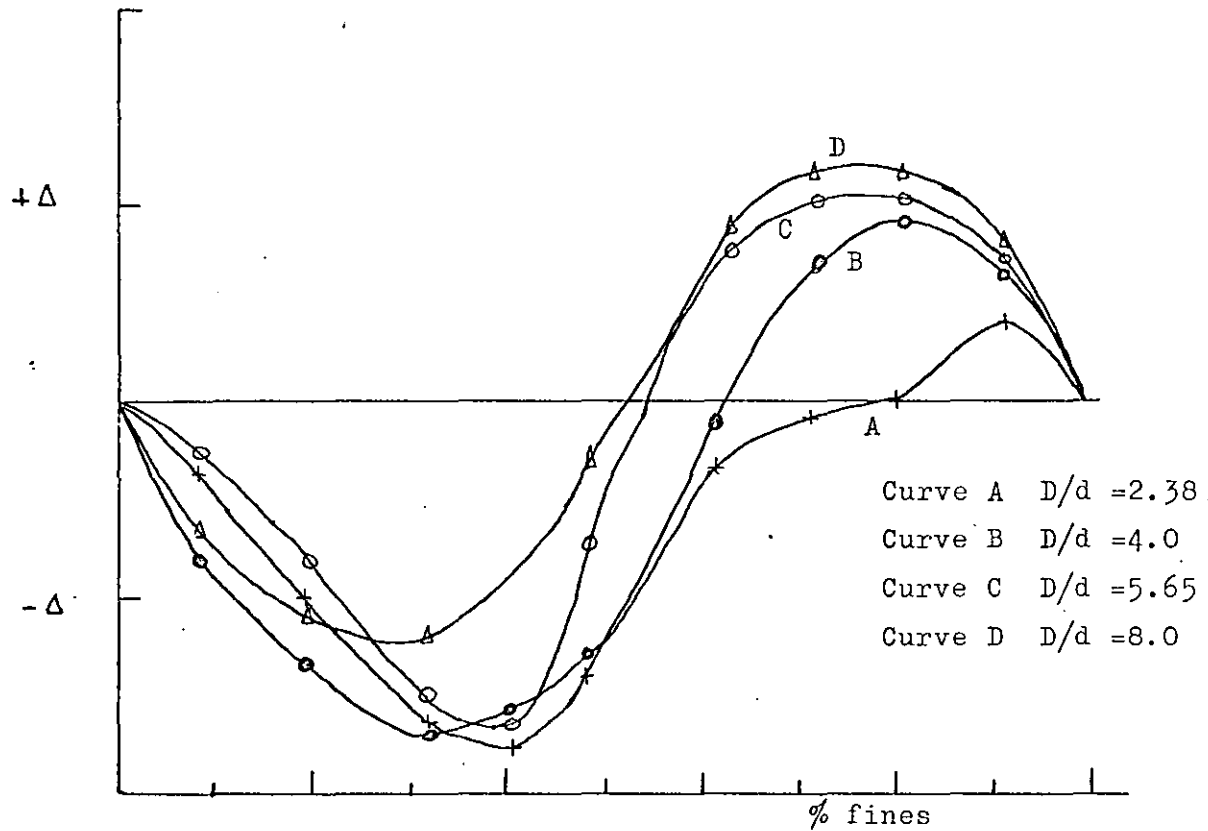


FIGURE 2.16
 A indicates the bottom of the die
 C indicates the top of the die
 Axial Effects

Segregation effects Δ % vs. % fines in the mixture (69)
 $\Delta = \%$ fines in sample - % fines in original mixture



D = diameter of course particles
 d = diameter of fine particles

FIGURE 2.17

Segregation effects % vs. % fines for different particle mixtures (69)

g) If the filling time is decreased, segregation decreases. This may be done by increasing the nozzle diameter or decreasing the die diameter. Table 2.10 shows the effects of both these variables on segregation.

TABLE 2.10 (Reference 69)

The effect of funnel orifice diameter and die diameter on segregation

Funnel orifice diameter (cm)	2	1	1
Die diameter (cm)	5	5	2.7
Fines %	Δ %	Δ %	Δ %
20	6	14	9
40	6	16	7
60	-2	2	6
80	-2	-9	6

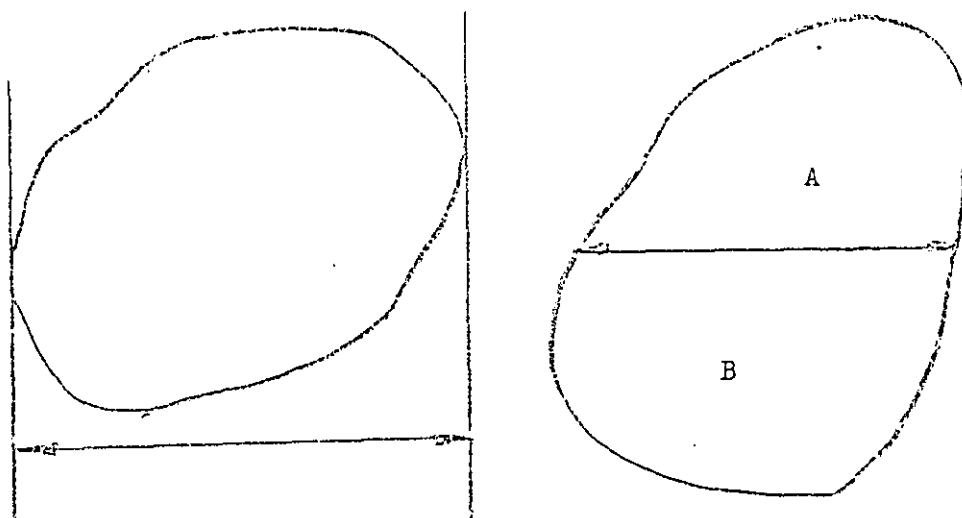
Where Δ = % fines in sample - % fines in layer

2.5 Particle Statistics

In the preceding pages the literature dealt with has mainly been concerned with macro properties of particle systems. At the outset it was stated that this was to be a 'microscopic' or particulate theory. It is therefore necessary to consider the particles individually. The essence of the object of this work is to link individual particle characteristics to system behaviour.

In recent years much attention has been paid to the mathematical (statistical) evaluation and definition of particle systems. This sub-section attempts to review these efforts and to choose those parameters which are likely to be useful for the purposes of this research.

There have been many methods in the past, of characterising particles and a number of these are based on the microscopic examination of the particles. The older, more established methods, use statistical diameters such as the Feret and the Martin's diameters (Figure 2.18)

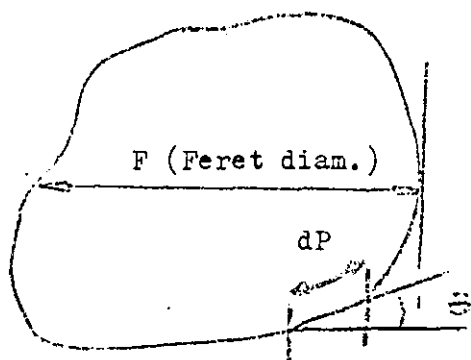


The distance between
two parallel tangents
FERET'S DIAMETER

Area A = Area B
MARTIN'S DIAMETER

FIGURE 2.18

The Feret diameter is the distance between two parallel tangents to the extremities of the particle. When measuring these diameters for an assembly of particles it is necessary to have all these tangents parallel to a fixed direction. A distribution of these diameters, characterises the system. The Martin diameter bisects the projected area of the particle. For convex particles, there is a relation between the average Feret diameter and the particle perimeter. (See Figure 2.19)



$$2 dF = dP \cos \theta$$

$$\bar{F} = \int_0^{\pi/2} dP \cos \theta d\theta / \int_0^{\pi/2} d\theta$$

$$\text{Thus } \bar{F} = P/\pi$$

$$\text{i.e. } P = \pi \bar{F}$$

Where P is the perimeter
and \bar{F} the average Feret diam.

FIGURE 2.19

In calculating most other parameters, however, both the Feret and Martins diameters give rise to inaccuracies, if they are used in place of equivalent sphere diameters (i.e. the diameter of a sphere of equivalent volume, projected area etc.). The Feret however has

a definite statistical significance and it will be shown later how it can be used with success in the building of a model. In recent years the best known attempt at applying statistics to particle systems came from Rumpf and Debbas (32). Their theory was applicable mainly to spheres and relate to the distribution functions of the diameters appearing in a section of a bed of spheres which had been previously set in resin. They obtained the following relations.

For equi-sized spheres the distribution function of the diameters appearing in a section is (See Figure 2.20)

$$z(y) = y / (x^2 - y^2)^{\frac{1}{2}}$$

where $z(y)$ represents the number of diameters of size y

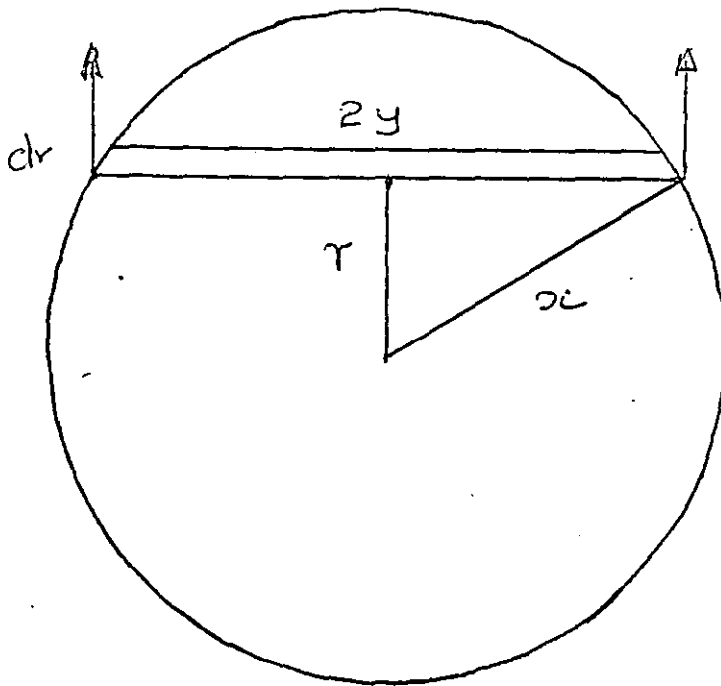
For mixed sizes the relation was,

$$z(y) = \frac{y}{\int_0^{x_{\max}} x h(x) dx} \int_y^{x_{\max}} h(x) dx / (x^2 - y^2)^{\frac{1}{2}}$$

If $M_{ny} = \int_0^{x_{\max}} y^n z(y) dy$ and $M_{nx} = \int_0^{x_{\max}} x^n h(x) dx$

where $h(x)dx$ is the number in the size class between x and $x+dx$. Then a number of relations obtainable from the projected size distributions may also be obtained from the sectioned distributions. These equations, it must be noted, have been derived for random packing of particles, but it has been found that with the use of the correct experimental techniques, it is possible to use them even with regular packings. In the experiments performed by the authors, packing which had been subjected to vibration for 30 secs at an amplitude of .5mm still produced results agreeing with the theory.

The newest attempt at characterising particle systems has been due to Scarlett (35,36). The particles (and the voids around them) are viewed as a collection of filaments of measurable length and finite, but immeasurable, cross-sectional area. These random filaments can be regarded as the intercepts made by an arbitrary straight line drawn through a random section of the packing of the particles.



Section (See Figure 2.20(b))

FIGURE 2.20 (a)

The probability of a circle of diameter $2y$ appearing in a section of a packing of spheres of size $2x$

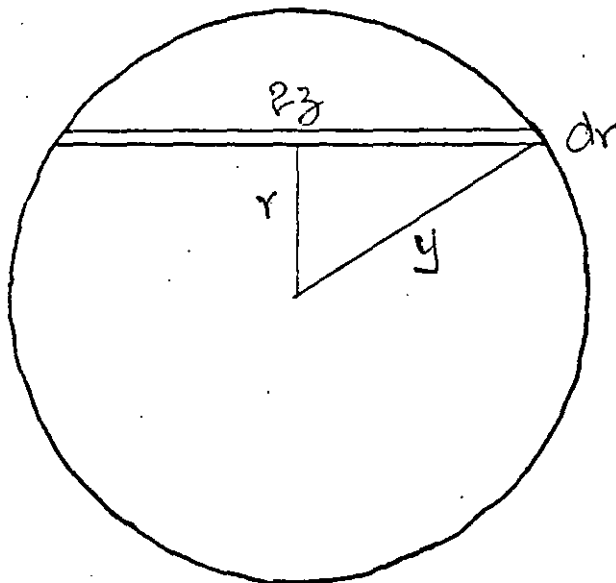


FIGURE 2.20 (b)

The probability of a chord of length $2z$ appearing in a circle of diameter $2y$.

The packing of the particles used in such a determination must be random and isotropic with regard to their location. Then the following relationships apply to the measurements made.

$$\text{Total number of filaments} = \int_0^{x_{\max}} f(x) dx$$

$$\text{Total length of filaments} = \int_0^{x_{\max}} x \cdot f(x) dx$$

Where $f(x) dx$ is the number of filaments with size between x and $x+dx$.

If the number of void filaments between the lengths z and dz were $g(z) dz$ then,

$$\frac{1 - e}{e} = \frac{\int_0^{x_{\max}} x \cdot f(x) dx}{\int_0^{z_{\max}} z \cdot g(z) dz}$$

Where e is the porosity of the system.

$$\text{Since } \int_0^{x_{\max}} f(x) dx = \int_0^{z_{\max}} g(z) dz$$

$$\frac{1 - e}{e} = \frac{\bar{x}}{\bar{z}}$$

Where \bar{x} and \bar{z} are mean lengths.

If any one of these filaments were to be divided randomly at all points along their length the distribution obtained would be the same as the distribution of the sectioned chords shown in Figure 3.3. Mathematically, if y is the length of the chord produced by such a section, then the probability of y is,

$$p(y) = 1 \quad \text{if } 0 < y < x$$

$$\text{and } p(y) = 0 \quad \text{if } y > x$$

If the distribution of such chords is represented by $h(y) dy$

$$h(y) dy = \int_{x=y}^{x=x_{\max}} f(x) dx \cdot dy$$

Which is the cumulative oversize distribution of the random filaments.

With spheres it is possible to derive a large number of relationships but these are of very limited application. (13,32). This is due to the definite, symmetrical shape of the sphere, which makes the application of statistical theory very easy. As an illustration of this two examples of how the filament size distribution can be obtained from particle size and vice versa can be found in references 35 and 13 respectively.

A more interesting feature of the filament size distribution is however the fact that the sectioned filament distribution (defined earlier), is identical to the distribution of sectioned chords when the chords are all drawn through a point in a section plane of a particle and this same point is regarded as the point of section (this is illustrated in Figure 3.3(c)). It has been demonstrated by Scarlett (15) that this is so, but it is quite easy to visualise. If in Figure 3.3 (b), we take any point on a random filament, it sections the filament. If that point corresponds to the point sectioning the chord in Figure 3.3 (c), then it is possible to see that if the whole assembly were considered, every possible orientation of the chord would be encountered in the measurement of the filaments and each filament would be sectioned in exactly the same way that the chord would have been sectioned.

It is customary to represent size distributions or filament distributions in graphical form. As explained, the number of sizes between size class x and the size class $x+dx$ is $f(x)dx$ or a similar function. A graphical distribution can be either a frequency vs size type or a cumulative frequency vs size type. The first type consists of plotting $f(x)$ as the ordinate against x as the abscissa, while the second uses a plot of $\int_0^x f(x)dx / \int_0^{\max} f(x)dx$ as the ordinate vs. x as the abscissa. An illustration of a curve of the first type is seen in Figure 2.22 and of the second in Figure 2.21. Since areas and volumes are proportional to diameters, it is also possible to plot volume-size and area-size curves, from this information if certain other parameters were known.

As far as this research is concerned, interest is centred on the

cumulative frequency curves. These curves contain valuable statistical information. For instance, if one wished to determine the most probable size one would encounter if a random selection were made from a packing of particles, then it is obvious that the gradient of this curve would show a maximum at the point required. Thus if the axis containing the ordinate were divided into a number of equal parts and any number, between 0 and the number of parts the axis were divided into, were chosen at random, then, if the size corresponding to that number were determined from the curve, then this selection would have been at random with the characteristics of the system taken into account. The significance of this selection is made clearer in sub-section 2.6 where Monte Carlo methods are described, and also in sub-section 3.3. More information on particle statistics is given in a book by Herdan (76) as well as in the number of papers referred to here.

The most important development recently has been the progress in the sizing techniques. For our purposes two of the parameters have been selected, the Feret diameter and the random filament distribution. Their use in building a model of a particle system is described in Section 3.

2.6 Monte Carlo methods

Monte Carlo methods is the term applied to what were formerly described as random or drunkards' walks. An excellent introduction to the basic techniques is given in a book by Hammersley and Handscomb (77). Monte Carlo methods deal with that branch of mathematics which is concerned with experiments with random numbers. The probabilistic type of Monte Carlo method involves the observation of random numbers chosen in such a manner that they simulate the physical random processes of the original problem and the inference of the desired solution from the behaviour of the chosen numbers. An example of the drunkards walk and many other applications of the Monte Carlo technique is given in a book by Chorafas (37). Consider Figure 2.22, the curves represent the lives of three components in an electronic system. The mean of such a system is given by

$$\bar{x} = \frac{\sum n_i X_i}{N}$$

where n_i is the frequency in the i th class and N the total number

On the other hand, if we wished to obtain the probability of obtaining a section OB of the Feret diameter starting from O perpendicular to the horizontal (Figure 3.3 (d)), and OB was of length y, then the probability of y is given by

$$P(y) dy = \frac{dy}{x} \quad \text{if } y < x$$

where x is the length of the Feret diameter. If $f(x) dx$ represents the density of the Feret diameters Then the distribution of y, $g(y) dy$ is given by

$$g(y) dy = \int_{x=y}^{x=x \text{ max}} \frac{f(x)}{x} \cdot dx \cdot dy$$

which can again be obtained from the density distribution of the Feret diameters.

in all classes. If the frequency distribution is represented by $f(x)dx$ then,

$$\bar{x} = \frac{\int_0^x xf(x)dx}{\int_0^{x_{\max}} f(x)dx}$$

The standard deviation of this distribution is the root mean square deviation and is given by

$$s = \sqrt{\frac{\sum (x_i - \bar{x})^2 n_i}{N}}$$

For the three curves in Figure 2.22 these values are

$\bar{x}_1=40$	$s_1=8$
$\bar{x}_2=65$	$s_2=12$
$\bar{x}_3=80$	$s_3=12$

Assume that parts belonging to these three populations are selected at random on the assembly line. By the use of the Monte Carlo method we can simulate this random selection and compute the anticipated life of the system. Fundamentally, there are two approaches to the problem. If cumulative curves are plotted of the distributions (Figure 2.23) and the vertical axis divided into n equal intervals and then a table of random numbers is used, it would be possible to locate a random ordinate and using the curve to find the corresponding abscissa or the hours of life of the component. This can be repeated until sufficient values have been taken for the three systems to get the distribution function for the life of the system. The second approach is not relevant to this research but is to be found in reference 37. Although the example quoted has little relevance to the problem being dealt with here, the technique is exactly the same.

2.7 Deformation and crushing of particles

It was decided to include this section in the literature survey because the many references made in the text to the possibility of extending the application of the proposed model, need justification in fact. A number of statistical parameters used here will change if the particles in the system are deformed and some of the assumptions made here will be invalidated. It must be stressed that there is insufficient current information on a number of points to make the further development of the model a possibility, but there is every

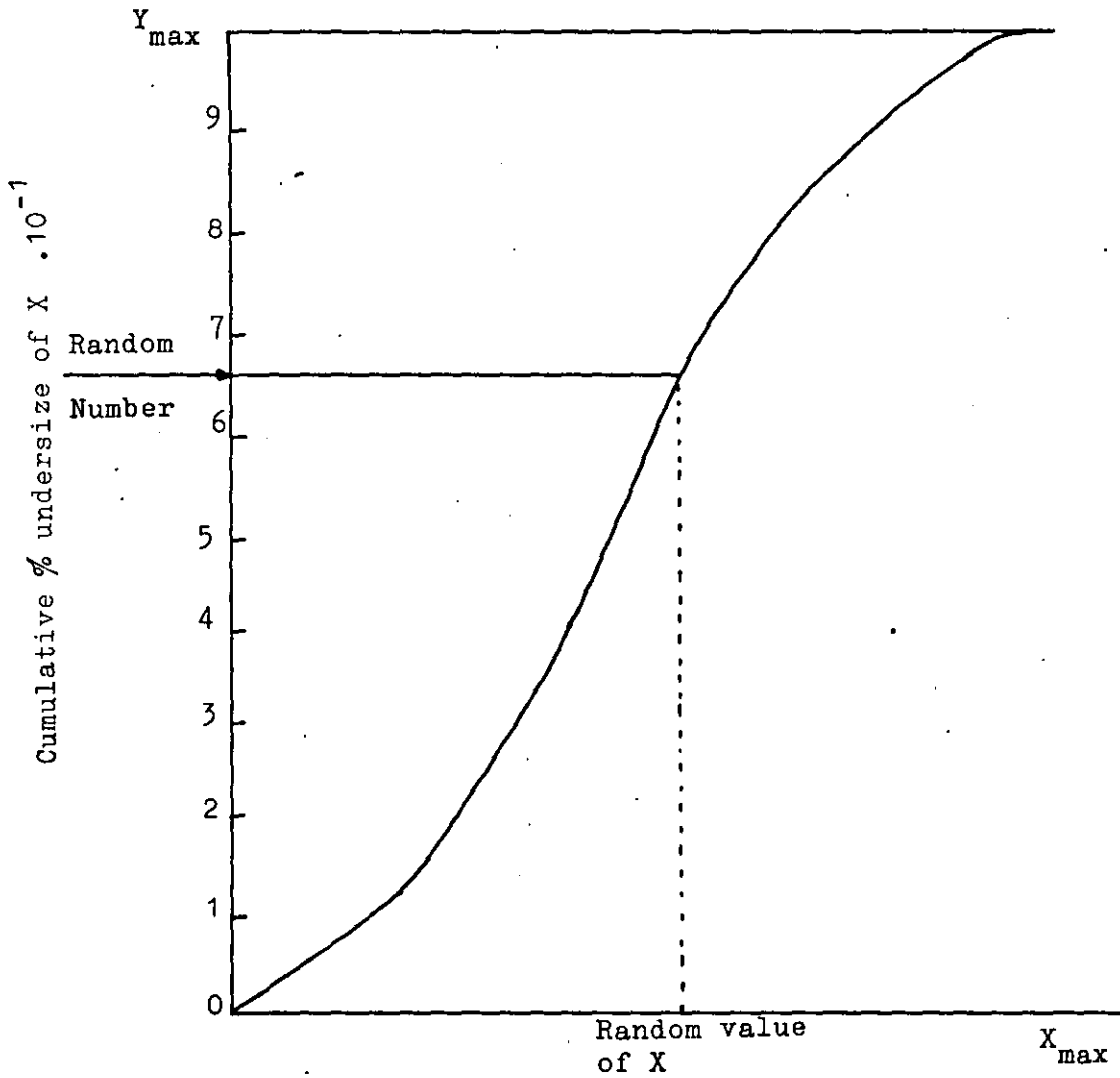


FIGURE 2.21

The random selection of values from a cumulative frequency curve

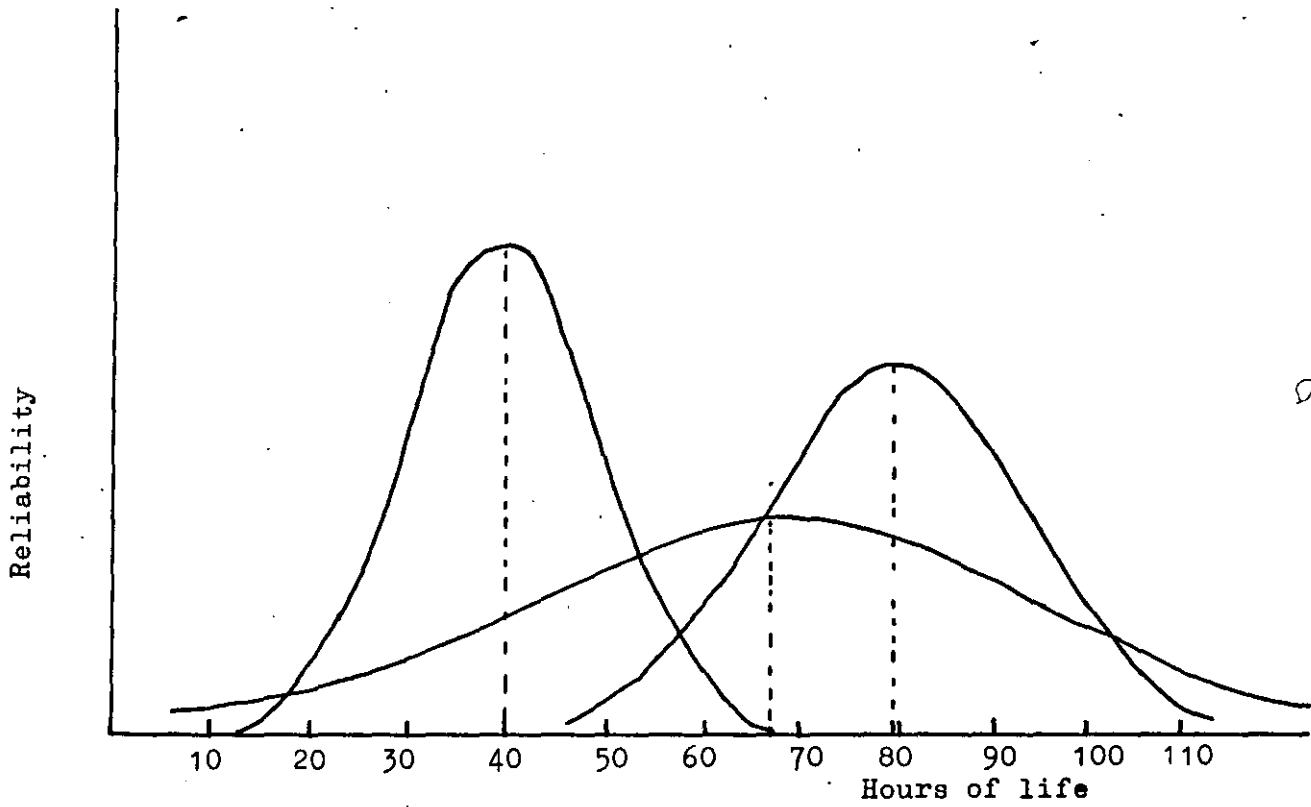


FIGURE 2.22

The hours of life of three components in an electronic system

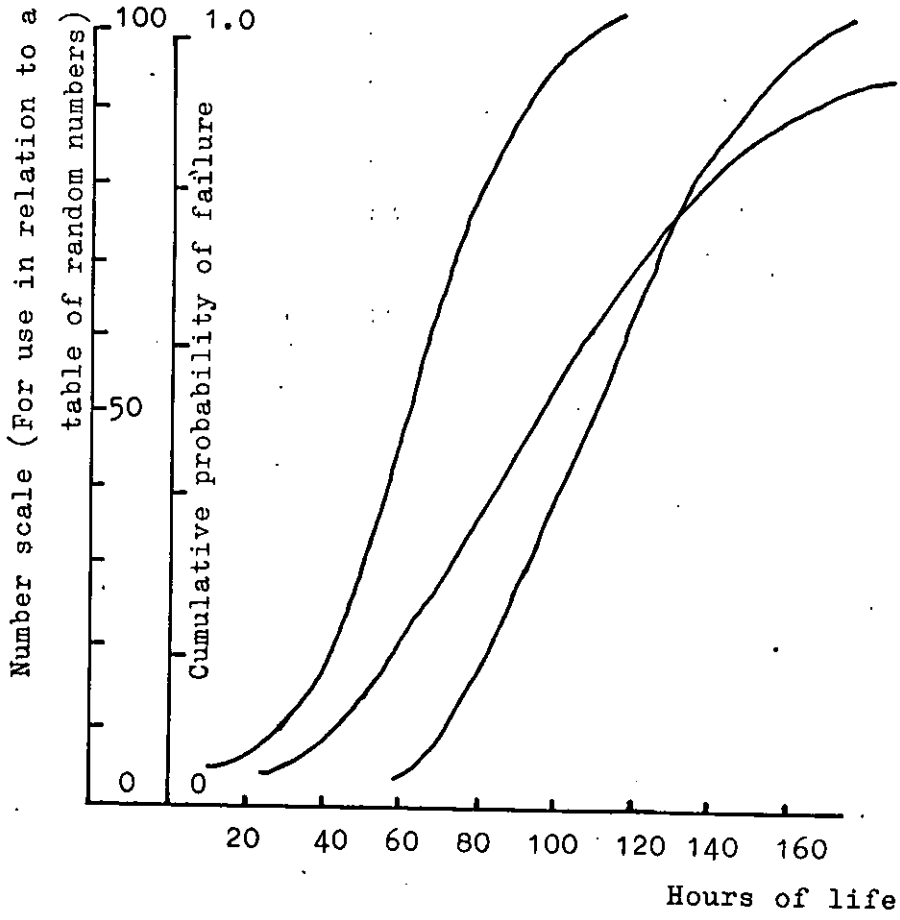


FIGURE 2.23

The hours of life expressed as cumulative undersize curves

possibility that this information is likely to be available in the near future.

One particular shortcoming of the model is its inability to predict the strength of compacts. Since this is dependant on the nature of the contact surfaces and the extent of contact, it would be impossible to make any predictions about strength until more was known about these quantities. The theories of Hertz (78) regarding the elastic deformation of bodies is of academic interest only, due to the fact that in real systems most of the deformations obtained are plastic, even at very low loads. Ishlinsky has developed a theory dealing with plastic deformation (79). Deresiewicz (80), Mindlin (81) and others have also written a large number of papers on the subject. So far it has been difficult to apply their results to particulate systems which have stress distribution within them. It is hoped that this model might, in time, overcome this problem.

A recent analysis of the plastic deformation of spheres and cylinders has been done by Johnson (83). He measured the surface strains and deduced the contact stresses using the flow rules of plastic theory. He points out that a layer in the contact surface is left in a state of residual tension when the surface is unloaded. The stresses in this layer are said to be between 0.56 and 1.0 times the yield stress. The material at the contact point, flows outwards during the compression, even in the presence of friction.

The solution of bulk deformation problems which occur in particle systems has yet to be attempted, but there seems to be an interest being currently shown in the problem. The application of tensor calculus and numerical analysis could conceivably give acceptable results in the near future. Experimental analyses of the crushing of single particles, which are likely to be of greater use than information obtained on a macroscopic scale, have been going on for some time in Germany. A report by Leschonski (84) describes these investigations. Schönert (85) has already published a model which takes into account the variable intensities of stress. As Rumpf (86) has pointed out, it is possible to calculate the output of a controlled grinding process, if enough data relating to materials under differing conditions of stress can be determined. It is these

determinations that can be made with controlled crushing experiments. It seems therefore that if the model proposed here can in fact predict the stress in the various parts of the system, then from the information obtainable from the controlled crushing experiments it would be possible to predict the behaviour of a particle at any point within the system.

The variables listed by Leschonski as being important in the experiments on controlled crushing might be recounted here as it seems likely that they will be just as important in compaction.

- a) Kind of material.
- b) The size of the particles.
Since the strength of individual particles increases with decreasing size due to the elimination of flaws, this is an important variable.
- c) The shape of particles
The state of tension developed by a particle depends on its shape in relation to the geometry of the compaction system.
- d) The history of the particles
- e) The stress intensity
- f) The velocity with which the stress is applied
- g) The rate of shear
- h) The system geometry
- i) The properties of the particle surfaces.
- j) The temperature
- k) The surrounding medium

Thus to be useful, any results obtained by these experiments must be performed with these variables carefully controlled.

2.8 Conclusion

In the preceding pages an attempt has been made to recall and correlate all the work done in recent years which have any relevance to the building of a model of a particle system, with a view to predicting the stress distributions obtained when the system, confined in a restricted space, is subject to an applied pressure. Since there is a vast quantity of information available on powder compaction it was necessary only to include here the most representative of these.

SECTION 3.

THEORY

- 3.1 Introduction to theory
- 3.2 The general conditions of equilibrium
- 3.3 The use of statistics and the application
of the Monte Carlo method
- 3.4 System description
- 3.5 Friction
- 3.6 Computer models
- 3.7 Extension to non-symmetrical systems

3.1 Introduction to the theory

In the preceding section much of the work of other investigators relevant to the building of a model, which may be used in the evaluation of particulate systems, has been recounted. It has been generally recognised that stress transmission in particulate systems takes place through those points at which the particles contact one another. Unlike liquid systems particles have the property of being able to support shear. Consequently any force applied to one surface of such an assembly is not transmitted uniformly through the system. The degree of non-uniformity depends on the restrictions imposed on the system and other parameters connected with the particles themselves.

It is relatively easy to derive, mathematically, parameters to describe or simulate Systems of Spheres. This has been undertaken here to illustrate the principles on which the model is based. With irregularly shaped particles, however, statistical parameters are not easy to determine and approximations have to be used. The statistics of particle systems has been the subject of much recent research, and the papers by Rumpf and Debbas(32), Bockstiegel(13), Scarlett(35, 36, 75), Todd(70), Eastham(71) and others illustrate how particle statistics may be applied in the evaluation of particulate assemblies.

In considering the application of force to particle systems, the force is transmitted, initially, while the particles move and rearrange themselves. This aspect of the process is not dealt with in the model presented here. At any stage of the pressure application, however, it is possible to hold the pressure constant and to let the system develop an equilibrium state and it is with this condition that the model has been constructed to evaluate.

The factors affecting the stress picture within the system are

- a) The particle characteristics
- b) The physical properties of the material of the particles
- c) The friction characteristics of the particles and the system
- d) The nature of the system

The model developed here takes these parameters into account in the prediction of the stress pattern set up within the system.

There are three distinct types of particles which must be dealt with. The simplest is the spherical shape which can be handled mathematically with relative ease, the second the irregular, but convex, particle which, although possible to handle needed special methods of characterisation (which have been developed here) and thirdly the completely irregular particle whose statistical definition has not been possible.

3.2 The general conditions of equilibrium

Any force, \vec{P} , acting at any point O' in space can be replaced by three forces P_x, P_y, P_z , at another point O , such that P_x, P_y, P_z are mutually perpendicular and such that $(P_x^2 + P_y^2 + P_z^2)^{\frac{1}{2}} = P$, and by three couples $(zP_x - xP_z), (yP_z - zP_y)$ and $(xP_y - yP_x)$ about the axes along which P_x, P_y, P_z act. Similarly all forces in Cartesian space (See Figure 3.1) can be replaced by similar forces and couples about the same axes at O . Then for equilibrium the following conditions must be satisfied.

1. $\sum P_x = 0$
2. $\sum P_y = 0$
3. $\sum P_z = 0$
4. $\sum M_x = \sum (yP_z - zP_y) = 0$
5. $\sum M_y = \sum (zP_x - xP_z) = 0$
6. $\sum M_z = \sum (xP_y - yP_x) = 0$

Applying these conditions it is possible to calculate six unknown quantities appearing in a force balance performed on any body at rest and it will be explained in the following sections how these conditions are used in simulating the transmission of a force through a system of particles.

3.3 The use of statistics and the application of the Monte Carlo method to the solution of the problem

3.3.1 The sphere model

Consider first, the model representing a system of mono-size spheres (Figure 3.2). The probability of one particle being contacted by another at any point on its surface, located by the angles α and β , and by the chord, length l , with respect to any other point on its surface is expressed by

$$P = 4r^2 \lambda \sin \alpha \sin \beta / 4\pi r^2$$

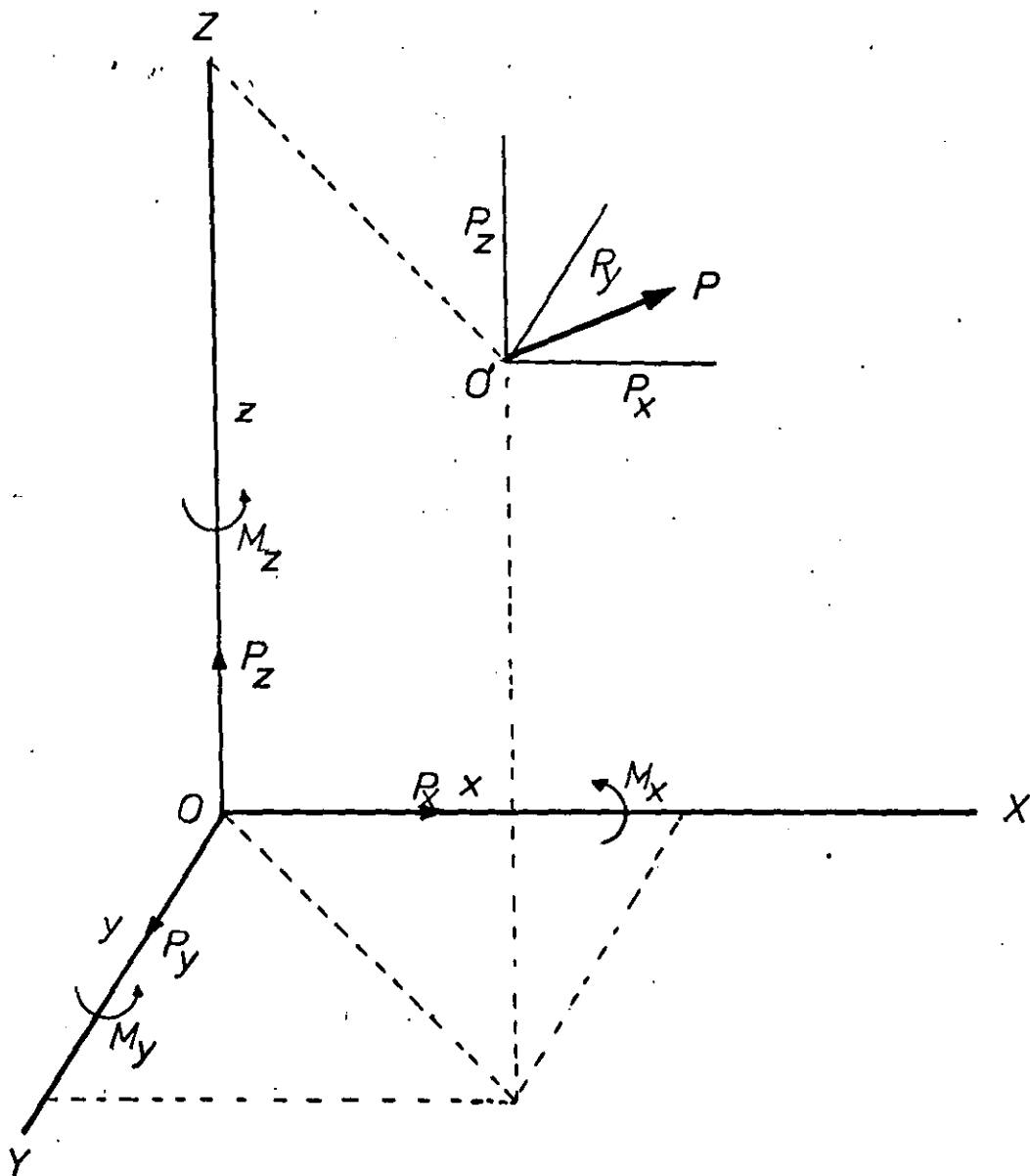


FIGURE 3.1

Representation of a force by three components
and three moments at a different point in space

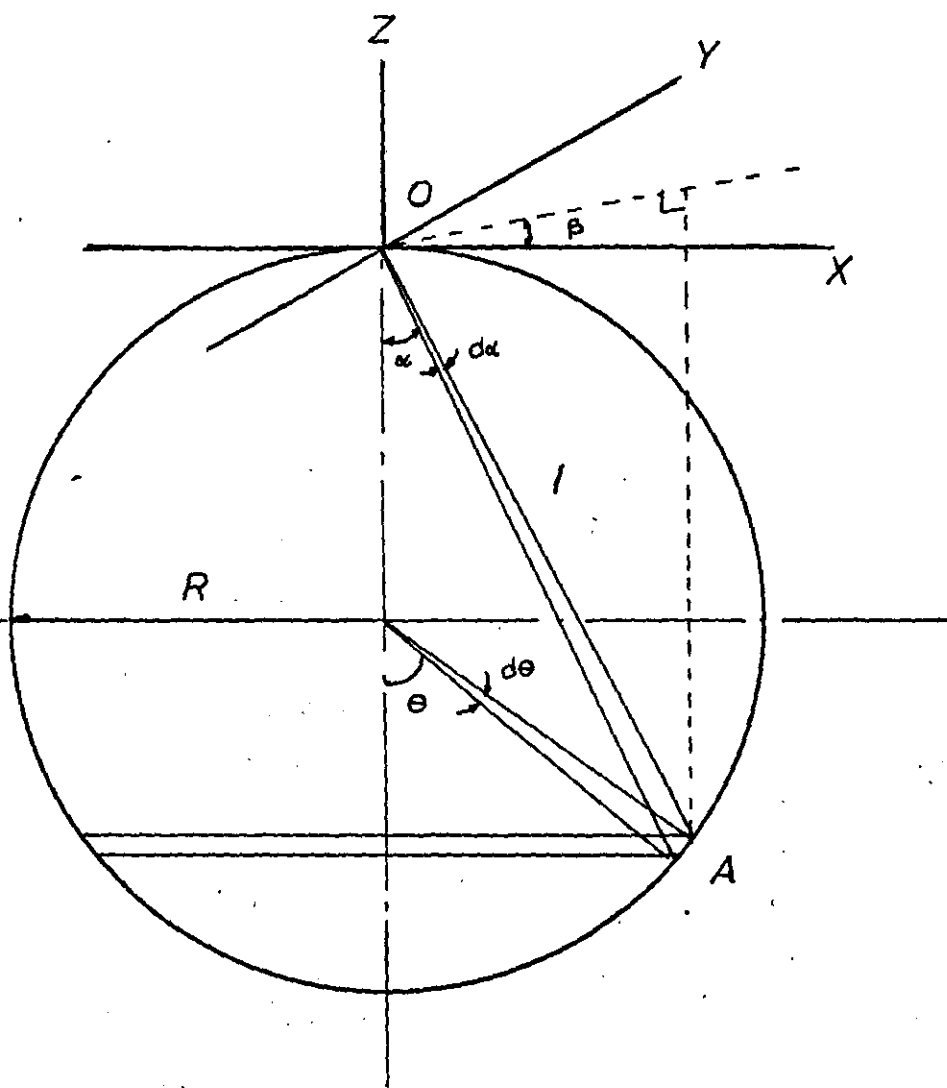


FIGURE 3.2
The probability of a contact on
the surface of a sphere

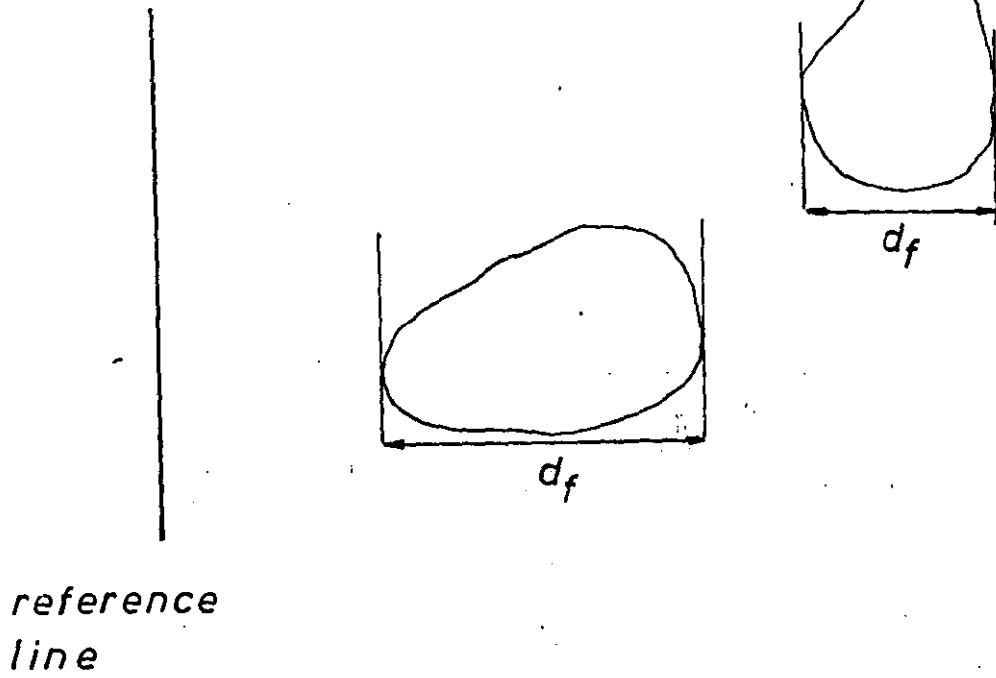
The probability distribution function (cumulative) for any contact is, therefore given by

$$\begin{aligned} F(p) dp &= \frac{\int_0^{\Theta} 2\pi r^2 \sin\theta d\theta}{\int_0^{\pi} 2\pi r^2 \sin\theta d\theta} \\ &= \frac{\cos\theta - 1}{-1} \\ &= 1 - \cos\theta \end{aligned}$$

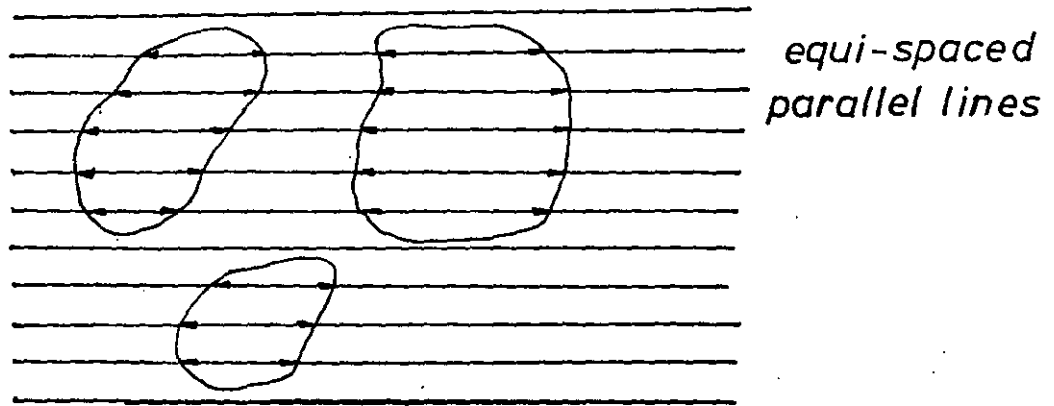
If we assume six contacts per sphere and three of these lie in positions where they can transmit force and two do not (the sixth being the point at which the force was applied); then we can proceed to build a model to which mathematical criteria for equilibrium can be applied. Although it is obvious that any system of mono-size spheres will have in it particles with many more than six contacts on average, the limitations of the mathematics used here pre-empt any consideration of such a case. This is due to the fact that in the case without friction the reactions at the points of contact are normal to the surface of the sphere, and are consequently concurrent, thus reducing the equations describing equilibrium to three.

To simplify the problem, the areas excluded by each successive contact to further contacts will not be considered. Since only three contacts have to be located by statistical means, it is proposed that it is reasonable to assume that the random location procedures used are highly unlikely to generate two points with identical coordinates in three attempts. The location of the contacts is found by using the probability distribution function, described earlier, and having found their coordinates it is then possible to apply the conditions of equilibrium to the particle and hence to determine the forces of reaction at the three points of contact.

That it is too complicated to trace every reaction force (henceforth called transmitted force) through the rest of the system is obvious, thus, at this point, use is made of the statistical advantages offered by the Monte Carlo technique. Since the three points of contact were chosen at random, if it was decided to follow the further transmission of any one of these forces, this decision would also be a random one. Provided therefore that the third (or first or second) point of contact were always chosen as the point from which further transmission of the force was to be followed then a statistically valid sampling technique would be used.

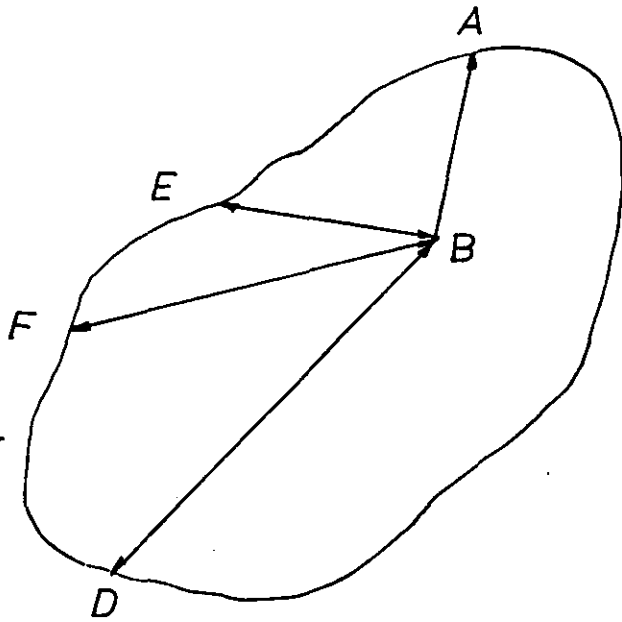


(a) Feret's diameters

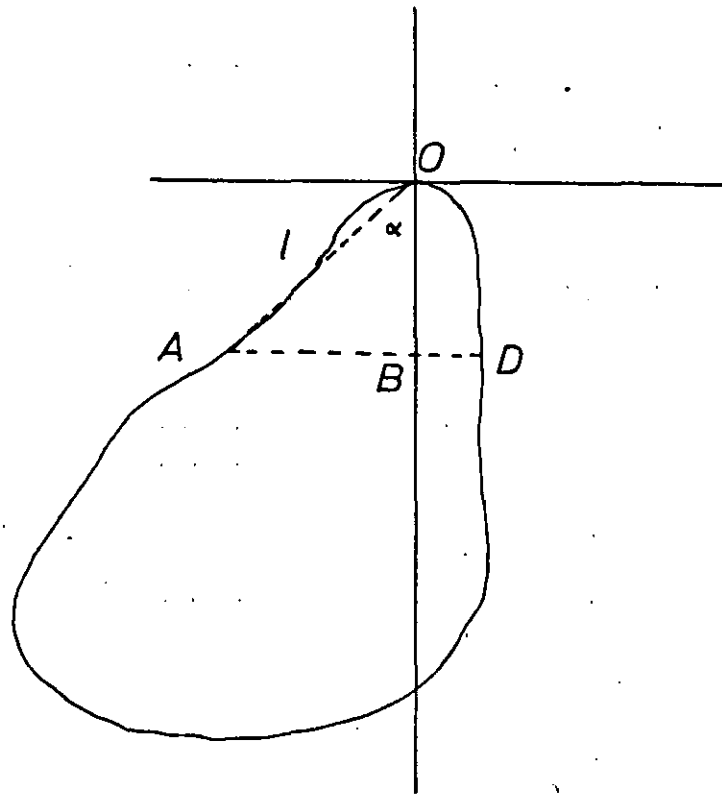


(b) Random filaments

FIGURE 3.3



(c) Sectioned random filaments



(d) α, l from particle characteristics

FIGURE 3.3

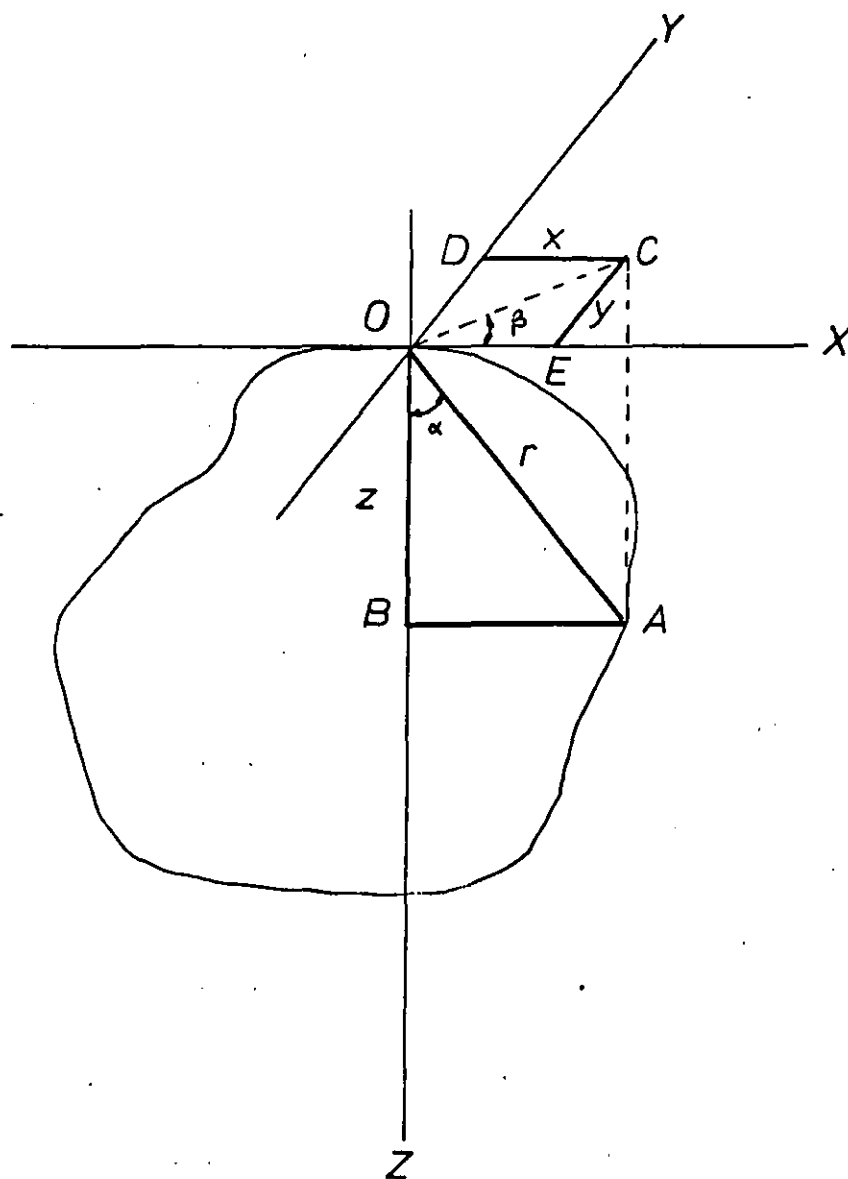


FIGURE 3.4

The coordinates of a point (Cartesian and cylinder)

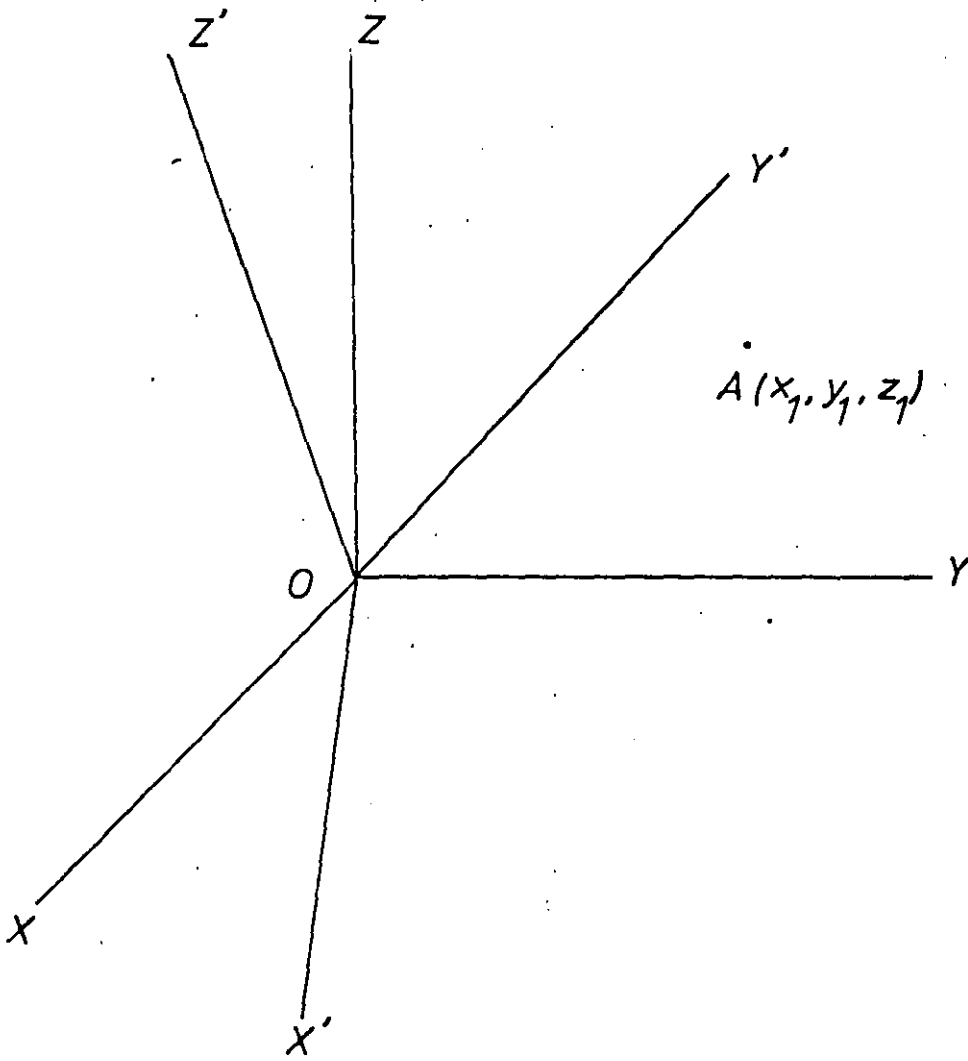


FIGURE 3.5

Rotation of axes (See also FIGURE 3.8)

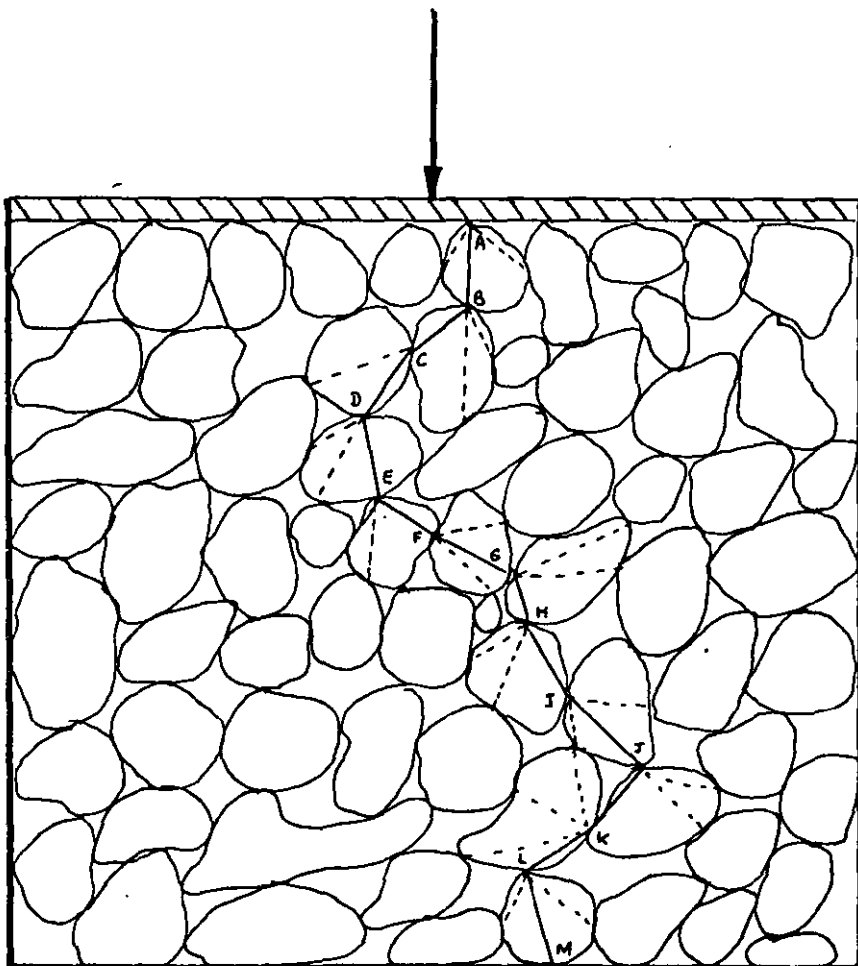


FIGURE 3.6

The transmission of a force through
a particulate system

The tracing of the output forces so obtained is carried out until a system boundary is reached. If this process is repeated a large number of times, then every possible path by which a force, applied to the surface of the system, could reach the system boundary, would have been evaluated (See Figure 3.6). At the boundary, the force is assumed to have been absorbed and no further transmission is considered. Now, if the total number of Monte Carlo runs is summed and normalised, by the balancing of the input and output forces (the forces said to have been 'absorbed' at the boundary), then the stress pattern within the system can be evaluated.

By the application of the Monte Carlo technique the effect of choosing only six contacts per sphere may be reduced, due to the fact that in making a fresh walk through the system, a different set of contacts is used for the first sphere. Thus in the final analysis, it can be assumed that a reasonable representation of all the force paths to the boundary has been obtained, and consequently, that although a physical representation of the system geometry has not been used, the simulation has been performed on a stochastic model of the system instead. How this is done is described in the following pages.

It is worth noting here, that if frictional effects between the particles themselves were considered, then it would be possible to consider up to twelve contacts for a sphere. (Six of which would be able to transmit force and five unable to do so with the sixth being the point at which the force is input). Unfortunately the variation of the coefficient of friction under these conditions is, as yet, inadequately understood and the resulting uncertainties caused by the consideration of friction between particles may far outweigh any advantage gained. In any case since the sphere model, alone, (which had been included for illustrative purposes only) is affected, it was decided not to pursue the matter further.

3.3.2 Extension to irregular particles

When irregular, frictionless particles are considered, because the resultant forces (even though they are still normal to the particle surface) are no longer concurrent, it is possible to use all six equations of equilibrium. This in turn enables the consideration of

upto six transmitting contacts.If we again assume this to mean a total of twelve contacts,then it is possible to say that we now have a reasonably representative system.

To illustrate what is meant by transmitting and non-transmitting contacts,consider a sphere with six contacts (Figure 3.7).If the force is input at the contact with sphere A,then it is obvious that, unless there is deformation,the transmission of the force is only possible through the contacts with spheres E,D and C.Thus these are referred to as transmitting contacts while the contacts with spheres F and B are referred to as non-transmitting contacts.If however the input force came in through F ,then A and E become the non-transmitting contacts.

3.3.3 The generation of the coordinates of the points of contact

How the points of contact are located on a sphere,using a random generation procedure has already been outlined.Unfortunately it is not possible to find the same exact mathematical definitons of the shapes and surfaces of irregular particles.Instead,however, a method by which the location of the contacts could again be picked with a similar basis in probability had to be devised. Since the systems encountered in everyday life are never mono-sized,the model proposed here deals with a mixture of sizes.The simulation of the force transmission is then performed on this a stochastic representation of the real system.

In Section 2.5 the significance of Feret diameter has been discussed. Consider Figure 3.3 (a).The Feret diameter is seen to be the largest dimension in the direction of measurement.If it is assumed that a contact may occur at any point on the surface of a particle with equal probability,then it should be possible to randomly intersect the Feret diameter with a plane perpendicular to it and say that a contact occurs at a point on the surface of the particle which is cut by this plane.(See Figure 3.3 (d)).If now, the sectioned view of the particle is examined it is possible to say that the Feret diameter cuts this plane at a point B.It has been proved by Scarlett(75) that the lengths of lines BA,BD,BC etc.,have the same distribution function as the sectioned random filaments (Figure 3.3 (b) and (c)).How this may be obtained from a distribution of random

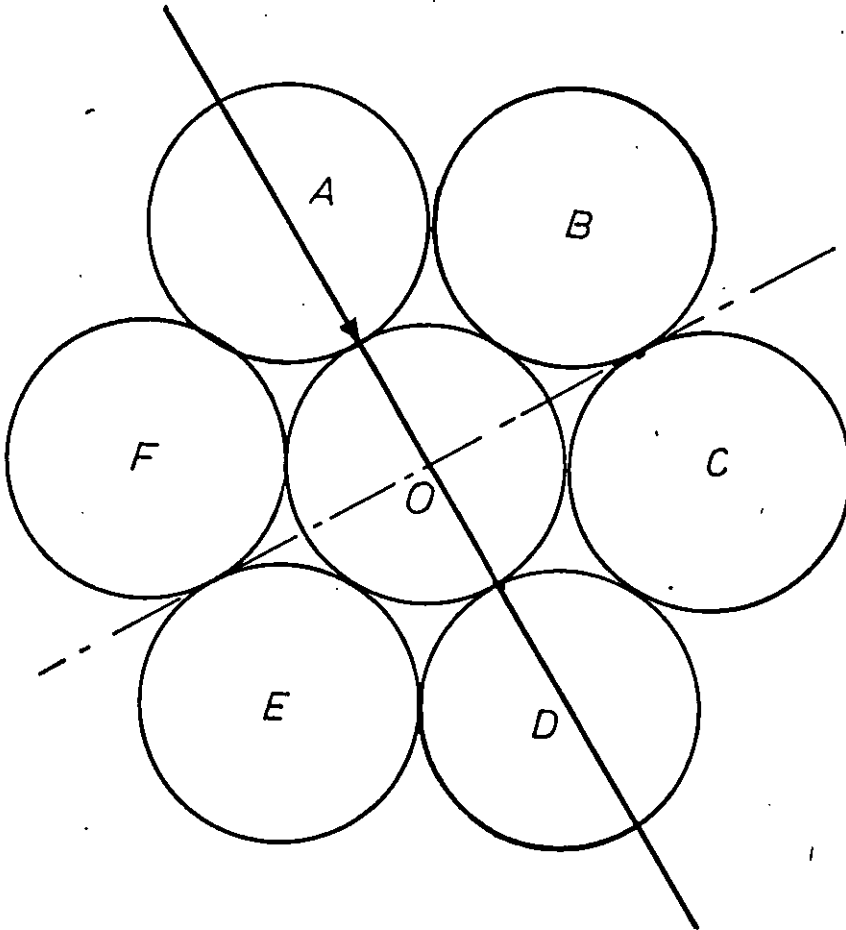


FIGURE 3.7

Transmitting and non-transmitting
contacts on a sphere

filaments has also been outlined in Section 2.5. Using the Monte Carlo technique, it is now possible to find two probable values for both OB and for one of the lengths such as BA , thus enabling us to determine α and OA . If now it is assumed that β is a uniformly distributed function, it is possible to find the polar coordinates of A , which is a point of contact. By similar means the other five points of contact may also be determined.

Now, it is necessary to find the angle that the normal at the surface at A makes with the direction in which the force was input. Since unlike in the case of spheres there is no rigorous mathematical law governing its value it was decided to assume a ^{uniform} normal distribution for these angles. Two angles are necessary to determine the direction of the normal and these are called θ and ϕ . Their exact physical significance will be defined later.

As in the case of the sphere model these generations are performed for each particle that the simulated path of the force passes through. The information obtained from the force balances and the positions of each particle involved in the transmission is then used in the determination of the stress diagram. How this is done is described in Section 3.6, together with the description of the computer programs prepared to perform the calculation.

3.4 System description

Polar, Cartesian and cylindrical coordinates have all been used at one stage or another of the calculation. Thus a brief explanation of their use seems desirable. The model uses a cylindrical system, as such systems are easier to analyse due to their being possessed of axial rotational symmetry. The use of such systems does not however detract from the generality of the approach ~~as is demonstrated in Section 3.7.~~

Consider Figure 3.4. The axes of the system are $X'OX$, $Y'OY$ and OZ .

If A is a point of contact

1. Its polar coordinates are OA, α, β
2. Its Cartesian coordinates are $OA \sin \alpha \cos \beta = OE,$
 $OA \sin \alpha \sin \beta = OD,$
 and $OA \cos \alpha = OB.$

3. Its cylindrical coordinates are OC and OB and β
 Thus in any one of three ways it is possible to locate the point
 A with respect to axes OX, OY, OZ .

The force paths to the system boundaries are followed by using these
 coordinates as follows:

As the transmission proceeds through the system, the coordinates
 of the points of contact are generated with respect to three
 mutually perpendicular axes which are normal and tangential to the
 surface at which the force is input. These axes may or may not be
 parallel to the axes of the system. Therefore to follow the transmis-
 sion of the force it is constantly necessary to refer back to the
 system axes and to transform coordinates obtained with respect to
 axes on the individual particles into coordinates which relate to
 them. This is essentially a problem involving the use of tensors.
 Consider Figure 3.5, the reference axes of the system are OX, OY, OZ
 and the axes of the particle are OX_1, OY_1, OZ_1 . The coordinates of A
 with respect to OX_1 etc are x_1, y_1, z_1 . In order to obtain the coordi-
 nates of A with respect to OX etc. we use the following relations.

$$\begin{aligned}x &= \lambda_{11} x_1 + \lambda_{12} y_1 + \lambda_{13} z_1 \\y &= \lambda_{21} x_1 + \lambda_{22} y_1 + \lambda_{23} z_1 \\z &= \lambda_{31} x_1 + \lambda_{32} y_1 + \lambda_{33} z_1\end{aligned}$$

where

$$\begin{aligned}\lambda_{11} &= \cos XOX_1 \\ \lambda_{21} &= \cos YOX_1 \\ \lambda_{12} &= \cos XOY_1 \quad \text{etc.}\end{aligned}$$

In order to simplify the problem, it was decided to always keep one
 axis in the system XY plane, thus there are only two rotations to
 consider when transforming coordinates from one set of axes to
 another. Thus to transform the particle axes into the system axes
 (Figure 3.8) it is necessary to rotate OX, OY in the XY plane
 through an angle ψ about OZ , and then to rotate the OX_1, OZ axes
 through an angle γ about OY_1 . This ensures that the OY_1 axis always
 remains in the same plane, regardless of the position of the particle.
 Now if the OX_2, OY_2, OZ_2 axes had a point A located with respect to
 themselves by the coordinates x_2, y_2, z_2 then the coordinates of A

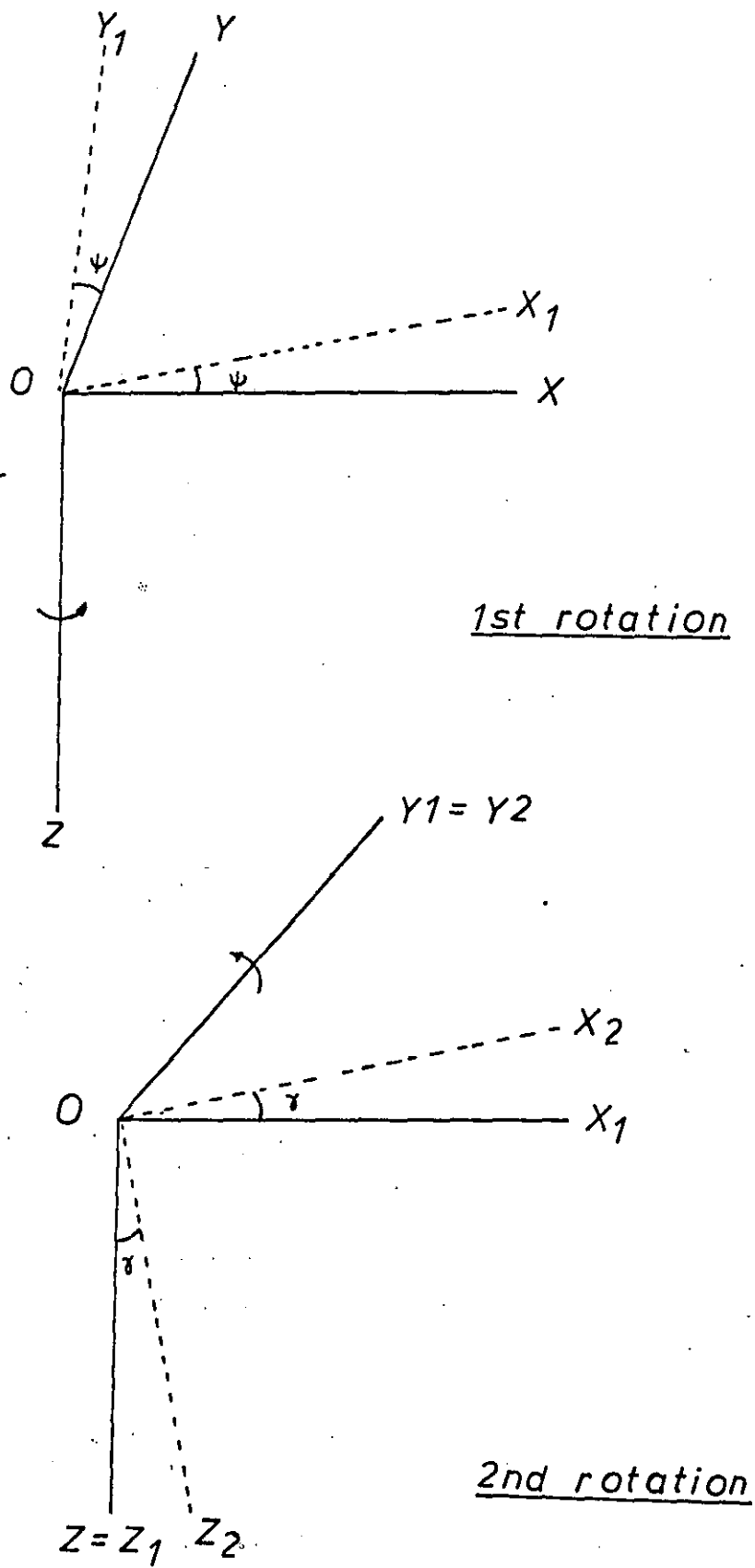
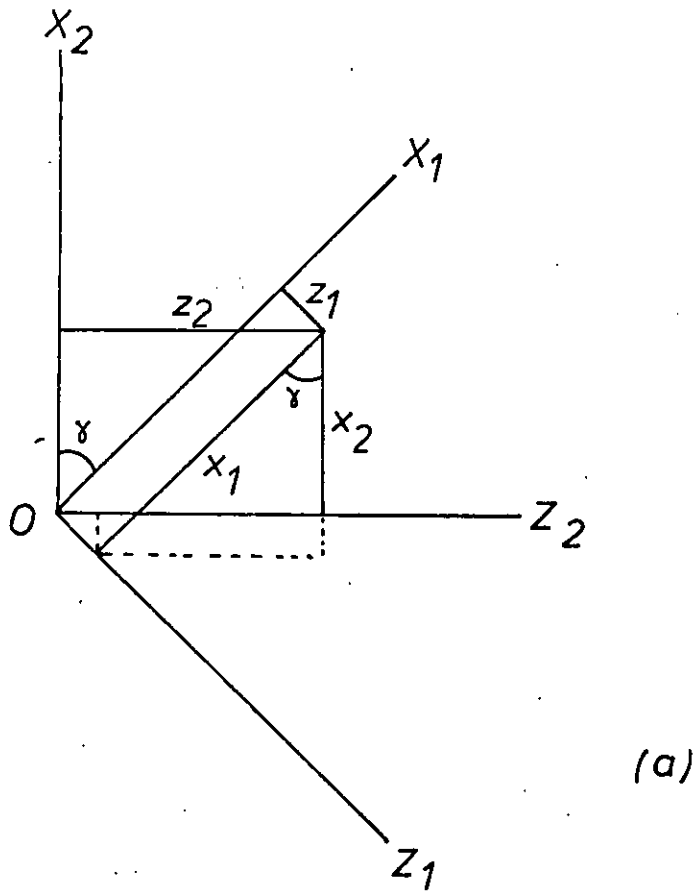
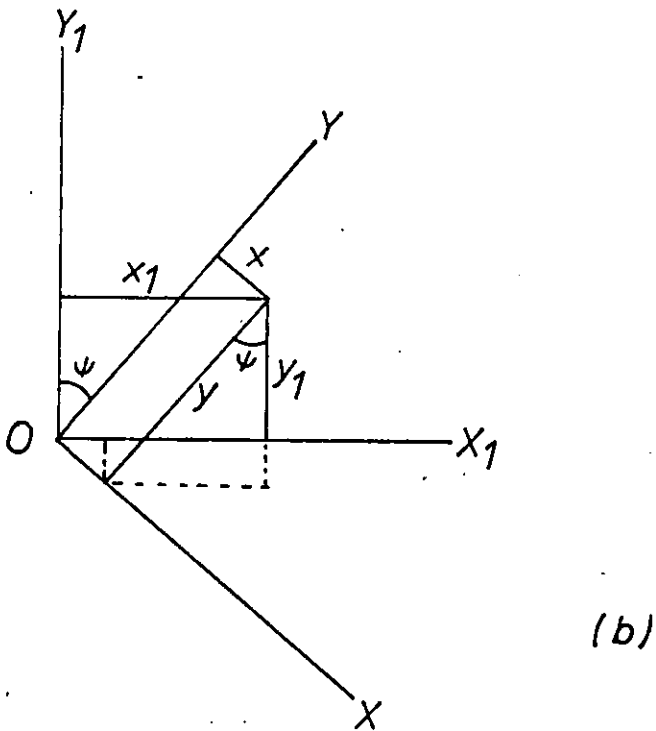


FIGURE 3.8

Rotation of axes



(a)



(b)

FIGURE 3.9

Rotation of axes

with respect to OX, OY, OZ can be determined as follows. First the rotation of the OX_2, OZ_2 axes about OY_2 . The coordinates of A with respect to OX_1, OZ_1 are

$$\begin{aligned}x_1 &= x_2 \cos \gamma + z_2 \sin \gamma \\z_1 &= -x_2 \sin \gamma + z_2 \cos \gamma \\(y_1 &= y_2)\end{aligned}$$

An illustration of the rotation is given in Figure 3.9 (a).

Consider next the Figure 3.9 (b). The coordinates of A with respect to OX, OY, OZ are now given by

$$\begin{aligned}x &= x_1 \cos \psi - y_1 \sin \psi \\y &= x_1 \sin \psi - y_1 \cos \psi \\(z &= z_1)\end{aligned}$$

from which

$$\begin{aligned}x &= x_2 \cos \gamma \cos \psi - y_2 \sin \psi + z_2 \sin \gamma \cos \psi \\y &= x_2 \cos \gamma \sin \psi + y_2 \cos \psi + z_2 \sin \gamma \sin \psi \\z &= -x_2 \sin \gamma + z_2 \cos \gamma\end{aligned}$$

If the axes with respect to the particle were taken at a point O_1 whose coordinates with respect to OX, OY, OZ were X, Y, Z then the coordinates of A would simply be $(X + x), (Y + y), (Z + z)$.

To conclude this part of Section 3 it is proposed to give a brief account of how γ and ψ can be determined. In order to locate a contact it has been mentioned that two angles are necessary these were α and β . Similarly in order to find the direction of the output forces two angles θ and ϕ were used as a description of the surface at the point of contact. It is then possible at any point to find γ and ψ by simply taking a point on the normal at any point of contact and calculating its coordinates with respect to a set of axes parallel to the system axes at the point of contact. If the coordinates are x, y, z then,

$$\gamma = \tan^{-1} \left(\left(x^2 + y^2 \right)^{\frac{1}{2}} / z \right)$$

and

$$\psi = \tan^{-1} (y / x)$$

In order to describe completely the whole of three dimensional space γ is allowed to vary between 0 and 2π and ψ to vary between $+\pi/2$ and $-\pi/2$. The decision to choose these intervals is related

to the use of the model on a computer.

3.5 Friction

As has been stressed in the literature survey section, there are three types of friction in powder compaction

1. Particle-Wall friction
2. Particle-Particle friction
3. Wall-Punch friction

Of these, only the first is considered to be relevant in any calculation. The others have been ignored because the evidence provided by the many experimenters in the field indicate that these other forms have a negligible effect on the system properties. Another but less valid reason for ignoring the effects of the other two types of friction, is the lack of knowledge of the coefficient of friction under these conditions. As far as this model is concerned the effect of the wall friction can be allowed for in the process of normalising the results from the Monte Carlo runs, and is therefore described in the next part of this section. In passing, it may be of interest to point out that, there is evidence to believe that it may be possible to determine the angle of internal friction from the particle characteristics, and thus it would be possible to determine the exact values of the coefficient of friction at the wall in a powder compact.

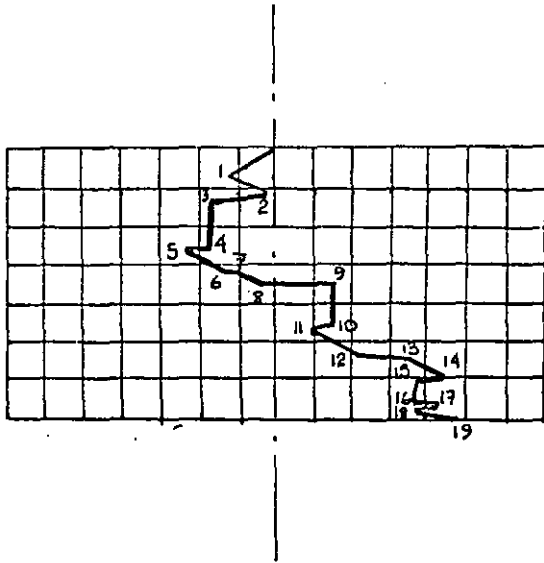
3.6 Computer models

In any form of mathematical model building, it is necessary to determine those parameters which are absolutely necessary to the solution of the problem and to eliminate those that are not, otherwise all the advantages gained from the representation of the system by a model would be lost in the determination of a welter of irrelevant properties. On the other hand it is necessary to retain and use all the relevant parameters. In systems as complex as those encountered in particle technology such decisions are even more difficult to make and even having made them, the derivation of relationships between the measurable quantities and the parameters relating to the model may prove impossible, as has been the case with the completely irregular particles. There is however, a need to make some reasonable assumptions and to make a start, at this stage, in order that in the reasonably near future a usable model might emerge. The final forms of the models used are given in Appendix 3.2.

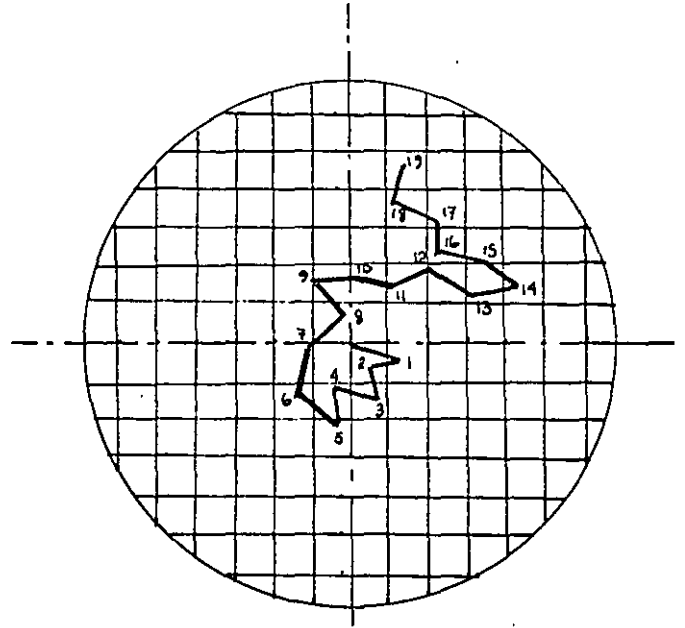
3.6.1 The Monte Carlo Model

The model was developed along the lines of the theory presented earlier. The assumption, made for spheres, that only six contacts actually transmit force, although up to twelve may exist was also extended to the model, which was however constructed for all convex particles. The model uses statistical methods to predict the points of contact, and several random walks of a 'quantum' of force is traced through the system. When the 'quantum' reaches an arbitrary, pre-designated, boundary, it is assumed to be absorbed. Since the process of simulating these 'walks' requires considerable computer time, and since at least 500 such walks are required to obtain even a reasonably representative picture, it was not thought desirable to repeat the process for each and every system that needed investigation. Thus the Monte Carlo walks were performed on one large system and all smaller systems could be evaluated using these results. The method of labelling the 'quanta' as they travel through the system is detailed in Appendix 3.2. The program which develops the model is shown in Appendix 3.1 together with brief comments and a flow diagram. The program that labels the force 'quanta' as they are propagated through the system is shown and discussed in Appendix 3.2 also.

In order to keep the number of simulations low, while still obtaining a representative result, it is of advantage to deal only with cylindrical (axi-symmetric) systems. In such systems all the forces can be represented by two components in the r and z directions. (Figure 3.10 (a) and (b) and 3.11). Further all the walks may be regarded as occurring in the r - z plane, thus increasing the walk density and the representability.



(a) A random walk (r-z plane)



(b) A random walk (r- plane)

FIGURE 3.10

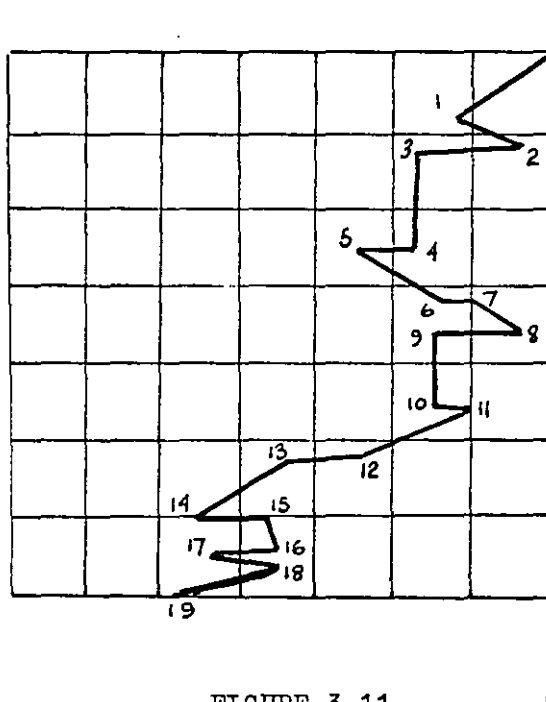


FIGURE 3.11

The representation of a three dimensional random walk on a two dimensional grid

3.6.2 Normalisation of the Force Diagram

The forces as traced and labelled above give effectively a picture of the distribution of the forces within the selected system. Due, however, to the fact that not all possible force paths have been simulated, the force diagram so-obtained must be normalised. The program shown in Appendix 3.2 does this also, the method being as follows. The only force applied to the system is that acting upon the original particle at the surface. No matter which sub-system we consider all forces leaving the boundaries of the sub-system must be equal to that input force. For example, consider the six force paths in Figure 3.12: if one considers the system AEMO, the input force at O must be equal to the total recorded forces at the boundaries AE and ME minus those (for example, the force 4) which have been recorded twice. Thus using the notation of Appendix 3.2, the total force at the boundaries of system OAEM are

- 1) $F(i,1,1,1)$ $i=1,2$
- 2) $F(i,1,1,1)$ $i=1,2$
- 3) $F(i,1,1,1)$ $i=1,2$
- 4) $F(i,1,2,1), F(i,1,1,1), F(i,1,1,2)$ $i=1,2$
- 5) $F(i,1,1,1)$ $i=1,2$
- 6) $F(i,1,2,1)$ $i=1,2$

or the total z-component is

$$5F(2,1,1,1) + 2F(2,1,2,1) - F(2,1,1,2)$$

which may then be compared with the total z-component of the input force at O. If the simulation was an absolute representation of the force paths, the two quantities would be equal, but since it is not their ratio can be used to normalise all the other forces within this system. This procedure is repeated for all possible sub-systems.

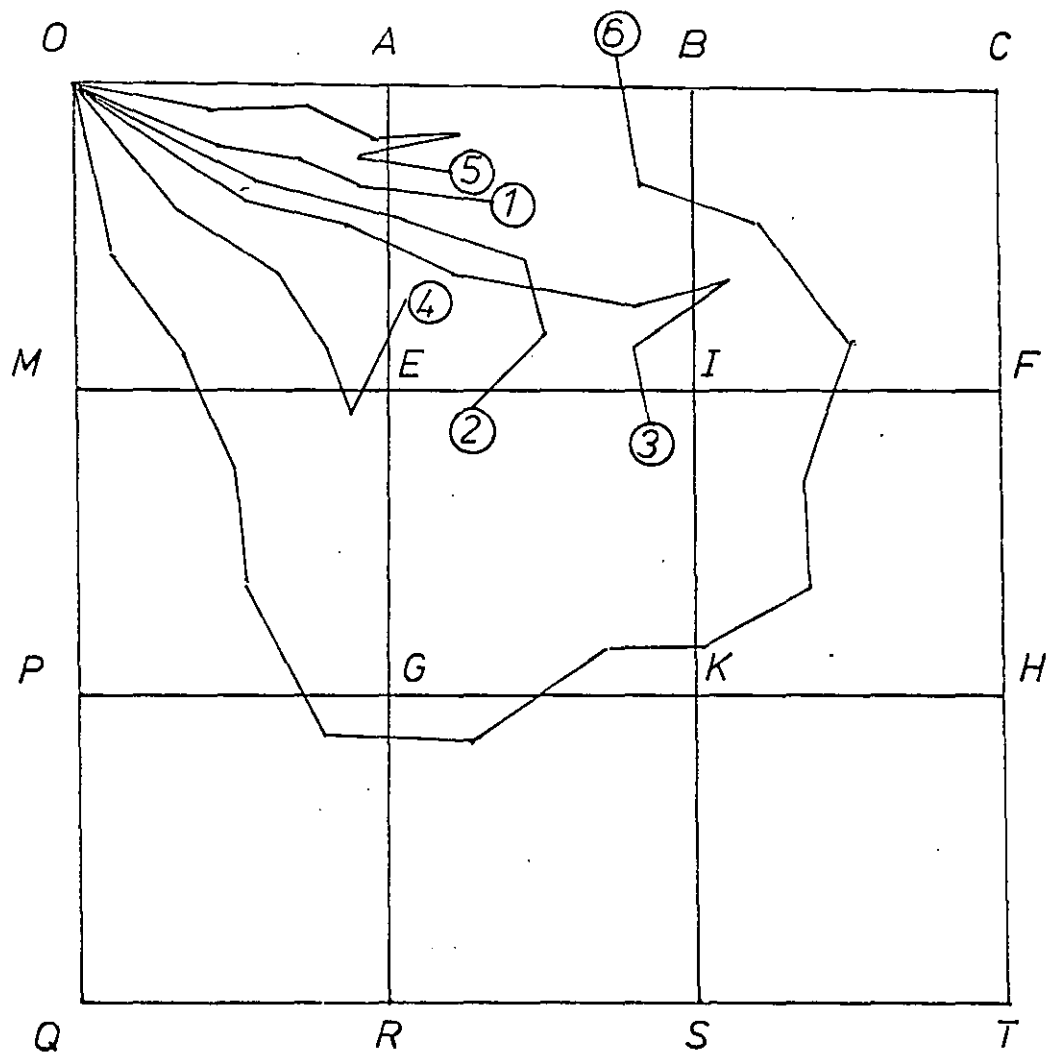


FIGURE 3.12

Sub-division of a large system
by grid lines

This procedure leads to the 'force diagram', which is a pictorial representation of the force distribution in the system. The forces crossing the grid lines AE, EG, BI etc. and the lines ME, EI, PG etc. are thus evaluated. The r-components of the forces crossing the vertical lines and the z-components of the forces crossing the horizontal grid lines are pressure forces while the r-components crossing the horizontal and the z-components crossing the vertical lines are shear forces. Thus by making the squares on the grid small enough it is possible to obtain a representation of the distribution of pressure in the system, as well as the order of magnitude of the shear on the various planes.

3.6.3 Total Particles on the Surface

What has been dealt with so far has been the force transmitted in the bed due to one surface particle. Obviously it is not possible, for reasons of economy, to repeat the simulation for each and every particle on the surface; fortunately it is not necessary either. All one needs is a distance distribution of the particles on the surface from all points at which the pressure and/or shear is to be determined. Appendix 3.3 shows how the position of the surface particles are computed and how the position distribution is calculated. In order to do this an assumption is made that the spatial distribution of particles on the surface is uniform and use is made of the value of voidage calculated from experimental work. Once the distance distribution of the surface particles is known, a reference to the force diagram shows the force due to a surface particle at any desired point. Multiplying this force by the number of particles lying at similar distances away gives the force diagram for the system.

Due, however to the fact that the force diagram so derived takes account only of a small portion of the surface particles, another normalisation of the force is necessary before the pressure at various bed depths can be calculated. This is done relatively easily by equating all the z-components at any particular level to the input force and multiplying all the forces on the force diagram by the appropriate factor.

3.6.4 The Effect of Friction and Non-symmetrical Systems

The friction between particles has been ignored in the construction of the model and cannot therefore be accounted for in the normalisation process. The wall friction, however, can be taken into account when the second normalisation is carried out. In fact if the absurd physical condition that the coefficient of friction exceeds 1, is to be avoided it is necessary to assume a value for the frictional coefficient along the die wall.

The problem of asymmetry is more complex and has not been dealt with here. A further more analytical approach to the particle system must be made before such systems will lend themselves to statistical evaluations of the type used here.

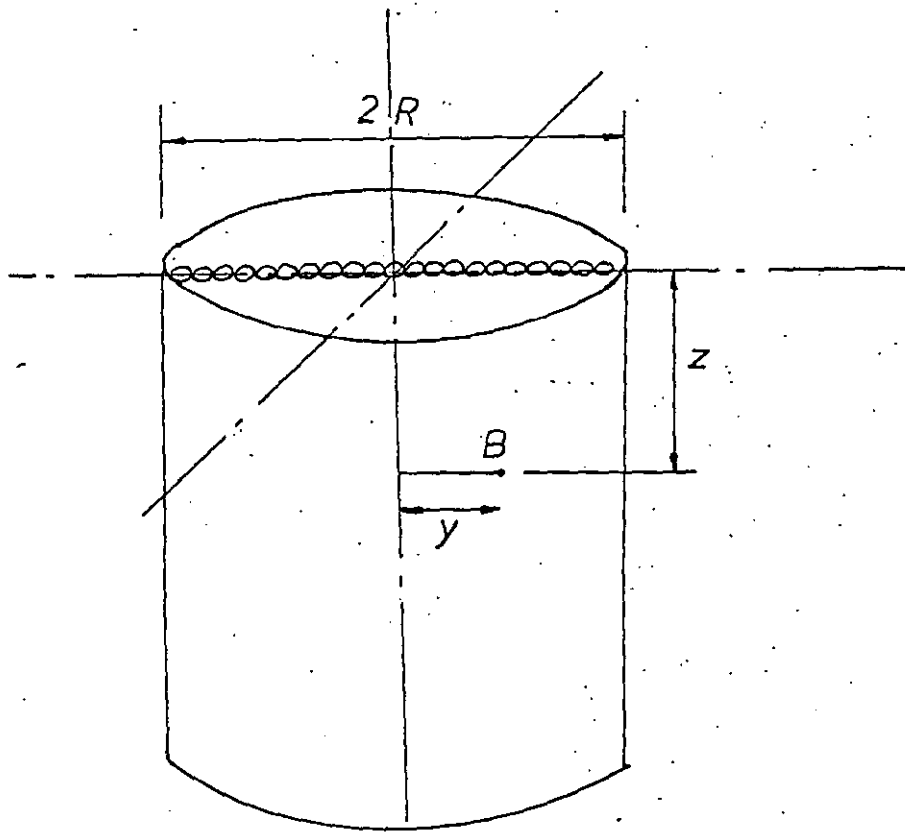


FIGURE 3.13

A cylindrical (axi-symmetric) system

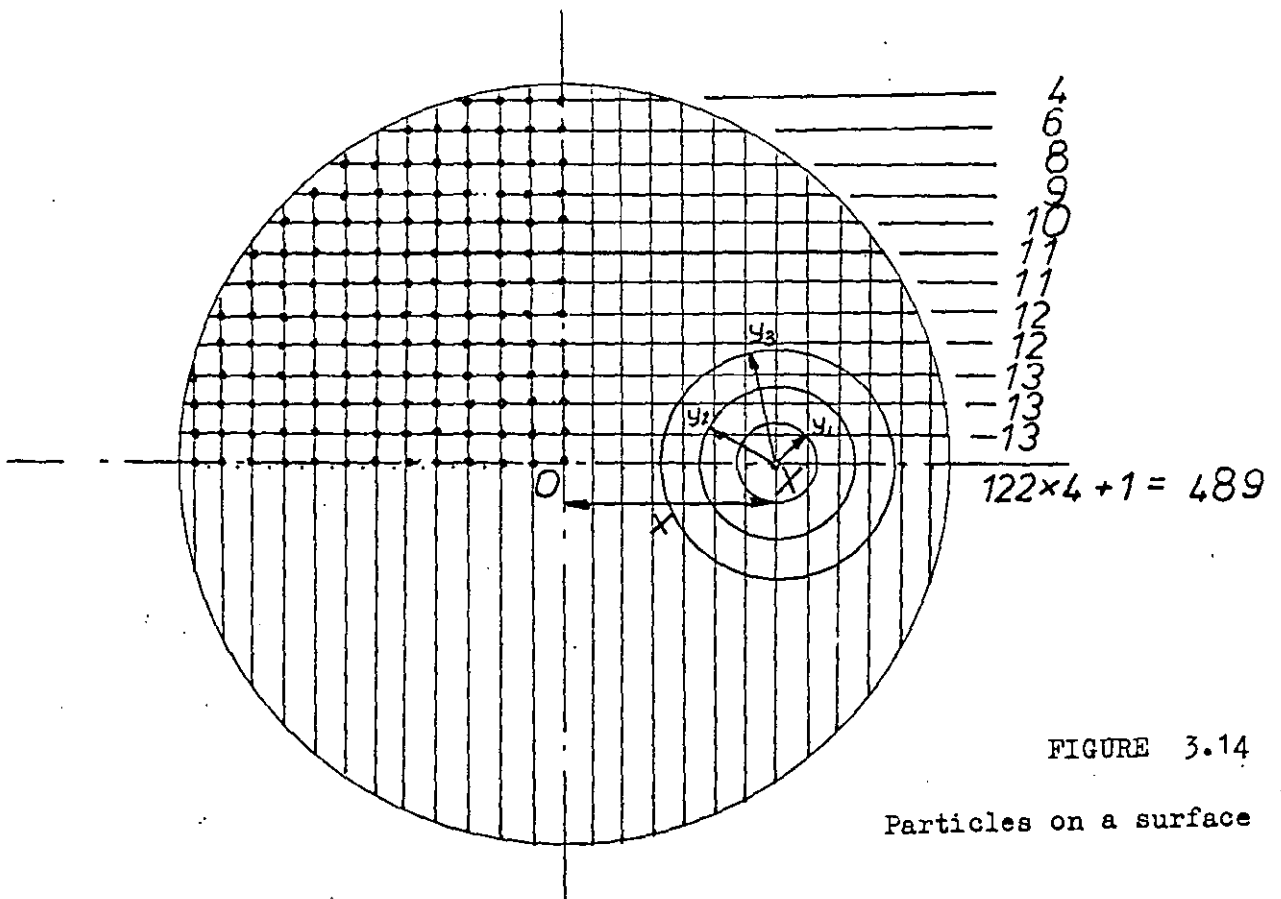


FIGURE 3.14

Particles on a surface

SECTION 4

APPARATUS AND EXPERIMENTAL METHOD

- 4.1 Particle sizing
- 4.2 The die assembly
- 4.3 The press
- 4.4 The experimental method

4.1 Particle sizing

It was necessary to use a powder in the experiments, that would conform with the assumptions made in the theory. Accordingly an iron powder, supplied by B.S.A Metal Powders was used. This powder had the characteristic of being irregular in shape, while also being more or less, ^{spheroidal} ~~convex~~. Since the model was not very sophisticated, it was also decided to use a narrow size range. The size range chosen for the experiments described here was the 200-300 micron range.

A distribution of Feret diameters was obtained using the standard microscope counting methods. In order to obtain filament size distributions, however, a more sophisticated, quicker method was required as it has been found by the Author that to be representative of a sample, at least 2000 filaments must be counted. An assembly of particles was allowed to settle in a resin, which was then allowed to set. The hardened mass was then sectioned at random, and polished on successive grades of emery paper and then on a cloth impregnated with diamond paste. The polished surface was then photographed and the photographs placed between two perspex sheets, one of which had equi-spaced lines drawn across its length. This allowed the measurement of the intercepts made by the lines with the outlines of the particles on the photographs.

These measurements were made with a pair of callipers, which were attached to the rider on a coil of variable resistance. The movement of the callipers changed the resistance of the coil which affected in turn the reading on a digital voltmeter. The signal from the volt meter was fed into a data logger, which recorded it on paper tape. The paper tape was then fed in as information into a computer program which calculated not only the filament size distribution but also the sectioned filament size distribution.

4.2 The die assembly

The experiments were performed, using a die similar to that devised by Duwez and Zwell (6). This is illustrated in Figure 4.2. The die assembly was mounted on an Apex PMPP7 floating die table but the springs were replaced with nuts in order to obtain uni-directional pressing, i.e. pressing from the top only, with the

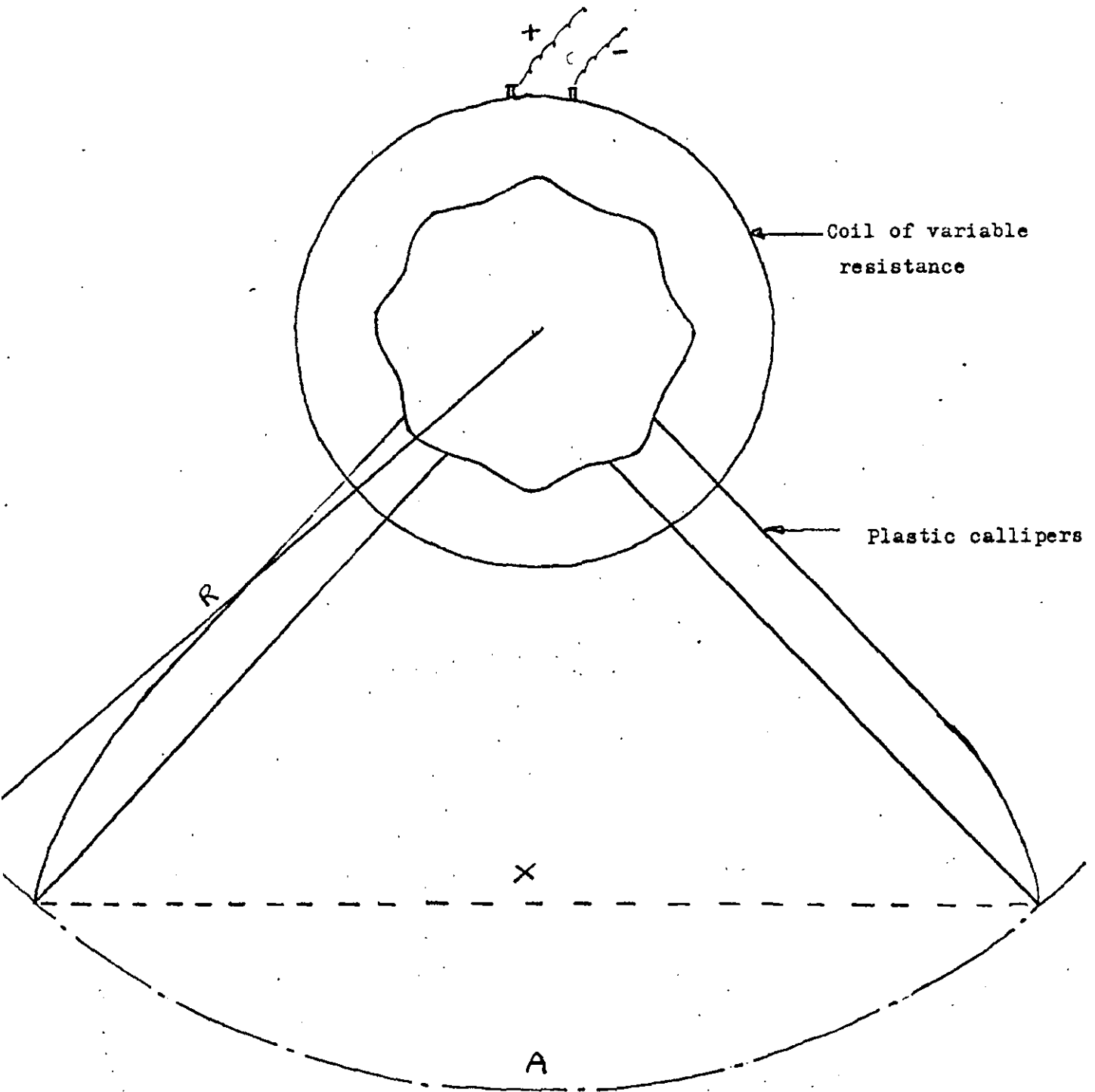


FIGURE 4.1

Measurement of filament sizes

$$X = 2R \sin (A / 2R)$$

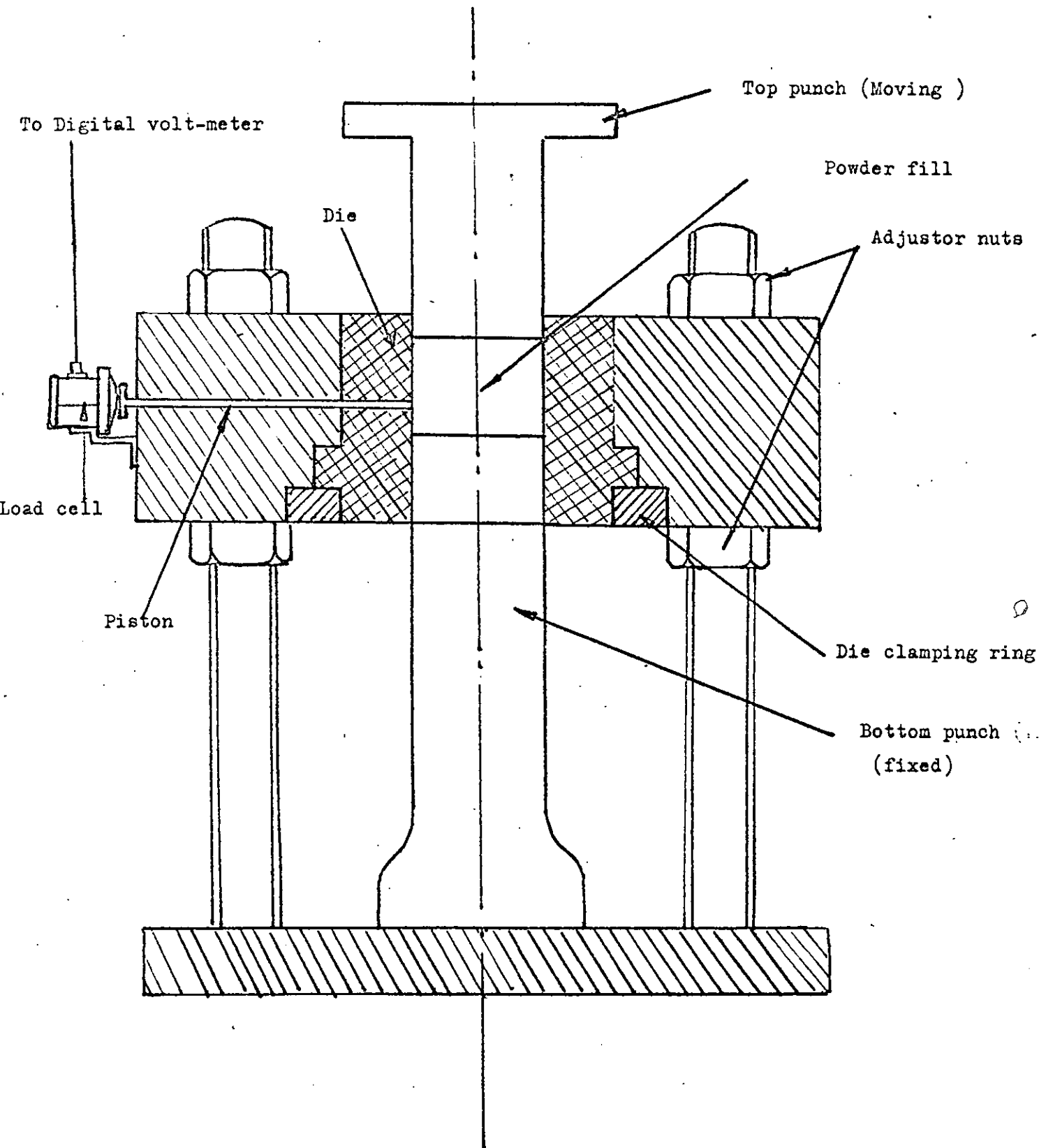


FIGURE 4.2

The -die assembly (sectioned view)

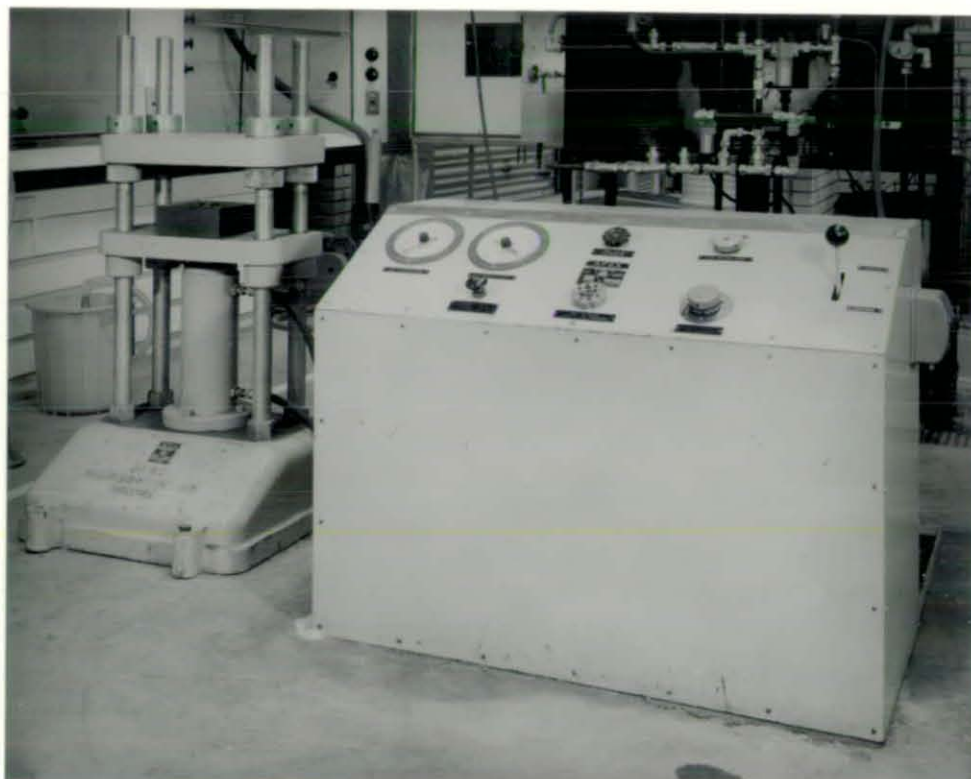


FIG. 4.3

THE PRESS

bottom punch held stationary, relative to the die. A $1/8$ " dia. piston was inserted into the side of the die, a distance of 1" from the top of the die. One end of the piston was filed to be flush with the walls of the die and the other rested on the head of strain gauge load cell supplied by Southern Instruments (type LC/1t). The load cell forms the measuring element in a four arm, bridge compensated circuit and has a repeatability of 0.1%. Thus any pressure exerted on the piston is transmitted to the load cell. Since the whole assembly was supported on four nuts it was possible to adjust the position of the bottom punch in relation to the position of the piston. Thus if the same die fill is used, assuming that the conditions of the experiments remain the same, by varying the position of the bottom punch in relation to the position of the piston, it is possible to obtain the pressure at all points on the side wall of the die. Thus it was possible to obtain for the different sets of experiments, graphs of the variation of side wall pressure at all points on the die wall with applied pressure.

4.3 The press

An Apex 175/A34/D, 35 ton power operated press was used in the experiments. The pressure exerted was indicated on a gauge calibrated to read between 1 and 5 tons. For higher pressures, which were not used in this work, a gauge calibrated between 1 and 35 tons was available. The speed of approach of the compacting ram could be controlled between 0 and 30 ins. per second. The whole die assembly was placed between the platens of the press and a dial gauge was used to calculate volume changes during compaction. (Figure 4.3). The dial gauge was set to zero when the top and bottom punches were just in contact. The expansion of the die was tested with a solid plug of iron, machined to fit exactly into the die.

4.4 Experimental Method

Two series of runs were made with the iron powder. The first series was with a 25 g. powder fill and no lubrication. The second with a 25 gram fill lubricated with 0.5% stearic acid. The porosity at the surface was thus determined.

A known weight of powder was poured into the die cavity through a funnel and the powder was then compacted to 5 tons gauge pressure, in steps of 1 ton. The piston, which was in contact with the load cell, was initially adjusted to be 0.1" from the bottom punch. This process was repeated with the piston being moved up in steps of 0.1" until the position of the piston was 0.1" from the final position of the top punch. To determine reproducibility of these experiments, they were repeated a number of times and in all cases the load cell readings were within 5% of one another for the same conditions. In this way it was possible to obtain curves of the side-wall pressure vs. the compact height. It was hoped that these tests would provide a check on the predictions made with the model.

SECTION 5

RESULTS

- 5.1 Calibration of the press and load cell
- 5.2 The Feret's diameter distribution function
- 5.3 The random filament distribution function
- 5.4 The pressing experiments
- 5.5 The results of the computer model

5.1 Calibration of the Press and Load Cell

The 0-5 ton pressure gauge mounted on the press was calibrated using a standard load ring. The calibration curve is shown in Figure 5.1. The load cell was calibrated by dead loading and the calibration curve is shown in Figure 5.2 .

5.2 The Feret's Diameter Distribution Function

The curves representing the normalised distribution function are seen in Figure 5.3 as cumulative undersize and cumulative oversize curves. From the cumulative oversize curve can be derived the function $g(y) dy$ (P 38) which represents the distribution of the probability of obtaining a section of a Feret diameter of length y , which is less than the length of the Feret diameter itself. The theory applicable has been discussed in Section 2.5.

5.3 The Random Filament Distribution Function

The curve representing the random filament distribution function are shown in Figure 5.4. The comments made with respect to the Feret distribution function also apply to these functions. The curves representing the distribution of a sectioned filament $h(y) dy$ (P 38) can be obtained from these curves.

5.4 The Pressing Experiments

The results of compacting 25 g. of iron powder in a 1" diameter die of cylindrical shape, are shown in Figures 5.5 and 5.6. The side wall pressure is plotted against the height of the compact. In Figure 5.5 the curves represent the behavior of the powder when 0.5% stearic acid has been added as lubricant, while the curves in 5.6 show the behaviour of untreated iron powder. The voidage of the compacts as a function of applied load and compact height is shown in Table 5.1.

TABLE 5.1

Voidage of the compact as a function of the applied pressure and compact height.

Voidage	Applied Load (tons)	Height (ins.)
0.49	2	0.1
0.48	4	0.1
0.43	6.5	0.1
0.51	2	0.2
0.455	6.5	0.2
0.53	2	0.4
0.50	4	0.4
0.472	6.5	0.4

These voidages are used in the determination of the number of surface particles transmitting the load.

5.5 The Results of the Computer Model

5.5.1 The Monte Carlo Simulation

The print out from the computer as it traces path and magnitude of a force as it is transmitted through the system are shown in Table 5.2. The order of the quantities as they appear in the print out are as follows.

Column	Variable	Explanation
1	E	Indicates the end of a walk. During a walk E=1, at the end E=2.
2	r	The r-coordinate of the point of contact, through which the force is transmitted.

Column	Variable	Explanation
3	G	If G=2 the Z boundary was crossed,if G=1 the force reaches the surface.
4	ITS	The number of the walk
5	z	The z-coordinate
6	NUMBER	The number of particles encountered upto that point in that walk
7	F_r	The r-component of the transmitted force
8	F_z	The z-component of the transmitted force

5.5.2 The Force Diagrams

The force diagram shown in Figure 5.7 was obtained by the analysis of 500 random walks such as the one shown in Table 5.2. The diagram shows the quantity of force reaching grid lines separated by 0.02 ins. in the r-direction and by 0.1 ins. in the z-direction. The forces shown are those due to a single particle at 0, which transmits a load of 10000 lb. normal to the surface. As may be seen the force decays rapidly as the distance of the grid lines become farther and farther away from 0.

5.5.3 Conclusions from the Force Diagram

Force diagrams similar to the one in Figure 5.7 are obtained for different die geometries and different compaction pressures.

These diagrams may then be used in predicting,

- a) The side wall pressure as a function of die depth. The curves obtained from the model are compared with the curves shown in Figure 5.6, in Figure 5.10 for 2, 4 and 6.5 tons applied load, and compacted in a 0.4 x 1.0 in. Dia. die.
- b) The pressure transmitted to various depths in the system, and determine the effect of the height:diameter ratio on these curves. This is shown in Figure 5.8
- c) The loss of force by friction at the wall, as a percentage of the applied force. The relevant curves are shown in Figure 5.9.

A complete discussion of all these results and their implications is found in Section 6.

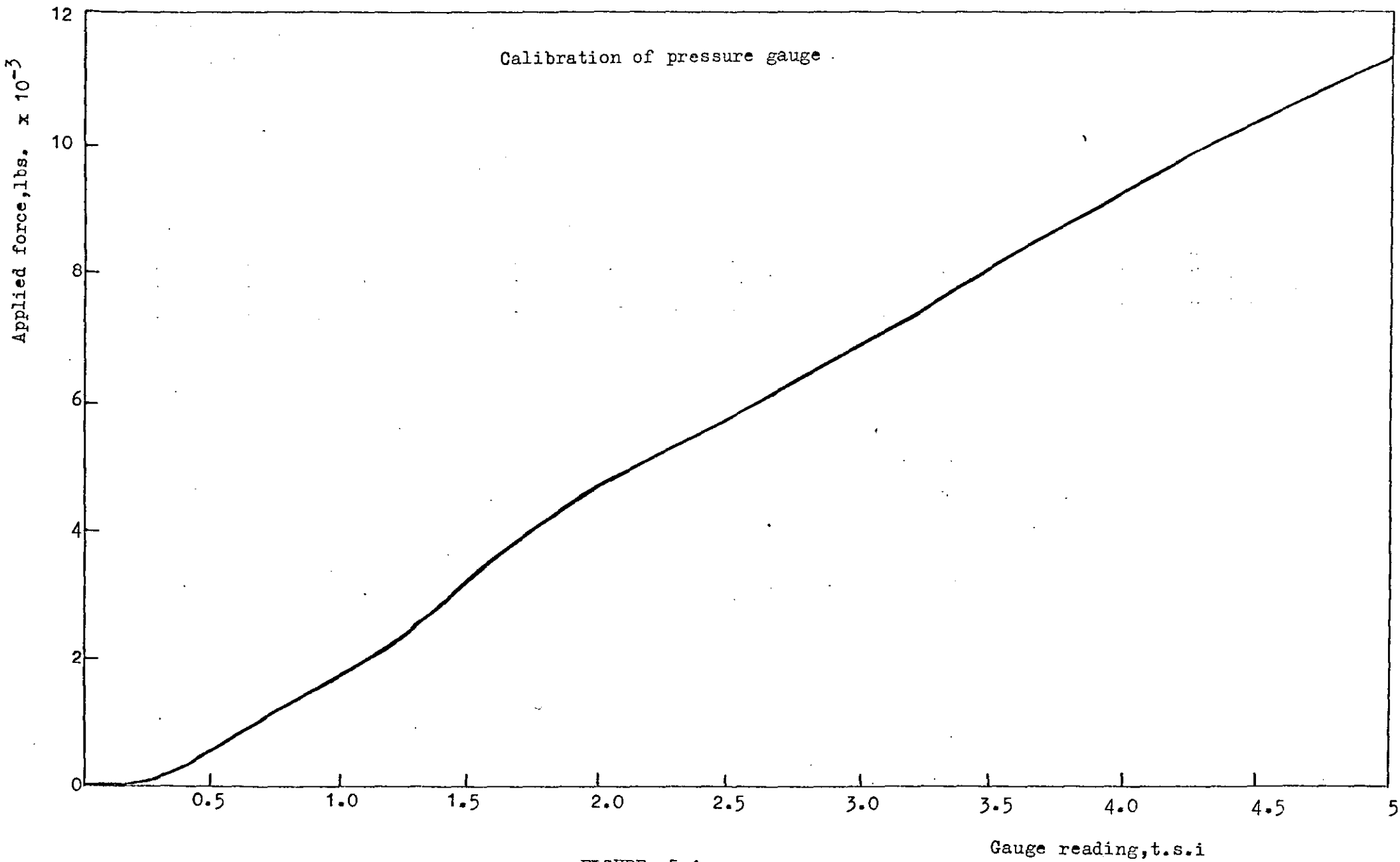


FIGURE 5.1

Gauge reading, t.s.i

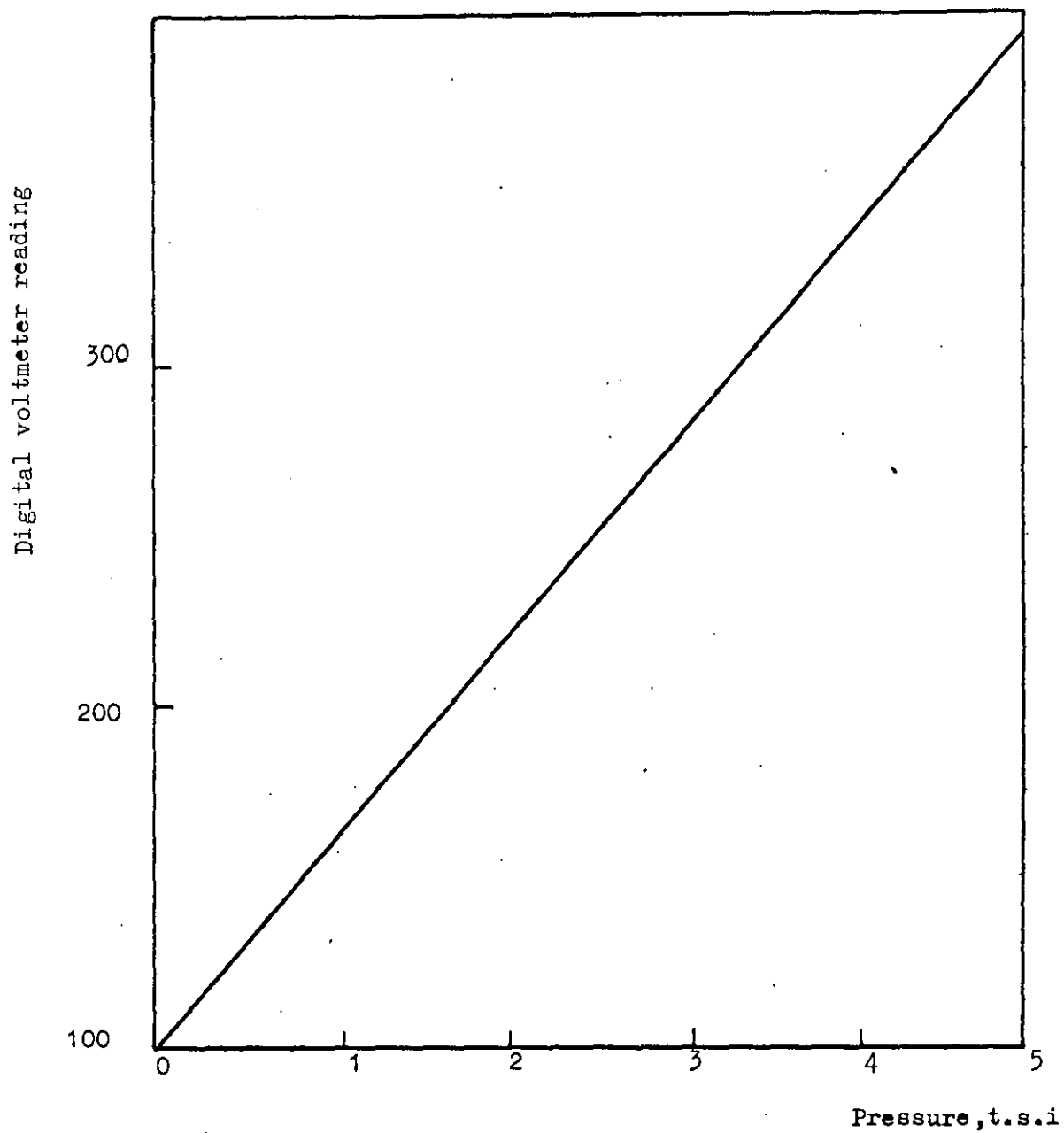


FIGURE 5.2

Calibration of the load cell

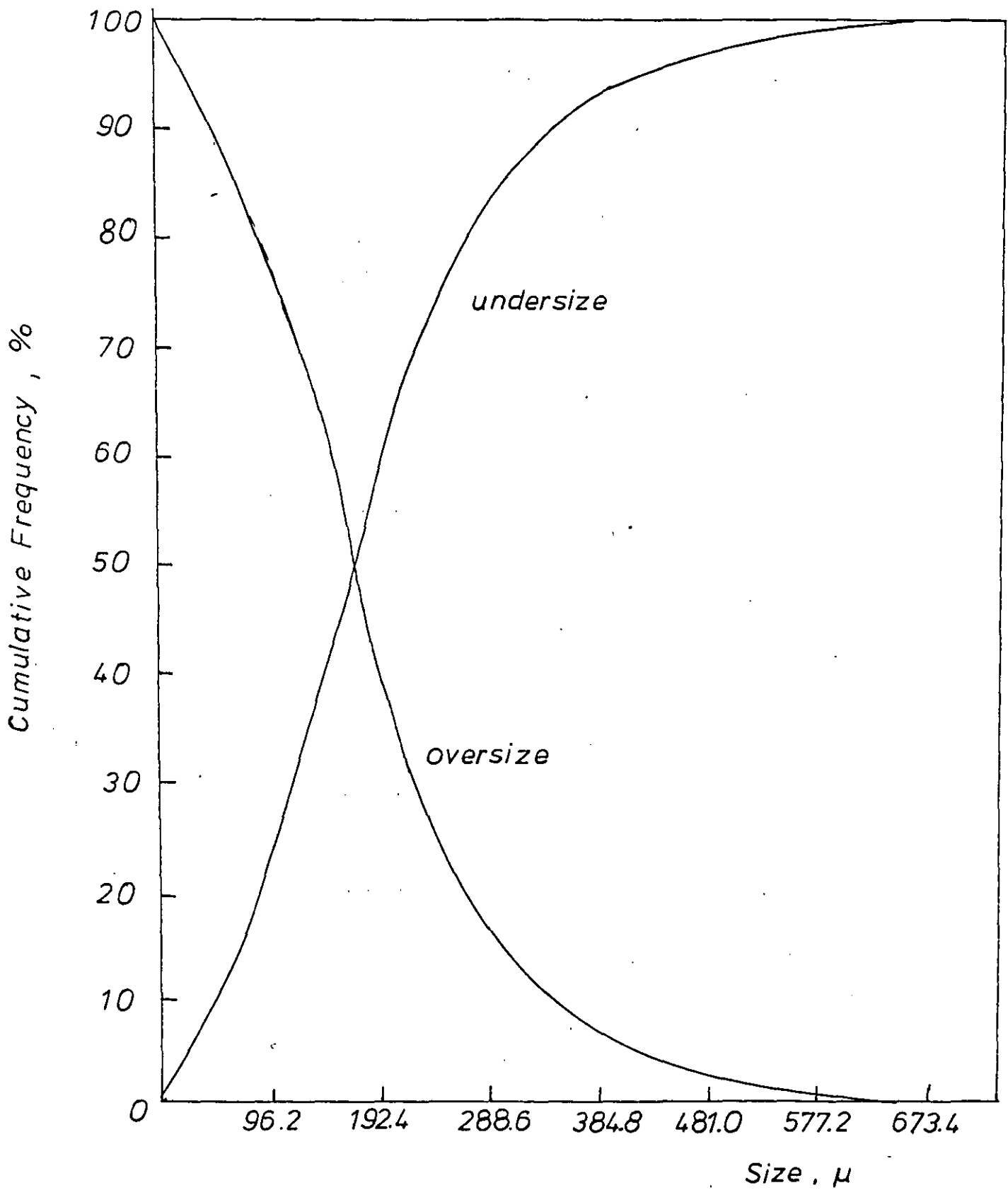


FIGURE 5.3

Feret's diameter distribution

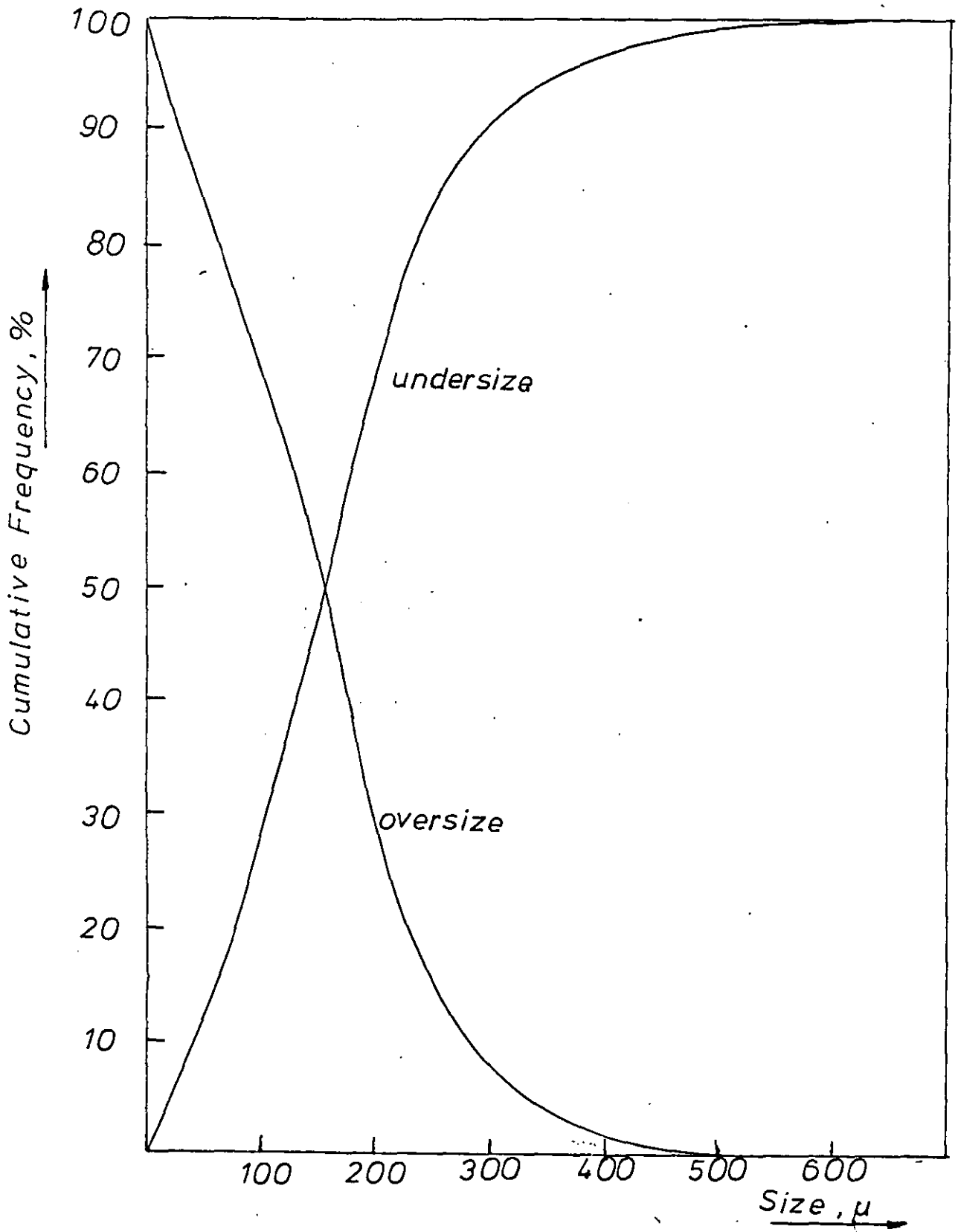


FIGURE 5.4
Random filament distribution

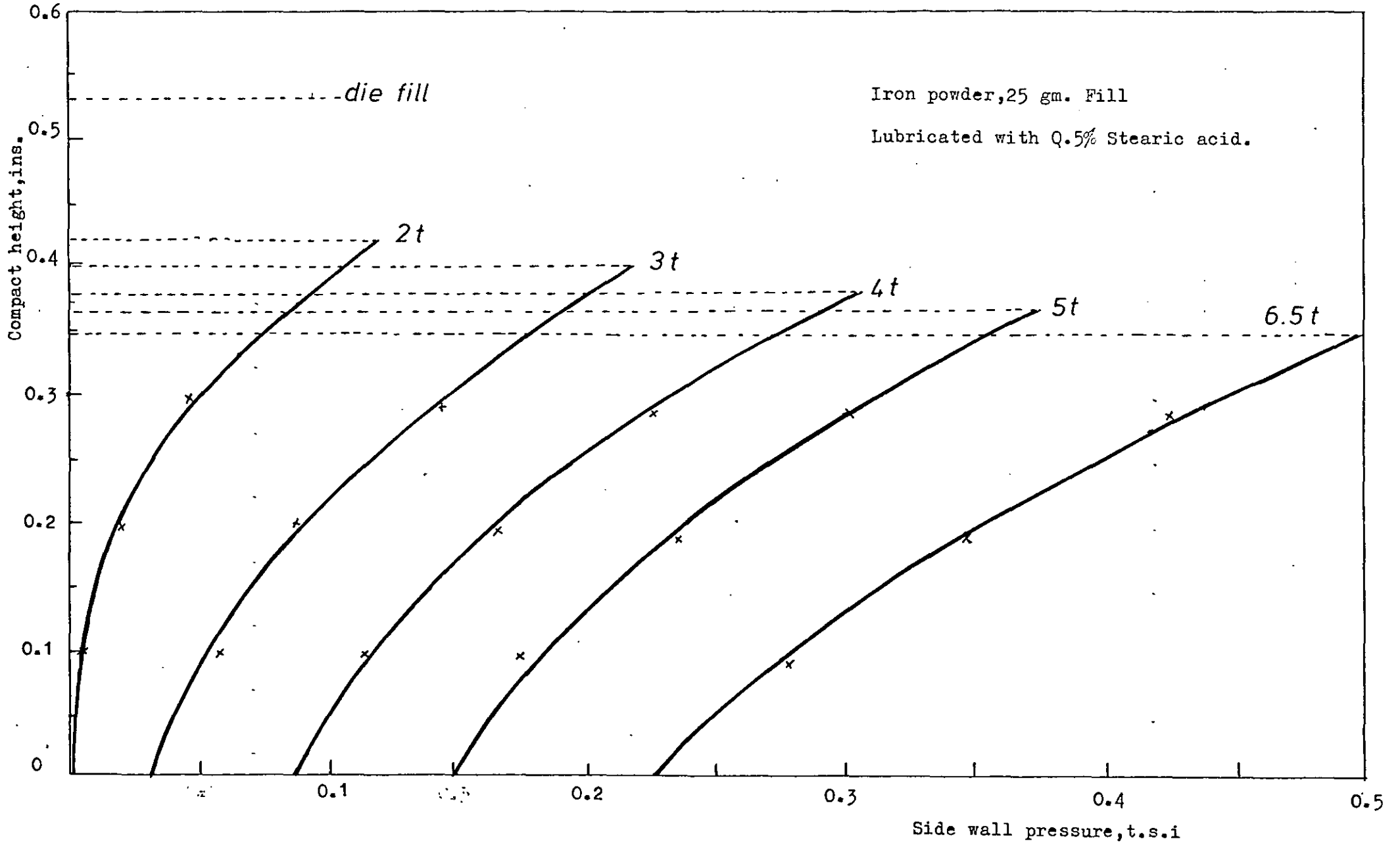


FIGURE 5.5

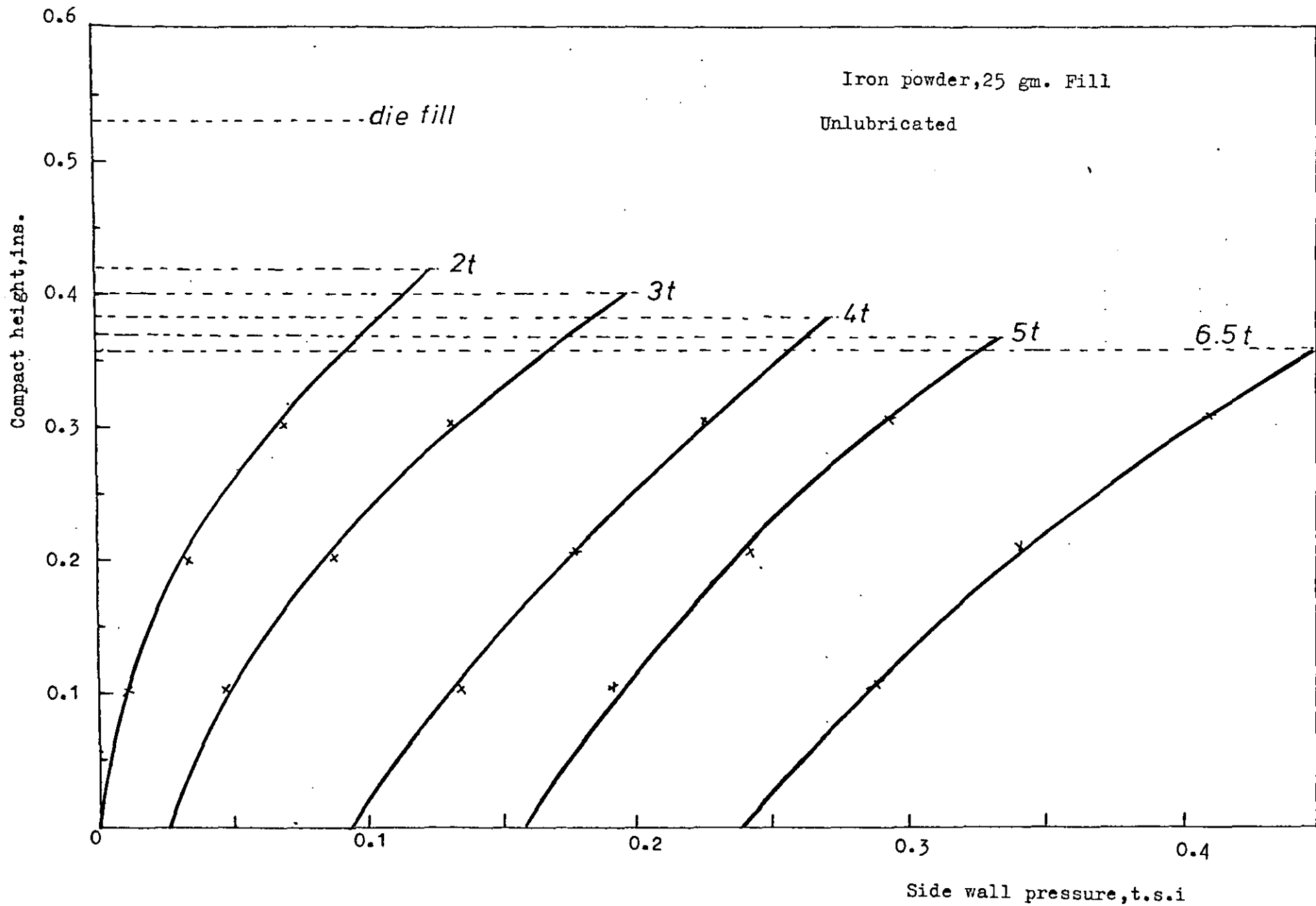


FIGURE 5.6

		Distance along r-axis, ins.										
		0	0.02	0.04	0.06	0.08	0.10	0.12	0.14	0.16	0.18	0.20
Distance along z-axis, ins.	0	0.2E+4	0.2E+4	0.5	0.3E-5	0	0	0	0	0	0	0
	0.1	0.1E+5	0.8E+4	8.9	0.3E-4	0	0	0	0	0	0	0
	0.2	0.3E-6	0.3	0.2	0.02	0.2E-22	0.4E-33	0	0	0	0	0
	0.3	0.1E-25	0.01	0.01	0.4E-11	0.6E-23	0.2E-32	0	0	0	0	0
	0.4	0.8E-25	0.5E-4	0.5E-8	0.3E-8	0.1E-11	0.2E-20	0.3E-36	0.2E-36	0.1E-41	0	0
	0.5	0.6E-24	0.4E-3	0.5E-8	0.7E-13	0.5E-17	0.2E-19	0.1E-35	0.3E-46	0	0	0
	0.6	0	0.2E-18	0.5E-9	0.2E-18	0.1E-23	0.3E-30	0.2E-45	0.2E-49	0.1E-49	0.1E-49	0.1E-49
	0.7	0	0.2E-18	0.1E-18	0.2E-17	0.7E-28	0.2E-37	0.3E-45	0.2E-49	0.2E-52	0.3E-59	0.3E-59

note: $E \pm N \equiv 10^{\pm N}$

FIGURE 5.7

A force diagram (transmission from wall neglected)

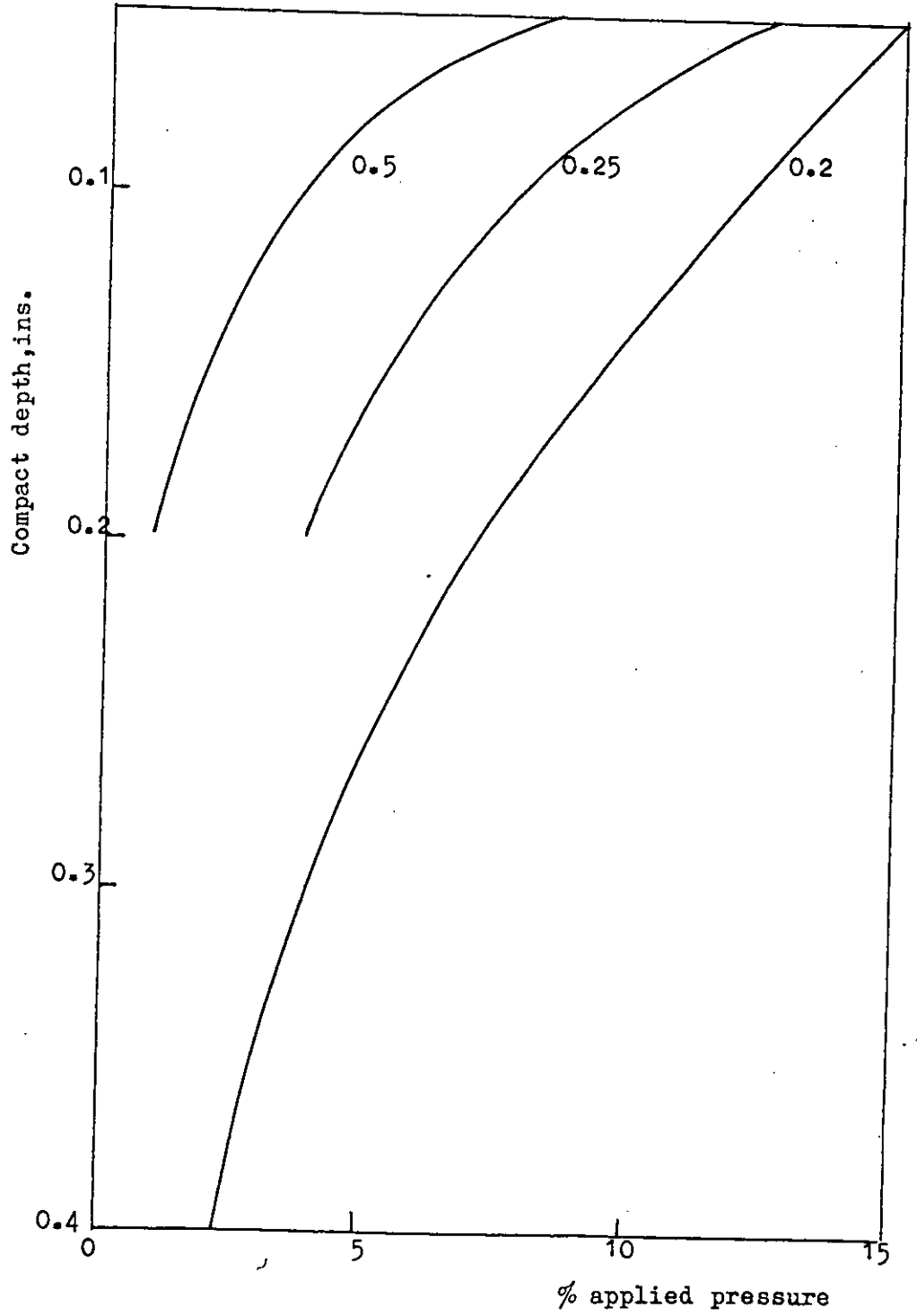


FIGURE 5.8

% of applied pressure transmitted vs. compact height for various height:diameter ratios (Computer Prediction)

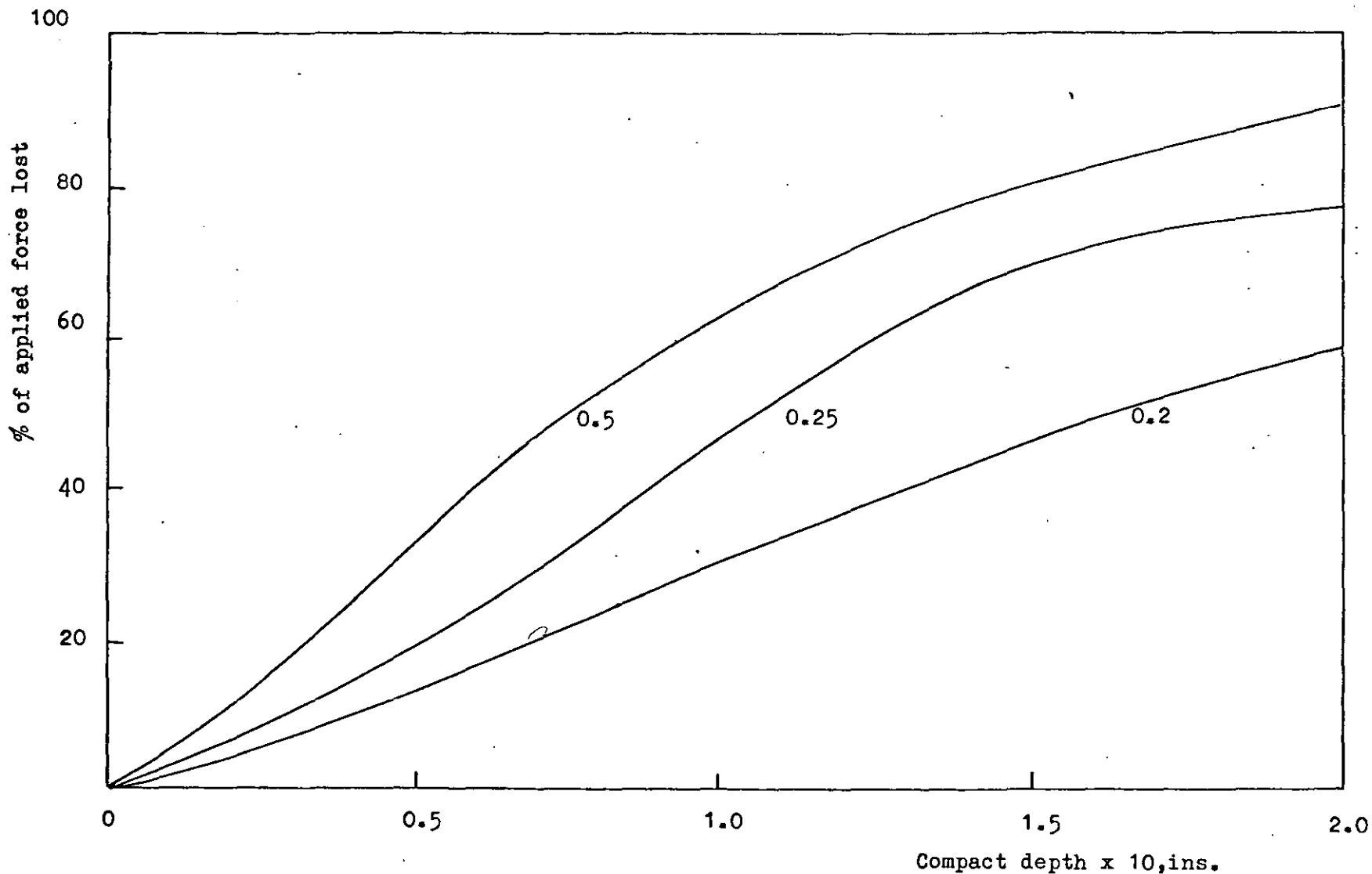


FIGURE 5.9

Friction losses at the wall as a function of compact height for various height:diameter ratios (Computer Prediction)

FIGURE 5.10

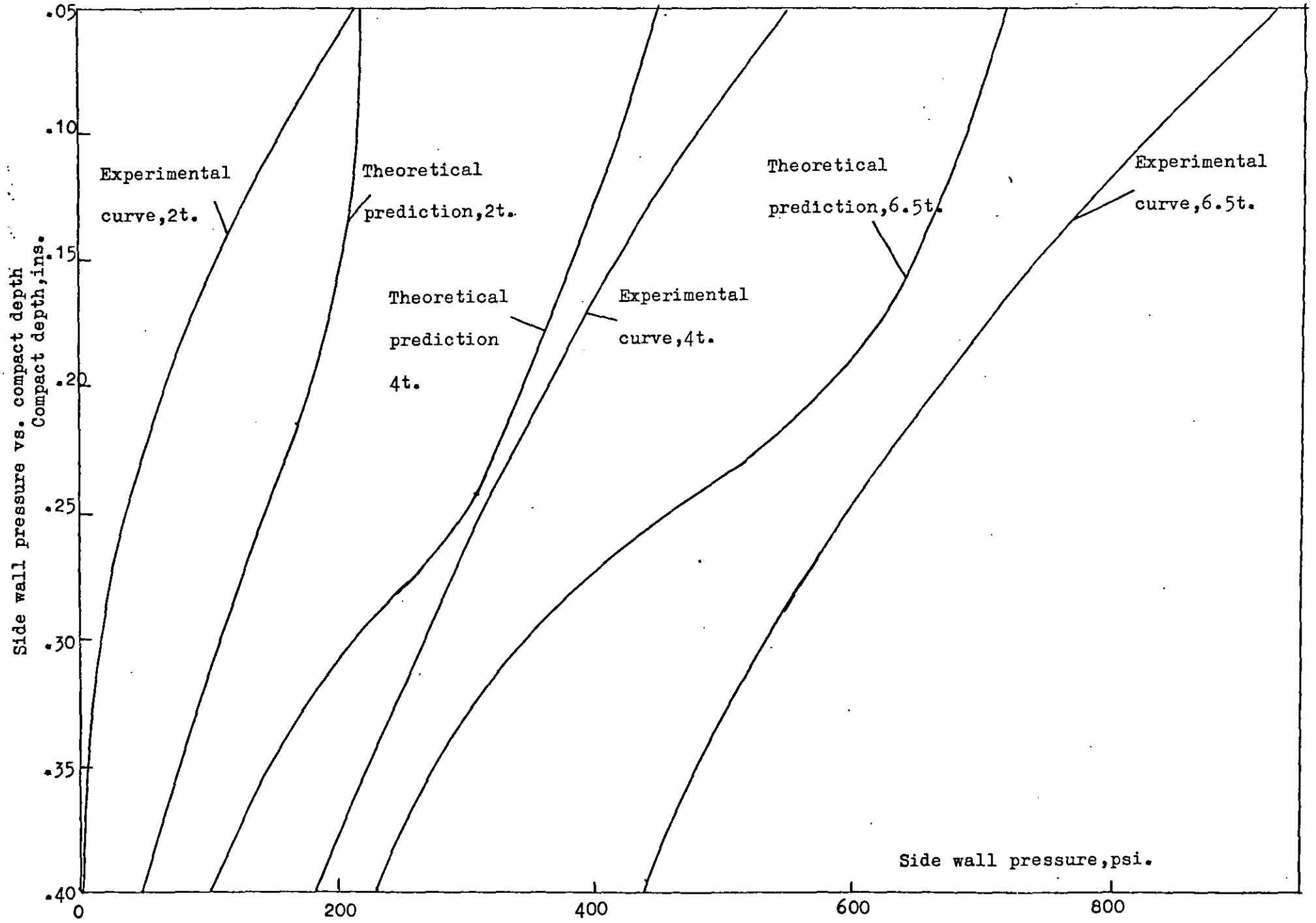


TABLE 5.2

The computer print out of a random walk

E	r	G	ITS	z	NUMBER	F _r	F _z
1	0.3026745E-02	0	1	0.5757370E-02	1	0.5315626E 51	0.0000000E 00
1	0.8514566E-02	0	1	0.7991000E-02	2	0.1102069E 50	0.0000000E 00
1	0.1640753E-01	0	1	0.9198609E-02	3	0.1690949E 48	0.0000000E 00
1	0.2257052E-01	0	1	0.1014653E-01	4	0.7022110E 46	0.2138212E 38
1	0.2056701E-01	0	1	0.7185520E-02	5	0.5044824E 48	0.0000000E 00
1	0.2584018E-01	0	1	0.9723594E-02	6	0.5889973E 47	0.1683044E 47
1	0.2445171E-01	0	1	0.1012283E-01	7	0.1476512E 46	0.0000000E 00
1	0.2494661E-01	0	1	0.1031838E-01	8	0.6996955E 45	0.3138928E 35
1	0.2690241E-01	0	1	0.1316250E-01	9	0.6816708E 45	0.2163092E 45
1	0.2796614E-01	0	1	0.1147454E-01	10	0.6593346E 44	0.0000000E 00
1	0.2988942E-01	0	1	0.1186907E-01	11	0.2163958E 45	0.0000000E 00
1	0.2976731E-01	0	1	0.1117761E-01	12	0.1202740E 45	0.2517046E 44
1	0.3362076E-01	0	1	0.9662957E-02	13	0.2597456E 45	0.8536784E 44
1	0.3363777E-01	0	1	0.9959915E-02	14	0.2866222E 45	0.0000000E 00
1	0.3034018E-01	0	1	0.1003892E-01	15	0.2162294E 44	0.2855536E 44
1	0.2613461E-01	0	1	0.1151694E-01	16	0.2489406E 41	0.1457334E 42
1	0.2732416E-01	0	1	0.1598106E-01	17	0.9420560E 39	0.2248824E 40
1	0.2416679E-01	0	1	0.2020207E-01	18	0.1088357E 39	0.0000000E 00
1	0.2780429E-01	0	1	0.1800668E-01	19	0.8163427E 38	0.5251574E 38
1	0.2336844E-01	0	1	0.2329971E-01	20	0.6087175E 38	0.5897198E 28
1	0.2174045E-01	0	1	0.2190657E-01	21	0.3761893E 39	0.2080273E 29
1	0.2206053E-01	0	1	0.1916588E-01	22	0.1651146E 37	0.6091337E 26
1	0.1618554E-01	0	1	0.2026744E-01	23	0.2045056E 37	0.1809706E 37
1	0.1475141E-01	0	1	0.2098265E-01	24	0.3626356E 37	0.0000000E 00
1	0.1258741E-01	0	1	0.1546398E-01	25	0.3043174E 36	0.1458139E 36
1	0.1803845E-01	0	1	0.1190708E-01	26	0.2302269E 36	0.1537776E 26
1	0.1314913E-01	0	1	0.8893575E-02	27	0.8750770E 34	0.8775369E 35
1	0.1633100E-01	0	1	0.1345944E-01	28	0.9595831E 36	0.0000000E 00
1	0.1691768E-01	0	1	0.1296099E-01	29	0.9285077E 36	0.1953521E 36
1	0.1843523E-01	0	1	0.1383523E-01	30	0.6802707E 36	0.0000000E 00
1	0.1903595E-01	0	1	0.1303115E-01	31	0.2357392E 37	0.1022204E 37
1	0.1358137E-01	0	1	0.1659945E-01	32	0.5723423E 35	0.0000000E 00
1	0.1880570E-01	0	1	0.1600035E-01	33	0.3482284E 36	0.1287619E 26
1	0.1669122E-01	0	1	0.1293345E-01	34	0.6711575E 33	0.1241988E 35
1	0.1441231E-01	0	1	0.1295001E-01	35	0.6826233E 33	0.4744535E 34
1	0.1226992E-01	0	1	0.1472684E-01	36	0.1789135E 34	0.3748841E 23
1	0.1561048E-01	0	1	0.1689555E-01	37	0.1017880E 34	0.3417620E 23
1	0.1514885E-01	0	1	0.1791967E-01	38	0.2233339E 34	0.0000000E 00
1	0.1714037E-01	0	1	0.1767123E-01	39	0.1945969E 34	0.5723933E 33
1	0.1682566E-01	0	1	0.2194611E-01	40	0.1878409E 35	0.5551444E 34
1	0.1390620E-01	0	1	0.2380293E-01	41	0.1421606E 35	0.0000000E 00
1	0.1714095E-01	0	1	0.2616432E-01	42	0.3240048E 34	0.0000000E 00
1	0.1878515E-01	0	1	0.2342376E-01	43	0.6163884E 33	0.2451949E 33
1	0.2188978E-01	0	1	0.2300071E-01	44	0.4010960E 32	0.1125418E 33
1	0.1866739E-01	0	1	0.3032141E-01	45	0.7595008E 31	0.4773181E 31
1	0.1398019E-01	0	1	0.3120423E-01	46	0.8183249E 31	0.5108581E 21
1	0.1300324E-01	0	1	0.3132460E-01	47	0.8720499E 31	0.0000000E 00
1	0.1441124E-01	0	1	0.3128568E-01	48	0.2636462E 33	0.4146458E 33
1	0.1385062E-01	0	1	0.3296597E-01	49	0.2390868E 31	0.1520260E 32
1	0.1278221E-01	0	1	0.3600317E-01	50	0.7023923E 29	0.0000000E 00
1	0.1486566E-01	0	1	0.3539346E-01	51	0.2406021E 31	0.7653195E 30
1	0.1577371E-01	0	1	0.3353930E-01	52	0.2353320E 32	0.0000000E 00

TABLE 5.2 (Contd.)

1.	0.1725065E-01	0.	1	0.3440434E-01	53	0.4624762E	32	0.0000000E	00
1.	0.1722216E-01	0.	1	0.3139624E-01	54	0.8183814E	29	0.7018225E	19
1.	0.1230116E-01	0.	1	0.3576038E-01	55	0.1113928E	28	0.1128676E	29
1.	0.1852399E-01	0.	1	0.3709760E-01	56	0.5437843E	25	0.1049685E	27
1.	0.1991466E-01	0.	1	0.3939468E-01	57	0.1228657E	27	0.6948601E	26
1.	0.1888351E-01	0.	1	0.4053653E-01	58	0.2775391E	26	0.8752054E	15
1.	0.1844295E-01	0.	1	0.4063150E-01	59	0.1310306E	27	0.7163796E	26
1.	0.1777887E-01	0.	1	0.4175218E-01	60	0.1550812E	26	0.8745175E	25
1.	0.1184144E-01	0.	1	0.4260686E-01	61	0.1212497E	24	0.0000000E	00
1.	0.1515815E-01	0.	1	0.4349620E-01	62	0.1010312E	24	0.1369131E	24
1.	0.1709689E-01	0.	1	0.4532759E-01	63	0.6982671E	23	0.1332472E	24
1.	0.1507011E-01	0.	1	0.4939783E-01	64	0.1861292E	22	0.9033250E	22
1.	0.1545738E-01	0.	1	0.5052350E-01	65	0.2244552E	22	0.6247375E	22
1.	0.1337718E-01	0.	1	0.5473611E-01	66	0.1578689E	22	0.2115670E	22
1.	0.1143009E-01	0.	1	0.6137155E-01	67	0.1294946E	21	0.5531029E	21
1.	0.1154609E-01	0.	1	0.6157931E-01	68	0.3615613E	21	0.1027906E	23
1.	0.1515957E-01	0.	1	0.6677226E-01	69	0.3681755E	21	0.0000000E	00
1.	0.9807624E-02	0.	1	0.6753810E-01	70	0.6214092E	21	0.2196287E	21
1.	0.9947272E-02	0.	1	0.6752778E-01	71	0.7911895E	20	0.0000000E	00
1.	0.8926814E-02	0.	1	0.6755672E-01	72	0.9026454E	18	0.8321275E	09
1.	0.4050048E-02	0.	1	0.6205755E-01	73	0.2431044E	20	0.0000000E	00
1.	0.7588992E-02	0.	1	0.6298575E-01	74	0.3293083E	19	0.2330962E	09
1.	0.1309412E-02	0.	1	0.6324732E-01	75	0.9792371E	18	0.1140400E	09
1.	0.9013052E-03	0.	1	0.6312424E-01	76	0.4908388E	17	0.0000000E	00
1.	0.4851882E-02	0.	1	0.6008188E-01	77	0.4497362E	19	0.1348803E	09
1.	0.9133752E-02	0.	1	0.5887371E-01	78	0.4245937E	16	0.4829311E	16
1.	0.1499814E-01	0.	1	0.5962634E-01	79	0.8190338E	16	0.2795823E	16
1.	0.1547947E-01	0.	1	0.5941127E-01	80	0.2703041E	17	0.0000000E	00
1.	0.1515188E-01	0.	1	0.6054125E-01	81	0.2821071E	17	0.1073643E	07
1.	0.1637863E-01	0.	1	0.5985533E-01	82	0.2152505E	17	0.0000000E	00
1.	0.1122512E-01	0.	1	0.6108067E-01	83	0.4941553E	16	0.1984191E	06
1.	0.1552149E-01	0.	1	0.6408881E-01	84	0.5291940E	15	0.1575919E	05
1.	0.1401059E-01	0.	1	0.6460557E-01	85	0.1653429E	14	0.4812113E	03
1.	0.1987319E-01	0.	1	0.6305115E-01	86	0.7037440E	14	0.2313175E	14
1.	0.1672022E-01	0.	1	0.6680783E-01	87	0.1668387E	14	0.9305340E	03
1.	0.1720005E-01	0.	1	0.6500215E-01	88	0.1040305E	15	0.7435306E	13
1.	0.1163872E-01	0.	1	0.6564263E-01	89	0.2236498E	15	0.2102829E	05
1.	0.1397361E-01	0.	1	0.6759508E-01	90	0.9851947E	14	0.1933501E	14
1.	0.1904915E-01	0.	1	0.6819119E-01	91	0.2580005E	15	0.0000000E	00
1.	0.1526535E-01	0.	1	0.6936309E-01	92	0.4088676E	14	0.0000000E	00
1.	0.1578152E-01	0.	1	0.6567323E-01	93	0.1906190E	14	0.4228774E	13
1.	0.1111990E-01	0.	1	0.6422346E-01	94	0.1894576E	13	0.0000000E	00
1.	0.7177357E-02	0.	1	0.6707768E-01	95	0.1257648E	16	0.5160557E	05
1.	0.6841273E-02	0.	1	0.6583829E-01	96	0.1101401E	15	0.8267104E	14
1.	0.7476252E-02	0.	1	0.6861634E-01	97	0.2344894E	14	0.0000000E	00
1.	0.3143039E-02	0.	1	0.7025538E-01	98	0.9220618E	13	0.1229913E	14
1.	0.3755967E-02	0.	1	0.7132036E-01	99	0.9018923E	13	0.2889110E	03
1.	0.8629602E-02	0.	1	0.6691337E-01	100	0.2111661E	12	0.9857634E	11
1.	0.9158093E-02	0.	1	0.6923522E-01	101	0.1007020E	13	0.0000000E	00
1.	0.4435803E-02	0.	1	0.7062738E-01	102	0.1958221E	13	0.0000000E	00
1.	0.9966684E-02	0.	1	0.6983608E-01	103	0.9282659E	12	0.3505867E	02
1.	0.5892900E-02	0.	1	0.6739891E-01	104	0.1023346E	13	0.0000000E	00
1.	0.7386808E-02	0.	1	0.6709051E-01	105	0.3472897E	13	0.0000000E	00
1.	0.9958116E-02	0.	1	0.6892395E-01	106	0.1921700E	12	0.8939544E	11
1.	0.1106387E-01	0.	1	0.6738462E-01	107	0.1525890E	11	0.8196147E	00
1.	0.8881809E-02	0.	1	0.6625102E-01	108	0.1957259E	09	0.9398137E-01	
1.	0.2404695E-02	0.	1	0.7108261E-01	109	0.1727473E	10	0.1102472E	09
1.	0.5208185E-02	0.	1	0.7039243E-01	110	0.8674892E	09	0.1204546E	10
1.	0.2603095E-02	0.	1	0.7075976E-01	111	0.2403967E	09	0.5586881E	09
1.	0.3000858E-02	0.	1	0.7126912E-01	112	0.2704048E	09	0.1244307E	09
1.	0.3276714E-02	0.	1	0.7923237E-01	113	0.2208572E	09	0.9650880E	08

1,	0.6799892E-02	0.	1	0.8285219E-01	114	0.1907238E	09	0.9251442E-02	
1,	0.1200996E-01	0.	1	0.7994382E-01	115	0.8345067E	09	0.2632366E	09
1,	0.1068157E-01	0.	1	0.7730902E-01	116	0.6061264E	09	0.4276988E	09
1,	0.8282856E-02	0.	1	0.8006184E-01	117	0.5882241E	09	0.0000000E	00
1,	0.6490309E-02	0.	1	0.8360114E-01	118	0.1573680E	09	0.1821797E	09
1,	0.9741506E-02	0.	1	0.8972626E-01	119	0.2548287E	08	0.8988915E	08
1,	0.1243808E-01	0.	1	0.9314450E-01	120	0.5218158E	07	0.1037874E-02	
1,	0.1101943E-01	0.	1	0.9595493E-01	121	0.3409477E	08	0.2133599E	08
1,	0.1383071E-01	0.	1	0.1004947E	00122	0.3863023E	07	0.3143173E	07
1,	0.1620378E-01	0.	1	0.1029504E	00123	0.2474778E	07	0.1324746E	08
1,	0.1254310E-01	0.	1	0.1080732E	00124	0.8038315E	07	0.2814372E	07
1,	0.7384611E-02	0.	1	0.1088498E	00125	0.3351010E	07	0.0000000E	00
1,	0.1954606E-02	0.	1	0.1124554E	00126	0.1573430E	07	0.0000000E	00
1,	0.4809267E-02	0.	1	0.1109464E	00127	0.3121746E	07	0.2923111E	07
1,	0.6561110E-02	0.	1	0.1124973E	00128	0.0032432E	07	0.1881042E-03	
1,	0.1089660E-01	0.	1	0.1111331E	00129	0.8404950E	05	0.1333036E	07
1,	0.1455987E-01	0.	1	0.1106033E	00130	0.1871699E	05	0.2358604E	06
1,	0.1643267E-01	0.	1	0.1118679E	00131	0.3176187E	06	0.0000000E	00
1,	0.1621329E-01	0.	1	0.1101077E	00132	0.6447815E	05	0.2838316E	05
1,	0.1634301E-01	0.	1	0.1128156E	00133	0.3531299E	02	0.1233100E-07	
1,	0.2091090E-01	0.	1	0.1082035E	00134	0.2231176E	02	0.1002488E	03
1,	0.2097836E-01	0.	1	0.1112751E	00135	0.4297675E	03	0.1288577E	03
1,	0.2534241E-01	0.	1	0.1097348E	00136	0.1914243E	04	0.8029310E	04
1,	0.2251009E-01	0.	1	0.1139129E	00137	0.5547051E	03	0.7293274E	03
1,	0.1902636E-01	0.	1	0.1185560E	00138	0.8143182E	03	0.5621162E	02
1,	0.1738604E-01	0.	1	0.1193958E	00139	0.9548352E	02	0.2869949E-08	
1,	0.1738003E-01	0.	1	0.1194704E	00140	0.1197072E	03	0.3590366E-08	
1,	0.1795868E-01	0.	1	0.1206079E	00141	0.2671173E	02	0.0000000E	00
1,	0.1639499E-01	0.	1	0.1241025E	00142	0.3928365E	02	0.1536579E-08	
1,	0.2058956E-01	0.	1	0.1211457E	00143	0.1438287E	02	0.2659094E	02
1,	0.1919662E-01	0.	1	0.1255110E	00144	0.4525400E	02	0.2216428E	02
1,	0.2030681E-01	0.	1	0.1225562E	00145	0.2294357E	02	0.7116312E-09	
1,	0.2113368E-01	0.	1	0.1215279E	00146	0.1828584E	01	0.9410012E	00
1,	0.1646645E-01	0.	1	0.1212953E	00147	0.1127648E	02	0.9695771E	01
1,	0.1807207E-01	0.	1	0.1250107E	00148	0.3088957E	01	0.4143572E	01
1,	0.1911776E-01	0.	1	0.1271357E	00149	0.5066805E	00	0.9415485E	00
1,	0.1757398E-01	0.	1	0.1289265E	00150	0.7577777E-01	0.	0.2628820E-11	
1,	0.1812131E-01	0.	1	0.1302904E	00151	0.4042547E-01	0.	0.9642496E-02	
1,	0.2404813E-01	0.	1	0.1309695E	00152	0.3646191E-01	0.	0.4699195E-01	
1,	0.2168862E-01	0.	1	0.1330124E	00153	0.1144869E-03	0.	0.0000000E	00
1,	0.1821931E-01	0.	1	0.1341970E	00154	0.8639230E-02	0.	0.0000000E	00
1,	0.1585643E-01	0.	1	0.1340212E	00155	0.8809324E-02	0.	0.6066955E-03	
1,	0.1553301E-01	0.	1	0.1338115E	00156	0.1569129E-02	0.	0.5471013E-02	
1,	0.1449268E-01	0.	1	0.1388790E	00157	0.3205540E-03	0.	0.3363006E-02	
1,	0.1444569E-01	0.	1	0.1440905E	00158	0.1430728E-02	0.	0.4206808E-13	
1,	0.1414759E-01	0.	1	0.1439454E	00159	0.1157983E-02	0.	0.4613018E-03	
1,	0.1412646E-01	0.	1	0.1452790E	00160	0.2545915E-03	0.	0.2022725E-03	
1,	0.1255887E-01	0.	1	0.1483636E	00161	0.2525574E-04	0.	0.2686515E-04	
1,	0.1826292E-01	0.	1	0.1477575E	00162	0.4805209E-04	0.	0.4478286E-04	
1,	0.1482247E-01	0.	1	0.1501666E	00163	0.9307389E-04	0.	0.0000000E	00
1,	0.1524199E-01	0.	1	0.1505435E	00164	0.2831086E-04	0.	0.9654855E-06	
1,	0.1496423E-01	0.	1	0.1503145E	00165	0.4224337E-04	0.	0.1678412E-04	
1,	0.1026253E-01	0.	1	0.1558591E	00166	0.9435548E-05	0.	0.4928702E-05	
1,	0.8335335E-02	0.	1	0.1609532E	00167	0.2912220E-05	0.	0.0000000E	00
1,	0.4766672E-02	0.	1	0.1585993E	00168	0.2207683E-04	0.	0.7970860E-04	
1,	0.6790746E-02	0.	1	0.1618717E	00169	0.9851096E-06	0.	0.0000000E	00
1,	0.9307867E-02	0.	1	0.1590967E	00170	0.8796288E-06	0.	0.4098430E-05	
1,	0.1006471E-01	0.	1	0.1639369E	00171	0.1164427E-06	0.	0.8252745E-17	
1,	0.1265873E-01	0.	1	0.1616397E	00172	0.9451114E-10	0.	0.3982663E-09	
1,	0.1571452E-01	0.	1	0.1658204E	00173	0.4027887E-08	0.	0.1247651E-18	
1,	0.1833755E-01	0.	1	0.1665170E	00174	0.8003077E-09	0.	0.1090975E-09	
1,	0.1437274E-01	0.	1	0.1642043E	00175	0.2950589E-10	0.	0.4471417E-11	

TABLE 5.2 (Contd.)

1	0.1799114E-01	0	1	0.1658778E	00176	0.2966582E-11	0.3662291E-11
1	0.2255724E-01	0	1	0.1669006E	00177	0.8729367E-12	0.3416989E-12
1	0.2402778E-01	0	1	0.1669629E	00178	0.9256281E-12	0.2259936E-12
1	0.2886278E-01	0	1	0.1712580E	00179	=0.4166552E-13	0.1474661E-23
1	0.2931808E-01	0	1	0.1736573E	00180	=0.8923508E-14	0.1036985E-23
1	0.2840751E-01	0	1	0.1766859E	00181	=0.1369186E-14	0.0000000E 00
1	0.2569697E-01	0	1	0.1765443E	00182	=0.4073066E-14	0.5827380E-15
1	0.2189125E-01	0	1	0.1775010E	00183	0.4863022E-14	0.2518223E-14
1	0.2670536E-01	0	1	0.1837948E	00184	0.3217452E-14	0.1150104E-13
1	0.2687876E-01	0	1	0.1891177E	00185	0.8950369E-14	0.5630189E-13
1	0.3183097E-01	0	1	0.1920526E	00186	0.2786981E-13	0.5992100E-13
1	0.3269972E-01	0	1	0.1934377E	00187	0.2219847E-13	0.5695835E-13
1	0.3329747E-01	0	1	0.1976304E	00188	=0.6283766E-14	0.0000000E 00
1	0.3096254E-01	0	1	0.1963624E	00189	0.4065984E-14	0.5097832E-14
1	0.3474268E-01	0	1	0.1995751E	00190	=0.1108702E-14	0.5199757E-25
1	0.3351959E-01	0	1	0.2000227E	00191	=0.1693862E-15	0.0000000E 00
1	0.3086250E-01	0	1	0.1992382E	00192	=0.5337334E-16	0.0000000E 00
1	0.2812419E-01	0	1	0.1991535E	00193	0.3248465E-16	0.0000000E 00
1	0.2806518E-01	0	1	0.1991309E	00194	=0.2281794E-16	0.1221809E-16
1	0.2545914E-01	0	1	0.2026488E	00195	=0.1642611E-16	0.1479807E-16
1	0.2252839E-01	0	1	0.2084248E	00196	0.7744322E-17	0.0000000E 00
1	0.2130661E-01	0	1	0.2083360E	00197	0.2317619E-17	0.6781784E-28
1	0.2472317E-01	0	1	0.2104867E	00198	0.9425419E-19	0.6646538E-20
1	0.2492496E-01	0	1	0.2138065E	00199	=0.7024179E-19	0.0000000E 00
1	0.2448791E-01	0	1	0.2140156E	00200	0.6527538E-19	0.0000000E 00
1	0.2513990E-01	0	1	0.2138935E	00201	=0.2777060E-19	0.8571879E-30
1	0.2193469E-01	0	1	0.2135749E	00202	0.1638897E-21	0.5798142E-32
1	0.2281438E-01	0	1	0.2129425E	00203	0.3118156E-21	0.9257257E-32
1	0.2462553E-01	0	1	0.2133919E	00204	=0.3782628E-19	0.2299348E-19
1	0.2261459E-01	0	1	0.2162759E	00205	=0.2089655E-19	0.4511077E-20
1	0.2239264E-01	0	1	0.2163294E	00206	0.6440353E-19	0.7560033E-20
1	0.2732469E-01	0	1	0.2156044E	00207	=0.6505635E-20	0.1514058E-21
1	0.2529856E-01	0	1	0.2160052E	00208	0.7800313E-21	0.1195350E-20
1	0.2018328E-01	0	1	0.2149277E	00209	=0.1775683E-21	0.3330231E-21
1	0.2061839E-01	0	1	0.2190054E	00210	=0.1109787E-21	0.5669218E-32
1	0.2713085E-01	0	1	0.2150333E	00211	=0.1203836E-22	0.3378069E-23
1	0.2897127E-01	0	1	0.2166853E	00212	=0.8572101E-23	0.5220139E-24
1	0.2406446E-01	0	1	0.2157407E	00213	=0.7821858E-23	0.0000000E 00
1	0.2057459E-01	0	1	0.2140329E	00214	0.2618043E-23	0.9256320E-34
1	0.2249861E-01	0	1	0.2151989E	00215	0.3025215E-24	0.1077480E-34
1	0.2367445E-01	0	1	0.2163946E	00216	0.1069499E-24	0.3156553E-35
1	0.2656629E-01	0	1	0.2137473E	00217	0.3346088E-26	0.6063222E-25
1	0.3181270E-01	0	1	0.2112957E	00218	0.6131250E-23	0.1784429E-33
1	0.3701816E-01	0	1	0.2121256E	00219	=0.3471917E-24	0.3115299E-24
1	0.3824335E-01	0	1	0.2178570E	00220	=0.4634352E-25	0.2246342E-25
1	0.3955288E-01	0	1	0.2226300E	00221	=0.1109953E-25	0.4751028E-36
1	0.4185776E-01	0	1	0.2256770E	00222	=0.4272638E-25	0.0000000E 00
1	0.3489620E-01	0	1	0.2278514E	00223	=0.3201175E-26	0.1554669E-26
1	0.3265954E-01	0	1	0.2280479E	00224	=0.4258679E-27	0.6185458E-28
1	0.3558883E-01	0	1	0.2282203E	00225	=0.3166005E-28	0.6946760E-28
1	0.4109160E-01	0	1	0.2301465E	00226	=0.6297933E-29	0.2874830E-28
1	0.3479675E-01	0	1	0.2315407E	00227	=0.9001609E-29	0.4278990E-29
1	0.3812675E-01	0	1	0.2319773E	00228	=0.5867634E-27	0.2746671E-27
1	0.4312188E-01	0	1	0.2348595E	00229	0.1954475E-28	0.2110713E-28
1	0.4220346E-01	0	1	0.2371920E	00230	=0.1535865E-28	0.2829724E-28
1	0.4291481E-01	0	1	0.2416443E	00231	0.1059014E-28	0.5082138E-39
1	0.4594818E-01	0	1	0.2431456E	00232	=0.4635470E-30	0.0000000E 00
1	0.4298536E-01	0	1	0.2462060E	00233	0.8239332E-29	0.4109426E-39
1	0.4725114E-01	0	1	0.2432371E	00234	0.5698862E-29	0.0000000E 00
1	0.4345069E-01	0	1	0.2390299E	00235	=0.2989501E-29	0.1474672E-39

TABLE 5.2 (Contd.)

1	0.4552808E-01	0.	1	0.2383452E	00236	0.6240161E-30	0.1953627E-39
1	0.5150831E-01	0.	1	0.2370881E	00237	=0.8313006E-31	0.0000000E 00
1	0.5094978E-01	0.	1	0.2391137E	00238	=0.1044739E-31	0.3389069E-42
1	0.5182293E-01	0.	1	0.2402295E	00239	=0.1355884E-31	0.0000000E 00
1	0.5051846E-01	0.	1	0.2400875E	00240	=0.1838710E-31	0.2891035E-31
1	0.5423669E-01	0.	1	0.2457483E	00241	0.1132832E-31	0.2927416E-31
1	0.4721429E-01	0.	1	0.2460600E	00242	=0.1075153E-31	0.3568889E-42
1	0.4799015E-01	0.	1	0.2460372E	00243	=0.1729907E-31	0.1545368E-32
1	0.4364324E-01	0.	1	0.2442601E	00244	0.5965332E-32	0.6511908E-33
1	0.5141538E-01	0.	1	0.2452707E	00245	=0.4553144E-33	0.0000000E 00
1	0.5057899E-01	0.	1	0.2467178E	00246	=0.2219616E-34	0.6090533E-34
1	0.5333622E-01	0.	1	0.2491478E	00247	0.1861251E-34	0.5464714E-45
1	0.5475451E-01	0.	1	0.2485961E	00248	0.3314314E-35	0.0000000E 00
1	0.4911946E-01	0.	1	0.2497681E	00249	=0.2921085E-35	0.1523454E-35
1	0.5352334E-01	0.	1	0.2489579E	00250	=0.7654904E-36	0.1706683E-35
1	0.5472849E-01	0.	1	0.2528634E	00251	0.3249832E-36	0.1850085E-36
1	0.5548872E-01	0.	1	0.2528634E	00252	0.2363187E-37	0.1085645E-37
1	0.5932841E-01	0.	1	0.2586009E	00253	0.4217990E-37	0.4126114E-37
1	0.6473377E-01	0.	1	0.2621671E	00254	0.1024191E-36	0.3757094E-47
1	0.7109500E-01	0.	1	0.2610828E	00255	0.5440240E-38	0.1679322E-37
1	0.7475227E-01	0.	1	0.2661004E	00256	=0.9583770E-38	0.4270926E-37
1	0.7327912E-01	0.	1	0.2724881E	00257	0.7035007E-38	0.7264450E-38
1	0.6964114E-01	0.	1	0.2730206E	00258	0.3220287E-38	0.3663571E-37
1	0.6548542E-01	0.	1	0.2756300E	00259	0.7427859E-38	0.1006243E-38
1	0.6311579E-01	0.	1	0.2775696E	00260	0.4830898E-38	0.0000000E 00
1	0.5879937E-01	0.	1	0.2778294E	00261	0.0000000E 00	0.8063672E-39
1	0.5508360E-01	0.	1	0.2812769E	00262	0.5194349E-41	0.1526046E-41
1	0.5442826E-01	0.	1	0.2852469E	00263	=0.4634945E-41	0.1637710E-51
1	0.5786838E-01	0.	1	0.2891986E	00264	0.1416197E-43	0.2324906E-42
1	0.5293046E-01	0.	1	0.2872163E	00265	0.1850880E-42	0.0000000E 00
1	0.5212203E-01	0.	1	0.2863294E	00266	=0.6823922E-43	0.1501730E-42
1	0.4910564E-01	0.	1	0.2911095E	00267	=0.1058872E-43	0.7409279E-54
1	0.4999286E-01	0.	1	0.2912630E	00268	=0.8889288E-44	0.9826368E-44
1	0.4918647E-01	0.	1	0.2922305E	00269	0.4359817E-44	0.1399057E-54
1	0.5364852E-01	0.	1	0.2950332E	00270	=0.4605758E-45	0.1046043E-44
1	0.5335494E-01	0.	1	0.2994226E	00271	0.9326756E-46	0.4010583E-45
1	0.5642024E-01	0.	1	0.3051026E	00272	=0.6538636E-47	0.7812175E-46
1	0.6021223E-01	0.	1	0.3092448E	00273	=0.1037687E-48	0.1376604E-49
1	0.5822912E-01	0.	1	0.3111586E	00274	0.3230285E-50	0.0000000E 00
1	0.5268981E-01	0.	1	0.3133207E	00275	=0.1366514E-49	0.0000000E 00
1	0.5045202E-01	0.	1	0.3130858E	00276	=0.2822250E-50	0.0000000E 00
1	0.4963820E-01	0.	1	0.3149865E	00277	0.1123156E-50	0.6581799E-51
1	0.4887327E-01	0.	1	0.3161471E	00278	=0.6108551E-51	0.1165318E-50
1	0.5138718E-01	0.	1	0.3179649E	00279	=0.1044102E-51	0.3482851E-62
1	0.5214584E-01	0.	1	0.3220397E	00280	=0.2279643E-52	0.3790024E-53
1	0.4952897E-01	0.	1	0.3211807E	00281	0.7712027E-53	0.2939370E-53
1	0.4879822E-01	0.	1	0.3207818E	00282	=0.5911003E-53	0.0000000E 00
1	0.4355024E-01	0.	1	0.3208895E	00283	0.3845032E-52	0.0000000E 00
1	0.4101826E-01	0.	1	0.3208895E	00284	=0.3461650E-52	0.1095389E-62
1	0.4806137E-01	0.	1	0.3227241E	00285	=0.1444749E-52	0.1643479E-53
1	0.4728762E-01	0.	1	0.3231097E	00286	0.6441211E-52	0.2312636E-62
1	0.5030441E-01	0.	1	0.3260569E	00287	=0.7711259E-53	0.7845567E-53
1	0.4383819E-01	0.	1	0.3242681E	00288	=0.8480618E-53	0.5371008E-54
1	0.4211764E-01	0.	1	0.3237653E	00289	=0.2928689E-52	0.9192107E-63
1	0.4756377E-01	0.	1	0.3226965E	00290	=0.1424900E-53	0.1154478E-63
1	0.5344620E-01	0.	1	0.3269163E	00291	0.3674634E-54	0.0000000E 00
1	0.5270307E-01	0.	1	0.3276217E	00292	=0.1878986E-54	0.7952752E-65
1	0.5922616E-01	0.	1	0.3244522E	00293	0.9549203E-56	0.1525524E-55

TABLE 5.2 (Contd.)

1	0.6012993E-01	0	1	0.3248999E 00294	=0.1639773E-55	0.1172718E-55
1	0.5889990E-01	0	1	0.3252635E 00295	=0.1456198E-56	0.4419417E-67
1	0.6372671E-01	0	1	0.3242419E 00296	0.1858031E-57	0.3259728E-59
1	0.6448734E-01	0	1	0.3214954E 00297	=0.2158020E-57	0.8650099E-58
1	0.6469881E-01	0	1	0.3219807E 00298	0.1764587E-58	0.1645377E-68
1	0.7254556E-01	0	1	0.3229571E 00299	0.1356529E-59	0.9062525E-61
1	0.7003131E-01	0	1	0.3227147E 00300	0.2817414E-61	0.0000000E 00
1	0.6410134E-01	0	1	0.3237767E 00301	0.6758617E-62	0.0000000E 00
1	0.5936452E-01	0	1	0.3273601E 00302	=0.1717548E-62	0.1835840E-72
1	0.6528497E-01	0	1	0.3224491E 00303	0.7354887E-63	0.7475947E-63
1	0.6010858E-01	0	1	0.3250623E 00304	0.5143793E-63	0.0000000E 00
1	0.5362730E-01	0	1	0.3232166E 00305	0.8704098E-64	0.2829310E-64
1	0.5110234E-01	0	1	0.3279684E 00306	=0.1852961E-63	0.5828285E-64
1	0.5399933E-01	0	1	0.3332231E 00307	0.1194865E-64	0.2432209E-64
1	0.4883462E-01	0	1	0.3337848E 00308	=0.8530390E-65	0.3748397E-75
1	0.5219726E-01	0	1	0.3345168E 00309	=0.4336172E-66	0.2724467E-76
1	0.5806424E-01	0	1	0.3318636E 00310	0.1286238E-66	0.1800006E-67
1	0.5427770E-01	0	1	0.3329667E 00311	0.2424929E-67	0.0000000E 00
1	0.4896662E-01	0	1	0.3331526E 00312	=0.2401505E-68	0.3971147E-68
1	0.4983391E-01	0	1	0.3357741E 00313	0.2719823E-68	0.0000000E 00
1	0.4409191E-01	0	1	0.3354653E 00314	0.6191833E-69	0.0000000E 00
2	0.4278176E-01	2	1	0.3350913E 00315	0.6191833E-69	0.0000000E 00

SECTION 6

DISCUSSION OF RESULTS AND COMPARISON WITH THEORY

The experimental work, which involved the measuring of side wall pressures, was carried out to provide a quantitative check on the predictions of the model. The side wall pressures obtained are a function of the type of powder, as well as of the geometry of the die and the method of pressing, thus it was not possible to deduce values from other research and use it to compare with the predictions of this model. Since the model proposed here was the first of its kind to be developed a great deal of effort has gone into developing the mechanics of the model and its programming for a computer; it was therefore necessary to make certain simplifications in its construction with the result that its predictions were not expected to extend to such complex features of compaction as the density variations or the ejection pressures. It was therefore decided to curtail the experimental program in favour of solving the mathematical difficulties pertaining to force simulation and model building. The results are produced by the model, therefore somewhat less than perfect, but encouraging, when the difficulties of simulating such complex entities as particle systems are considered.

The experimental side wall pressures vs. compact height curves are shown in Figures 5.5 and 5.6 for the powder which was characterised by the size distributions shown in Figures 5.3 and 5.4. These side wall pressures were obtained using the apparatus described in Section 4. At each stage of the pressing operation, it was possible to monitor the volume of the compact and thus its average porosity could be determined. This value was used in activating the calculation of the force diagram.

This value was an average and its use was probably unjustified, but the error introduced as a result was expected to be acceptable. What was less justifiable was the assumption of an even distribution of pressure over the punch surface, which was made for the sake of simplicity alone. The experimental results are re-plotted in Figure 5.10, where they are compared with the predictions of the model for 2, 4 and 6.5 tons applied load. At the lower pressures (2 tons) the model predicts higher values than those obtained experimentally, while at higher pressures the predictions are too low. At 4 tons, applied load, there is fairly good agreement between prediction and experiment. The type of force diagram used in the calculation of the side wall pressure is shown in Figure 5.7. This shows the distribution of transmitted force in the system when a force of 10000 lb. is applied to a particle at 0. The diagram was constructed on the basis of 500 random walks and seems to indicate that this number was inadequate to give a representative diagram. Since, however, even 500 walks took up 20 hours of computer time, it was considered unjustifiable to increase this number until further improvements were made to the model. In spite of these comments, the force diagram does demonstrate that the force is not transmitted to any great extent in the lateral direction, a fact which becomes only too clear when trying to make non-symmetrical compacts. It also indicates that the force is transmitted in a cone from 0.

The predictions of higher side wall pressures at low values of applied pressure, and vice versa, can be explained to some extent

by the invalidity of the assumptions. At lower values of applied load, the assumption of 12 contacts (6 of which were expected to transmit force) is probably untrue and the number is probably less. It has further been demonstrated, that, at low pressures interparticle friction has a greater effect than at high values, the model ignores both these effects since no usable values were available at the time it was constructed. At higher pressures there not only are more than twelve contacts, but, more significantly, deformation also. Until such time as deformation can also be represented statistically the model cannot be used at higher pressures. It appears therefore that at about 4 tons, applied load, the deformation is not serious and that the assumption of six transmitting contacts is reasonably true.

The curves of Figure 5.8 represent the % of applied pressure transmitted to various depths in the die for different height:diameter ratios. The decay indicated by these results is far in excess of observed values. This phenomenon is partly bound up with the number of significant digits that the computer can store, and as shown in Table 5.2 an applied force of 10^{50} decreases to 10^{-70} in about 350 transmissions. Since unfortunately only about 0.5 " is penetrated during the travel through 350 particles, there is a false indication that all the applied force is lost after this distance, whereas the truth is that height:diameter ratios of about 15 are required before the applied force is totally lost. The model does however predict the expected trend and shows that the increase of the height:diameter ratio lowers the transmitted pressure. It needs a change in the application

of the Monte Carlo method to solve this problem but this should not prove too difficult.

The final prediction concerns the friction loss at the wall and again the model overestimates rather badly. The results are shown in Figure 5.9. The reason for this is partly the same reasons given above and partly the assumption of a constant coefficient of friction along the die wall. It is now known that it is the product of $\mu \times \beta$ i.e the coefficient of friction \times ratio of axial to radial stress, that remains constant and a variation in the coefficient of friction between .6 and .1 has been demonstrated by some workers in the field. It is however difficult to take this into consideration until some method of finding β is proposed, preferably as a function of particle characteristics.

Thus the discussion of the results obtained demonstrate that the model, although producing encouraging predictions, has to be further developed before it may be used as a useful research tool. The fact that the model cannot be yet used in the prediction of density distributions in the die, stem from the assumption that the transmitted force stops on reaching a boundary. Although this makes handling of the results easier, it is possible to take into consideration the force that is not absorbed at the wall, and which continues being transmitted. It is this type of force that causes density variations and more attention must be paid to them in the further development of the model. Suggestions concerning the improvement of the model are given in detail in the next section.

SECTION 7

CONCLUSIONS AND SUGGESTIONS FOR FURTHER WORK

7.1 Conclusions

From what has been said in the foregoing sections, it is apparent that powder systems are impossible to define analytically and difficult to define statistically. The attempt made here has been the first of its kind, and had as a consequence, to define parameters, determine mathematical techniques to handle the statistical methods proposed, build a credible model and make the assumptions necessary to get it off the ground. It is therefore not particularly surprising that the results obtained to date can only be described as encouraging. The work done here is a necessary prerequisite to any further improvement of the model and goes a long way towards providing the guidelines for future developments.

The model predicts, directly or indirectly, the following known features of die compaction.

- a) Increased diameters lessen die wall friction
- b) For the same height:diameter ratio larger diameters increase the the transmission of force, lessen wall friction and hence decrease the variations in density.
- c) Increasing the height:diameter ratios lessens the force transmission, increases wall friction and causes the density variations to increase.

The model is unable to make quantitative predictions of density variations or of ejection pressures.

Thus it may be concluded that, subject to improvement along the lines suggested hereafter, the model promises to be a possible

means of evaluating the compaction process without arduous experimentation. It seems likely however that it will prove an expensive process.

7.2 Suggestions for Further Work and Discussion of the Future

Performance of the Model

In the immediately preceding sections the failings and the inadequacies of the model have been discussed as well as its achievements and advantages. In order to improve the model, the assumptions that have proved questionable must be examined, and, where possible, improved.

The first major assumption was that there are twelve contacts per particle, and that six of these transmit force. The reasoning behind this assumption, was that dense packings of spheres exhibit twelve contacts, six of which, lying on the 'opposite' side to the contact to which a load was applied, could transmit force. A force balance on such a sphere could thus solve, by analytical means, the values of the output forces. Since the system examined here was restricted to convex particles of a not very diverse size distribution, it was decided to extend the assumption to these particles as well. As also indicated by the degree of compaction obtained at the lower applied loads (50% vs. a theoretical maximum of 64% for close packed spheres) it is apparent that twelve contacts do not occur. Inter-particle friction, which was neglected, may also play a part at these pressures. Thus steps should be taken to determine what effect pressure has on packing of spheres and other particle shapes. Further information should be sought on inter-particle friction,

and the information incorporated into the model. The general type of model used here does not seem feasible, and calculations will have to be done for each type of load separately. As this would mean an unacceptable increase in computing time, methods must be investigated that quicken the random walk. With computers becoming faster it is likely that this problem is capable of being overcome.

The problem of more than six transmitting contacts can be solved by the use of relaxation methods and the like, but it is unlikely to occur in the range of interest and even if it did, the problem of deformation would become predominant. As regards deformation, information currently becoming available on single particle crushing and stresses at the points of contact can be used in determining what effect deformation has on the statistical parameters defining the system. This information could again be built into the model. It is, however, difficult to say just how far these proposals will go towards eliminating the divergence of the predicted and experimental results, but there is a good chance that the side wall pressures, at least, could be improved in this way.

In order to determine the variations in density, again, more than one set of random walks seem likely to be required. These would take account of force 'quanta' being 'reflected' off the wall from particles in their vicinity. Further there needs to be superpositioning of force diagrams before building up the final stress distribution pattern for the die. It is possible to

from walks
 obtain these diagrams performed for the surface particles, the
 only difference being in the normalisation procedure.

The method of determining the number of surface particles could
 also be improved. The present method depends on an average size,
 an assumption that can no longer be made if size distributions
 with a greater variety of sizes were being used. *Investigation
 replaced by the actual surface voidage, determined after compaction*
 of the angle of internal friction, the coefficient of friction
 at the die wall under different conditions and their use with the
 model would also increase the accuracy of its predictions. The
 inaccuracy with regard to the transmitted pressure which results
 mainly from the limits imposed on the storage of numbers by the
 computer could be overcome by changing the application of the
 Monte Carlo method. Some means of bringing decaying numbers up to
 the significance limits of the computer, without destroying the
 validity of the normalisation process has to be discovered. This
 together with the knowledge of both the coefficients of internal
 and wall friction, should solve the remaining inadequacies of the
 model.

To conclude this thesis, therefore, it is claimed that the
 statistical characterisation of a system of particles restrained
 in a rigid die has been achieved, and the practicability of
 applying statistical techniques such as the Monte Carlo method
 to such systems has been demonstrated. Where the model falls short
 of expectations has been made clear and suggestions which should
 improve it have been made. Although the successful development of
 such a model might eliminate the need for a great deal of tedious

experimentation, the cost of operating it seems likely to be high unless faster computers and new techniques are able to quicken the simulation procedure appreciably.

APPENDICES

2.1 Unckel's mathematical evaluation of the compaction process	i
3.1 The computer model	iv
3.2 Labelling of the forces	v
3.3 The particles on a surface	viii

Appendix 2.1 (Reference 30)

If it is assumed that the pressure applied to the punch surface is uniformly distributed over its surface, then the average pressure, p_s , is given by

$$p_s = \bar{p} / (D^2 \pi / 4) \quad \text{-----1}$$

where D is the diameter of the punch and \bar{p} is the force applied to punch.

Since particle systems do not behave as liquids, the fraction of this pressure reaching the wall is $\beta \bar{p}$ and the friction at the wall is: $\beta \mu \bar{p}$ where μ is the coefficient of friction at the wall. If we consider two cross sections a distance dh apart,

$$\tau dh D \pi = -d\bar{p} (D^2 \pi / 4) \quad \text{-----2}$$

where $\tau = \beta \mu \bar{p}$ -----3

$$\therefore \frac{-d\bar{p}}{\bar{p}} = (dh \cdot 4 \cdot \beta \cdot \mu) / 4 \quad \text{-----4}$$

integrating between $h=0$ and $h=H$ (top and bottom, respectively) and using $h=0$ to evaluate the constant,

$$p = (4\bar{p}/D^2 \pi) e^{-4\beta\mu h/D} \quad \text{-----5}$$

$$= (4\bar{p} / D^2 \pi) e^{-4\beta\mu h/D} \quad \text{-----6}$$

For plastic flow to occur the following condition must be satisfied

$$k = \sqrt{((\sigma_a - \sigma_r)/2)^2 + \tau^2} \quad \text{-----7}$$

where σ_a and σ_r are axial and radial stresses respectively.

The minimum resistance to displacement is given by

$$k = \mu_1 \sigma_2 \quad \text{-----8}$$

where μ_1 is the coefficient of internal friction.

$$\sigma_1 \text{ or } \sigma_2 = ((\sigma_a + \sigma_r)/2) \pm \sqrt{((\sigma_a - \sigma_r)/2)^2 + \tau^2} \quad \text{-----9}$$

if $\tau = (\sigma_a + \sigma_r)/2$ -----10

(replace outer shear stress by mean shear stress x coefficient of friction at the outer edge), then using eqtns. 8 and 10 and 9 in 7

$$\sigma_r = \sigma_a \frac{1 + \mu_i - \sqrt{\mu_i^2 - (1 + \mu_i)^2 \mu^2}}{1 + \mu_i + \sqrt{\mu_i^2 - (1 + \mu_i)^2 \mu^2}} \text{-----11}$$

i.e. $r = a$

This gives $\beta = .72$ if $\mu = .15$ and $\mu_i = .25$
 and $\beta = .66$ if $\mu = 0$ and $\mu_i = .25$

If 2α is the angle formed by the direction of principal stress with the radial direction then,

$$\tan 2\alpha = 2E / (\sigma_a - \sigma_r) \text{-----12}$$

at the wall $E = \sigma_r \mu$ and $\sigma_r = \beta \sigma_a$, thus

$$\tan 2\alpha = 2\beta\mu / (1 - \beta) \text{-----13}$$

The assumption that the pressure is uniformly distributed is, however, incorrect. It is lowest at the centre of the punch and increases to a maximum at the outer edge. It is also less at the bottom outer edge, following a relation of the form

$$p_{\text{wall}} = c_1 e^{-ch} \text{-----14}$$

where h is the depth.

It is assumed that the pressure under the punch is proportional to the radial distance from the centre. Then,

$$\frac{dp_s}{dr} = c_2 r \text{ or } p_s = c_2 r^2 + c_3 \text{-----15}$$

where c_2 and c_3 are constants. This is the equation of a parabola.

A similar equation describes the pressure on the bottom punch.

$$p_b = -c_4 r^2 + c_5 \text{-----16}$$

$$T_{\text{punch}} = \int_0^R (c_2 r^2 + c_3) / \beta \cdot 2\pi r \, dr$$

$$T_{\text{bottom}} = \int_0^R (-c_4 r^2 + c_5) / \beta \cdot 2\pi r \, dr$$

from eqtn.15

$$R^2 c_2 + c_3 = c_1 / \beta \quad \text{-----17}$$

and from eqtn.16

$$-c_4 R^2 + c_5 = c_1 e^{-cH} / \beta \quad \text{-----18}$$

The sum of the punch force, bottom pressure and total friction must be zero.

$$\int_0^R (c_2 r^2 + c_3) \cdot 2\pi r \, dr - \int_0^R (-c_4 r^2 + c_5) \cdot 2\pi r \, dr - \int_0^H c_1 e^{-ch} \cdot \pi D \, dh = 0 \quad \text{-----19}$$

and hence

$$\bar{p} - 2\pi (-c_4 R^4/4 + c_5 R^2/2) - \pi D \int_0^H c_1 e^{-ch} \, dh = 0$$

If we now assume that wall friction is the same regardless of whether the pressure is uniform over the punch face or not, then,

$$\int_0^H \frac{\bar{p}}{D^2 \pi / 4} e^{-4\beta r^2 h/D} \, dh = \int_0^H c_1 e^{-ch} \, dh \quad \text{--- 20}$$

$$-\bar{p} / D \pi \beta \pi (e^{-4\beta r^2 H/D} - 1) = -c_1 \cdot (e^{-cH} - 1) / c \quad \text{-----21}$$

If the cross section at which the pressure is independent of the radius is known c_1 can be calculated, since

$$\bar{p} / (2\pi D/4) \cdot e^{-(\beta r^2 / D) \cdot H'} = c_1 e^{-cH'} \quad \text{---22}$$

where H' is the depth of such a cross section

$$H' = 7/12 H$$

Thus

$$\bar{p} - 2\pi (-c_4 R^4/4 + c_5 R^2/2) - \bar{p} (e^{-4\beta r^2 H/D} - 1) = 0 \quad \text{-----23}$$

now from eqtns.21 and 22 c_1 and c_2 are found hence

$$-c_4 R^2 + c_5 = c_1 e^{-cH/\beta} \quad \text{can be evaluated. Hence } c_4$$

and c_5 can be determined.

Appendix 3.1The Computer Model

The program generating the points of contact and tracing the force transmission through the system is attached as series of print outs. Print out 1 shows the master program, which is also shown in Flow Diagram 1. Print out 2 shows the program that generates the points of contact, based on the theory described in the text. Print out 3 shows the program that calculates the coordinates of each point of contact that the force passes through with reference to the system axes. The theory used is that given in section 3.4. Print out 4 shows the program that sets up the force balance on each particle as set out in section 3.2. Finally print out 5 shows the program that solves the six equations to output the transmitted force at the point of contact through which the propagation is followed. The method used is the standard Gauss elimination with partial pivoting.

Appendix 3.2

Labelling of the Forces

See Figure 3.12. For the purpose of using the results of random walks performed on a large system to analyse smaller systems it is necessary to first subdivide the system as shown in the figure. If the runs were performed on the system OCTQ, an analysis of all the systems represented by a combination of the several smaller squares (or rectangles) such as OAEM, OAGP, or OBIM is possible provided the forces crossing the boundaries of such systems could be labelled. A system by which each force is labelled with four indices was devised for this purpose. Thus a force is always remembered as $F(I,X,Z,J)$ where the indices are evaluated as follows.

a) The index I

Any force, as mentioned in the text, can be represented by two components in the r- and z- directions. Thus $I=1$ represents the r-component and $I=2$ represents the z-component.

b) The index X

As a force progresses on its way to the boundary, it crosses the grid lines represented by lines such as AR, BB, CT etc. The index X indicates which vertical boundary is crossed at the moment the force is labelled. Within the grid lines themselves the force is not labelled. Thus an r-component of a force crossing AE will be remembered as $F(1,1,Z,J)$.

c) The index Z

This signifies either which horizontal grid line has been crossed by the force or, if it has crossed a vertical line, its horizontal position. If it crosses AR between A and E, $Z=1$, if it crosses between E and G, $Z=3$ and so on. The even numbers are used similarly for the horizontal grid lines, starting with $Z=2$ for MF through to $Z=6$ for .

QT.

d) The index J

In order to calculate the force due to a surface particle at any point in the system, one needs to consider the system bounded by the particle and the point. In order to obtain the information from the results of the random walks performed on a larger system, therefore it is necessary to devise some way in which we can meet our postulate that force transmission stops at the boundary of a system. Consider system OCTQ for which the walks were performed. Then consider system OAEM for which the analysis is required. If a force crosses ME then as far as the subsystem OAEM is concerned, that force has left its boundaries. Since however the walks were performed on the larger system OCTQ this force may reenter the system and be recorded crossing AE. If however we were considering AOPG we would wish to record this force, since ME is not one of its boundaries. Thus the index J was introduced to indicate which vertical or horizontal line was the furthest crossed before it was recorded crossing a horizontal or vertical line respectively. Odd numbers from 3 onwards are used to describe the vertical lines AR(J=3), BS(J=5) and CT(J=7) and even numbers from 2 onwards for the horizontal lines MF(J=2), PH(J=4) and QT(J=6). Forces leaving any system at the surface are labelled with J=20. The following examples should make the process clear.

a) A force crosses AE having not crossed any grid lines previously

It is remembered as $F(I,1,1,1)$ $I=1,2$

b) A force crosses EI, having previously crossed AE

It is remembered as $F(I,2,2,1)$ $I=1,2$

c) A force crosses EI having previously crossed AE and BI. It is remembered as $F(I,2,2,5), F(I,2,2,1)$ $I=1,2$

i.e. it will be considered in system OCFM but not in system OBIM.

d) A force crosses AE having crossed ME. It is remembered as

$F(I,1,1,2)$ and $F(I,1,1,1)$ $I=1,2$

i.e. it will be considered in OAGP but not in OAEM.

e) A force crosses AE having previously crossed it.

It is not remembered.

f) A force having previously crossed PH and BS leaves the system

along OC. It is remembered as $F(I,3,5,20)$ $I=1,2$

Note: In all cases the forces are also recorded at the previous boundaries crossed.

Print out 6 shows the program written to label forces as described here. Using these labels the program proceeds to normalise the force diagrams.

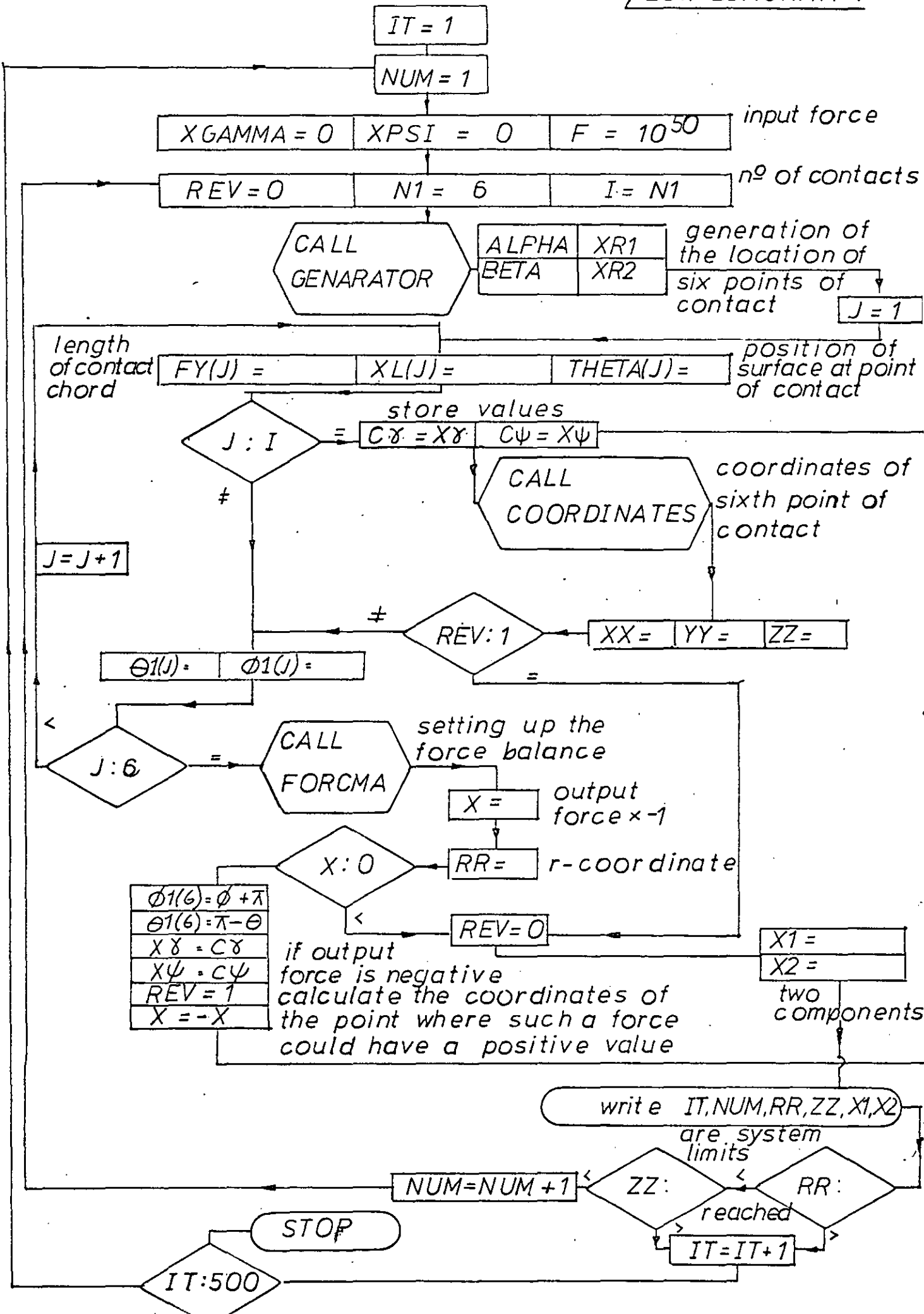
Appendix 3.3

The Particles on the Surface

Before normalisation can take place it is necessary to know how many particles lie on the surface so that the applied force per particle may be calculated. Consider Figure 3.14, If the voidage after the application of a load is known, and one makes the assumption that the voidage is uniform over the surface, then using an average particle size it is possible to calculate the number of particles on the surface. The distance between neighbouring particles will be $\frac{2r}{1-\epsilon}$ where r is the radius of the average particle and ϵ the voidage. Having calculated the number on the surface it is also necessary for the construction of the force diagram, to know the distance distribution of these particles from any point, within the system, at which the force is required. It is found that the force transmission in a lateral direction is very small, of the order of about ten diameters. Thus, there is unlikely to be transverse particle movement in a die. In order to determine this, however, not only the distance distribution of particles surrounding a point is required, but also, where the particles are non uniformly distributed, the numbers lying to one side which are in excess of the numbers lying to the other.

Print out 7 shows the program designed to calculate the necessary information. Print out 8 shows the results produced by this program for the system shown in figure 3.14.

FLOW DIAGRAM 1



PRINT OUT 1

X

MASTER G378

C FORCE DISTRIBUTION IN BED DUE TO ONE PARTICLE
CTHE CASE WITHOUT FRICTION

```
    DIMENSION GAMMA(6),PSI(6),XR1(6),XR2(6)
    COMMON THETA(6),ALPHA(6),BETA(6),FY(6),XX,ZZ,YY,X,XL(6),F,
    1 XGAMMA,XPSI,XMU1(6),XMU2(6),THETA1(6),FY1(6),P1(11),R2(11),DAT
    CALL ITIME(I1)
    PV=3,1415926535897932384626433832795
    LIMIT1=10
    LIMIT2=4
    READ(1,40)MM
40  FORMAT(I1)
    IF(MM.EQ.2) GO TO 207
206 CONTINUE
    READ(1,39)K1,K2,K3,K4,K5,K6,ITERATIONS
59  FORMAT(1H ,6I10,I4)
    GO TO 208
207 CONTINUE
    DO 210 ITERATIONS=1,10
208 CONTINUE
    NUMBER=1
    XGAMMA=0.
    XPSI=0.
    F=(10.**50)
32  CONTINUE
    REV=0.
    N1=6
    I=N1
    CALL GENERATOR(J,K1,K2,K3,PV,N1,XR1,XR2)
    DO 2 J=1,N1
    FY1(J)=UTR1(1,1,K4)*2.*PV
    XL(J)=SQRT((XR1(J)**2)+(XR2(J)**2))
    THETA1(J)=UTR1(2,1,K5)*PV
    IF(J.LT.1) GO TO 20
300 CGAMMA=XGAMMA
    CPSI=XPSI
21  CALL COORDINATES(NUMBER,PV,REV,I,XC,XD,XE)
    IF(REV.EQ.1.) GO TO 73
20  CONTINUE
    THETA(J)=THETA1(J)
    FY(J)=FY1(J)
2  CONTINUE
    XTHETA=0.
    XFY=0.
6  CALL FORCMA(XTHETA,XFY,N1,NUMBER)
    J=6
    F=-X
    RR=SQRT((XX**2)+(YY**2))
    IF(X)73,7,74
74  FY1(J)=FY(J)+PV
    THETA1(J)=PV-THETA1(J)
    XGAMMA=CGAMMA
    XPSI=CPSI
    REV=1.
    J=1
    F=X
    GO TO 300
73  REV=0.
    X1=F*SIN(XGAMMA)+COS(XPSI)
501 X2=F*COS(XGAMMA)
    IF(ZZ.GT.0.) GO TO 72
    RP=RR+.1
```

```
G=2.  
GO TO 202  
72 IF(ZZ.GT.(LIMIT2/10.)) GO TO 7  
IF(RR.GT.(LIMIT1/10.)) GO TO 8  
E=1.  
WRITE(2,35)E,RR,G,ITERATIONS,ZZ,NUMBER,X1,X2  
35 FORMAT(1H ,F3.0,E15.7,F3.0,I3,E15.7,I3,2E15.7)  
GO TO 201  
7 G=2.  
GO TO 202  
8 G=1.  
202 E=2.  
WRITE(2,36)E,RR,G,ITERATIONS,ZZ,NUMBER,X1,X2  
36 FORMAT(1H ,F3.0,E15.7,F3.0,I3,E15.7,I3,2E15.7)  
GO TO 200  
201 NUMBER=NUMBER+1  
GO TO 32  
200 CONTINUE  
212 IF(ITERATIONS.LT.10)GO TO 210  
GO TO 213  
210 CONTINUE  
213 CONTINUE  
E=3.  
WRITE(2,37)E,RR,G,ITERATIONS,ZZ,NUMBER,X1,X2  
37 FORMAT(1H ,F3.0,E15.7,F3.0,I3,E15.7,I3,2E15.7)  
GO TO 1001  
211 IF(ITERATIONS.EQ.500)GO TO 213  
NUMBER=0  
WRITE(2,1000)E,RR,G,ITERATIONS,ZZ,NUMBER,X1,X2  
1000 FORMAT(1H ,F3.0,E15.7,F3.0,I3,E15.7,I3,2E15.7)  
1001 STOP  
END
```

```

SUBROUTINE GENERATOR(J,K1,K2,K3,PY,N1,XR1,XR2)
DIMENSION AN(4),XR1(6),XR2(6)
COMMON THETA(6),ALPHA(6),BETA(6),FY(6),XX,ZZ,YY,X,XL(6),F,
1 XGAMMA,XPST,XMU1(6),XMU2(6),THETA1(6),FY1(6),R1(11),R2(11),DAT
IF(DAT.EQ.1.) GO TO 60
READ(1,25)(R1(L),L=1,11)
25 FORMAT(F6.5)
READ(1,26)(R2(N),N=1,11)
26 FORMAT(F6.5)
DAT=1.
60 DO 20 J=1,N1
30 XM=UTR1(1,0,K1)
XN=UTR1(2,0,K2)
L=XM*10.+1
N=XN*10.+1
28 IF(L.GT.1) GO TO 31
XR1(J)=R1(1)*(XM/.1)
GO TO 33
31 XR1(J)=((R1(L)-R1(L-1))*(XM-((L-1)/10.)))+R1(L-1)
33 IF(N.GT.1) GO TO 32
XR2(J)=R2(1)*(XN/.1)
GO TO 34
32 XR2(J)=((R2(N)-R2(N-1))*(XN-((N-1)/10.)))+R2(N-1)
34 IF(XR1(J).EQ.0.) GO TO 30
ALPHA(J)=ATAN(XR2(J)/XR1(J))
IF(ALPHA(J).GT.(PY/4.)) GO TO 30
1 CONTINUE
AN(1)=2.*PY*(UTR1(4,0,K3))
L=1
IF(ABS(SIN(AN(L))).GT..0872) GO TO 4
IF(COS(AN(L)))5,6,6
5 AN(L)=PY+.1
GO TO 7
6 AN(L)=0.+1
GO TO 7
4 IF(ABS(COS(AN(L))).GT..0872) GO TO 7
IF(SIN(AN(L)))8,9,9
8 AN(L)=(3.*PY/2.)*.1
GO TO 7
9 AN(L)=(PY/2.)*.1
7 BETA(J)=AN(1)
IF(J.EQ.1) GO TO 10
IF(J.GE.3) GO TO 10
IF(ABS(BETA(J)-BETA(J-1)).LT.(PY/2.)) GO TO 1
GO TO 10
10 CONTINUE
20 CONTINUE
59 RETURN
END
```

```

SUBROUTINE COORDINATES(NUMBER, PY, REV, I, XC, XD, XE)
COMMON THETA(6), ALPHA(6), BETA(6), FY(6), XX, ZZ, YY, X, XL(6), F,
1 XGAMMA, XPSI, XMU1(6), XMU2(6), THETA1(6), FY1(6)
IF(NUMBER.GT.1) GO TO 1
YY=XL(I)*SIN(ALPHA(I))*SIN(BETA(I))
XX=XI(I)*SIN(ALPHA(I))*COS(BETA(I))
ZZ=XI(I)*COS(ALPHA(I))
YGAMMA=0.
XPSI=0.
GO TO 2
1 AN1=ALPHA(I)
  AN2=BETA(I)
  EQTN=1.
  GO TO 3
2 AN1=THETA1(I)
  AN2=FY1(I)
  EQTN=2.
3 P=SIN(AN1)*COS(AN2)*XL(I)
  Q=SIN(AN1)*SIN(AN2)*XL(I)
  R=COS(AN1)*XL(I)
4 C1=COS(XGAMMA)
  C2=COS(XPSI)
  S1=SIN(XGAMMA)
  S2=SIN(XPSI)
  C=P+C2*C1-Q*S2+R*S1*C2
  D=Q+S2*C1+Q*C2+R*S1*S2
  E=-P+S1+R*C1
33 IF(ABS(C).GT.(1./(10.**5))) GO TO 50
   C=0.
50 IF(ABS(D).GT.(1./(10.**5))) GO TO 51
   D=0.
51 IF(ABS(E).GT.(1./(10.**5))) GO TO 52
   E=0.
52 IF(EQTN.EQ.1.) GO TO 5
   IF(SQRT(C**2+D**2).EQ.0.) GO TO 53
   IF(E.LT.(1./(10.**6))) GO TO 7
   XGAMMA=ATAN((SQRT(C**2+D**2))/E)
   IF(E)30,32,32
32 IF(C)30,31,31
30 XGAMMA=-XGAMMA
31 IF(ABS(SIN(XGAMMA)).GT..0872) GO TO 13
53 XGAMMA=0.
   IF(E)21,13,13
21 XGAMMA=PY
   GO TO 13
7 IF(C)15,16,16
15 XGAMMA=-(PY/2.)
   GO TO 13
16 XGAMMA=PY/2.
13 IF(D.EQ.0.) GO TO 54
   IF(ABS(C).LT.(1./(10.**6))) GO TO 10
   XPSI=ATAN(D/(ABS(C)))
   IF(D)300,23,23
300 XPSI=XPSI+PY
23 IF(ABS(SIN(XPSI)).GT..0872) GO TO 6
54 XPSI=0.
   GO TO 6
10 XPSI=SIGN(PY/2.,D)
   GO TO 6
5 IF(REV.EQ.1.) GO TO 9
  XE=E
  XC=C

```

```
XD=D
9 ZZ=ZZ+F
  XX=XX+C
  VV=VV+D
  IF(REV.EQ.0.) GO TO 8
  YX=XY-YC
  VY=VY-XD
  ZZ=ZZ-XE
8 CONTINUE
  IF(NUMBER.EQ.1) GO TO 6
GO TO 2
6 RETURN
END
```

PRINT OUT 4

```

SUBROUTINE FORCMA(XTHETA,XFY,N1,NUMBER)
DIMENSION A(6,7)
COMMON THETA(6),ALPHA(6),BETA(6),FY(6),XX,ZZ,VY,X,XL(6),F,
1YGAMMA,XPSI,XMU1(6),XMU2(6),THETA1(6),FY1(6)
DO 6 I1=1,N1
1 A(1,I1)=COS(THETA(I1))
2 A(2,I1)=SIN(THETA(I1))*COS(FY(I1))
3 A(3,I1)=SIN(THETA(I1))*SIN(FY(I1))
4 A(4,I1)=(COS(THETA(I1))+SIN(ALPHA(I1))*COS(BETA(I1))
1-COS(ALPHA(I1))*SIN(THETA(I1))*COS(FY(I1)))*XL(I1)
5 A(5,I1)=(SIN(THETA(I1))*SIN(FY(I1))+COS(ALPHA(I1))
1-COS(THETA(I1))*SIN(ALPHA(I1))+SIN(BETA(I1)))*XL(I1)
6 A(6,I1)=XL(I1)*SIN(THETA(I1))*SIN(ALPHA(I1))+SIN(BETA(I1)-FY(I1))
A(1,7)=-F
A(2,7)=0.
A(3,7)=0.
A(4,7)=0.
A(5,7)=0.
A(6,7)=0.
CALL EQSOLV(A,X,N1)
RETURN
END

```

```

SUBROUTINE EQSOLV(A,X,N1)
DIMENSION XM(6,7,4),A(6,7)
200 CONTINUE
N=2
J1=N1+1
I2=N1-1
L1=N1-2
DO 90 L=1,L2
DO 89 I=N,N1
DO 89 J=N,J1
IF(L.GT.1) GO TO 4
IF(J.GT.2) GO TO 5
DO 2 I1=1,N1
IF(ABS(A(I1,1)).EQ.0.) GO TO 2
M1=I1
IF(M1.EQ.1) GO TO 5
GO TO 3
2 CONTINUE
3 DO 4 K1=1,J1
R=A(1,K1)
A(1,K1)=A(M1,K1)
4 A(M1,K1)=R
5 XM(I,J,1)=(A(1,1)*A(I,J)-A(I,1)*A(1,J))
GO TO 89
1 IF(N1.GT.3) GO TO 26
GO TO 16
26 IF(L.GT.2) GO TO 6
IF(J.GT.3) GO TO 7
DO 8 I2=2,N1
IF(ABS(XM(I2,2,1)).EQ..0) GO TO 8
M2=I2
IF(M2.EQ.2) GO TO 7
GO TO 9
8 CONTINUE
9 DO 10 K2=2,J1
R=XM(2,K2,1)
XM(2,K2,1)=XM(M2,K2,1)
10 XM(M2,K2,1)=R
7 XM(I,J,2)=(XM(2,2,1)+XM(I,J,1)-XM(I,2,1)*XM(2,J,1))
GO TO 89
6 IF(N1.GT.4) GO TO 27
GO TO 16
27 IF(L.GT.3) GO TO 11
IF(J.GT.4) GO TO 15
DO 12 I3=3,N1
IF(ABS(XM(I3,3,2)).EQ..0) GO TO 12
M3=I3
IF(M3.EQ.3) GO TO 15
GO TO 13
12 CONTINUE
13 DO 14 K3=3,J1
R=XM(3,K3,2)
XM(3,K3,2)=XM(M3,K3,2)
14 XM(M3,K3,2)=R
15 IF(ABS(XM(3,7,2)).GT.(10.**10))GO TO 501
XM(I,J,3)=(XM(3,3,2)*XM(I,J,2)-XM(I,3,2)*XM(3,J,2))*(10.**20)
GO TO 89
501 XM(I,J,3)=(XM(3,3,2)*XM(I,J,2)-XM(I,3,2)*XM(3,J,2))
GO TO 89
11 IF(N1.GT.5) GO TO 28
GO TO 91
28 IF(L.GT.4)GO TO 91

```

```

IF(J.GT.5) GO TO 17
DO 18 I4=4,N1
IF(ABS(XM(I4,4,3)).EQ..0) GO TO 18
M4=I4
IF(M4.EQ.4) GO TO 17
GO TO 19
18 CONTINUE
19 DO 20 K4=4,J1
R=XM(4,K4,3)
XM(4,K4,3)=XM(M4,K4,3)
20 XM(M4,K4,3)=B
17 XM(I,J,4)=(XM(4,4,3)*XM(I,J,3)-XM(I,4,3)*XM(4,J,3))
89 CONTINUE
90 N=L-2
91 CONTINUE
IF(ABS(XM(N1,J1,4)).LT.(10.**40)) GO TO 16
DO 30 I=5,N1
DO 30 J=5,J1
XM(I,J,4)=XM(I,J,4)/(10.**20)
30 CONTINUE
16 IF(XM(L2,L2,L1).EQ.0.)GO TO 21
X=(XM(N1,J1,L1)+XM(L2,L2,L1)-XM(L2,J1,L1)+XM(N1,L2,L1))/
1(XM(N1,N1,L1)+XM(L2,L2,L1)-XM(L2,N1,L1)+XM(N1,L2,L1))
GO TO 22
21 Y=XM(L2,J1,L1)/XM(L2,N1,L1)
22 RETURN
END

```



```

COMMON E,RP,PAO,ITS,ZZ,X1,X2,NUMBER,LIMIT1,LIMIT2,G
PAO=.L1
LIMIT1=10
LIMIT2=2
MIT=5
WRITE(A,2000)

```

2000 FORMAT(1H ,97H SUMMATION OF FORCES BASED ON THEIR POSITION WITH RESPECT TO A GRID WITH .02X.05 SQ. IN. SEPERATION//1H ,17H RE-ENTRANT FORCES,22Y,29FX AND Z NON RE-ENTRANT FORCES,9X,3HITS,4X,6HNUMBER)

```

READING RESULTS OF RANDOM WALK
4 READ(5,1)E,RP,G,ITS,ZZ,NUMBER,X1,X2
1 FORMAT(F2.0,F4.3,F2.0,I1,F4.3,I2,2F2.0)
IF MAG TAPE HAS ENDED START USING THE NEXT MAG TAPE
IF(NUMBER)1001,1002,1001
1002 MIT=MIT+1
GO TO 4
1001 CONTINUE
H=0.

```

```

IF RANDOM WALKS HAVE BEEN COMPLETED GO TO 14
IF(IFIX(F).EQ.3)GO TO 14
IF A RANDOM WALK HAS ENDED GO TO 8
IF(E.LT.2.)GO TO 8
H=1.

```

```

HAS FORCE LEFT SYSTEM AT THE TOP,IF SO CALL PLOT WITH G=2
8 IF(ZZ)15,15,16
15 G=2.
GO TO 2

```

```

HAS WALK ENDED AT THE FARTHEST Z BOUNDARY
IF SO, CALL PLOT WITH G=2
16 IF((ZZ*100.)/5..LT.FLOAT(LIMIT2))GO TO 5
G=2.
GO TO 2

```

```

HAS WALK ENDED AT THE X BOUNDARY,IF SO GO TO 7
5 IF((RP*100.)/2..GE.LIMIT1)GO TO 7
WALK STILL WITHIN THE CONFINES OF THE SYSTEM CALL PLOT WITH E=1
G=0.
E=1.
CALL PLOT
GO TO 4

```

```

WHEN WALK ENDS AT X BOUNDARY G=1 AND E=2
7 G=1.
WHEN WALK HAS ENDED AT THE Z BOUNDARY,E=2 AND G=2
2 E=2.
CALL PLOT
IF(ITS.LT.5)GO TO 17
GO TO 14

```

17 IF(IFIX(H).EQ.1)GO TO 4
WHEN SYSTEM FOR WHICH THE WALK WAS PERFORMED IS LARGER THAN THE SYSTEM FOR WHICH THE FORCES ARE SUMMED, READ THE REMAINING DATA CARDS FROM THE MAIN PROGRAM UNTIL THE WALK IS COMPLETE THEN RETURN AND READ THE FIRST DATA CARD FROM THE NEXT RANDOM WALK

```

1005 READ(5,3)E,RP,G,ITS,ZZ,NUMBER,X1,X2
3 FORMAT(F2.0,F4.3,F2.0,I1,F4.3,I2,2F2.0)
IF(NUMBER)1008,1009,1008
1009 MIT=MIT+1
GO TO 1005
1008 CONTINUE

```

```

IF(IFIX(F).EQ.2)GO TO 6
IF(IFIX(E).EQ.3)GO TO 14
GO TO 1005
14 E=3.
CALL PLOT
STOP
END

```

```

SUBROUTINE FPL01
DIMENSION SS(2,10,16,20),X5(5,10,2),SUM(2,10,10,2)
COMMON E,RR,PAD,ITS,ZZ,X1,X2,NUMBER,LIMIT1,LIMIT2,G
SSP=0.
PY=3.141592653
C APPLIED FORCE
FORCE=489.*5.
C NUMBER OF Z SUBDIVISIONS EACH SPACED .050 APART ON THE SUMMATION GRID
M=LIMIT2*2
C NUMBER OF X SUBDIVISIONS EACH SPACED .020 APART ON THE SUMMATION GRID
N=LIMIT1/2
C RANDOM WALKS COMPLETE
IF(E.LT.3.)GO TO 1
C PROGRAM YIELDING THE POSITION DISTRIBUTION DISTRIBUTION OF SURFACE PARTICLE
CALL SMULT(N,M,S,K5)

GO TO 5
1 IF(NUMBER.GT.1)GO TO 3
IF(ITS.GT.1)GO TO 13
DO 2 K=1,2
DO 2 KXX=1,LIMIT1
DO 2 KZZ=1,M
DO 2 L=1,20
2 SS(K,KXX,KZZ,L)=G.
C SETTING X,Z COORDINATES TO ZERO VALUES AT THE START OF EACH RANDOM WALK
13 KXY=1
KZZ=1
C TEST FOR FORCES LEAVING SYSTEM AT THE TOP
3 IF(ZZ.GT.0.)GO TO 4
C Y COORDINATE AT POINT OF EXIT
KX=IFIX((RR*100.)/2.)*1
C X,Z COMPONENTS OF THE FORCE BEING ADDED TO OTHERS HAVING LEFT AT THE SAME
TIME WITH THE IDENTICAL PENETRATION BEFORE HAND
SS(1,KX,KZZ,20)=SS(1,KX,KZZ,20)+X1
SS(2,KX,KZZ,20)=SS(2,KX,KZZ,20)+X2
WRITE(6,164)KX,KZZ,SS(1,KX,KZZ,20),ITS,NUMBER
164 FORMAT(1H ,3HSS(.3H 1.,2(I2,1H.),6H20) = ,E15.7,43X,2(I2,5X))
IF(KX.LE.KXX)GO TO 5
SS(1,KXX,KZZ,20)=SS(1,KXX,KZZ,20)+X1
SS(2,KXX,KZZ,20)=SS(2,KXX,KZZ,20)+X2
KX=KXX
WRITE(6,164)KX,KZZ,SS(1,KX,KZZ,20),ITS,NUMBER
GO TO 5
C Y POSITION LOCATOR
4 KXX1=IFIX((RR*100.)/2.)*1
C Z POSITION LOCATOR
KZZ1=2*IFIX((ZZ*100.)/5.)*1
C IS RANDOM WALK FINISHED? IF NOT GO TO 104
IF(E.LT.2.)GO TO 104
C IF FINISHED DID FORCE LEAVE AT X OR Z BOUNDARY?
IF(IFIX(G).EQ.2)GO TO 103
C IT REACHED X BOUNDARY
KXX1=KXX1-1
GO TO 104
C IT REACHED Z BOUNDARY
103 KZZ1=KZZ1-2
104 NPOS1=(KZZ/2)+1
C FURTHEST Z BOUNDARY CROSSED BY FORCE PRIOR TO THIS MOVEMENT
POS1=FLOAT(NPOS1)
C FURTHEST X BOUNDARY CROSSED BY FORCE PRIOR TO THIS MOVEMENT
100 POS2=FLOAT(KXX)

```

```

IS THE FORCE CURRENTLY WITHIN THE PREVIOUSLY CROSSED X BOUNDARIES OR HAS I
CROSSED A NEW BOUNDARY
    IF((PR*100.)/2..LI.POS2)GO TO 111
IT HAS NOT
ACTUAL POSITION OF FORCE IN TERMS OF ITS Z COORDINATE
    NZZ=FIX((ZZ+100.)/5.)*1
IS FORCE WITHIN Z BOUNDARIES ALREADY CROSSED OR HAS IT CROSSED A NEW ONE
    IF(POS1.LI.FLOW)(NZZ)GO TO 102
IT HAS NOT BUT IS THE LAST Z BOUNDARY CROSSED THE SAME AS THE FURTHEST
    IF(KZZ.LE.KZ7)GO TO 101
THE LAST BOUNDARY IS WITHIN THE FURTHEST PREVIOUSLY CROSSED
ADDING THIS FORCE TO THOSE HAVING CROSSED THIS BOUNDARY BEFORE
    SS(1,KXX,KZZ,KZ7-1)=SS(1,KXX,KZZ1,KZ7-1)+X1
    SS(2,KXX,KZZ,KZ7-1)=SS(2,KXX,KZZ1,KZ7-1)+X2
THE LAST BOUNDARY IS FURTHER THAN ANY FORMERLY CROSSED
101 SS(1,KXX,KZZ1,1)=SS(1,KXX,KZZ1,1)+X1
    SS(2,KXX,KZZ1,1)=SS(2,KXX,KZZ1,1)+X2
    K3Z=KZ7-1

    IF(K3Z.EQ.0)GO TO 160
    WRITE(6,160)KXX,KZZ1,K3Z,SS(1,KXX,KZZ1,KZ7-1),KXX,KZZ1,SS(1,KXX,KZ
171,1),ITS,NUMBER
160 FORMAT(1H ,6HSS( 1,,2(I2,1H, ),I2,4H) = ,E15.7,5X,6HSS( 1,,2(I2,1H,
1),6H 1) = ,E15.7,5X,2(I2,5X))
    GO TO 168
168 WRITE(6,160)KXX,KZZ1,K3Z,SS(1,KXX,KZZ1,1),ITS,NUMBER
INCREASING NUMBER OF X BOUNDARIES CROSSED
168 KXY=KXY+1
CONTINUE WITH THE NEXT STAGE OF THE WALK
    GO TO 5

IF IT HASN'T CROSSED A NEW X BOUNDARY, HAS IT CROSSED A NEW Z BOUNDARY
110 IF((ZZ+100.)/5..LI.POS1)GO TO 5
IF YES IS IT WITHIN THE BOUNDARIES ALREADY CROSSED WRT X OR HAS IT CROSSED
A NEW ONE
102 IF(KXX1.GE.KXX)GO TO 105
IT HAS RE-CROSSED A PREVIOUSLY CROSSED BOUNDARY
ADDING THIS FORCE TO OTHERS HAVING ALREADY CROSSED THIS BOUNDARY
    KKXX=2+KXX-1
    SS(1,KXX1,KZ7+1,KKXX)=SS(1,KXX1,KZZ+1,KKXX)+X1
    SS(2,KXX1,KZ7+1,KKXX)=SS(2,KXX1,KZZ+1,KKXX)+X2
IT HAS CROSSED A NEW BOUNDARY
105 SS(1,KXX1,KZ7+1,1)=SS(1,KXX1,KZZ+1,1)+X1
    SS(2,KXX1,KZ7+1,1)=SS(2,KXX1,KZZ+1,1)+X2
    K3Z=KZ7+1
    IF(KXX.EQ.0)GO TO 167
    WRITE(6,161)KXX1,K3Z,KKXX,SS(1,KXX1,K3Z,KKXX),KXX1,K3Z,SS(1,KXX1,K
132,1),ITS,NUMBER
161 FORMAT(1H ,6HSS( 1,,2(I2,1H, ),I2,4H) = ,E15.7,5X,6HSS( 1,,2(I2,1H,
1),6H 1) = ,E15.7,5X,2(I2,5X))
    GO TO 173
167 WRITE(6,161)KXX1,K3Z,KKXX,SS(1,KXX1,K3Z,1),ITS,NUMBER
INCREASING NUMBER OF Z BOUNDARIES CROSSED
170 KZZ=KZZ+2
HAS IT CROSSED A X BOUNDARY AT THE SAME TIME AS AN Z
    IF((PR*100.)/2..LI.KXX)GO TO 5
    SS(1,KXX,KZZ-2,1)=SS(1,KXX,KZZ-2,1)+X1
    SS(2,KXX,KZZ-2,1)=SS(2,KXX,KZZ-2,1)+X2
    K3Z=KZ7-2
    WRITE(6,162)KXX,K3Z,SS(1,KXX,KZZ-2,1),ITS,NUMBER
162 FORMAT(1H ,3HSS(,3H 1,,2(I2,1H, ),3H 1),3H = ,E15.7,43X,2(I2,5X))
IF YES INCREASE NUMBER OF X BOUNDARIES CROSSED
    KXX=KXX+1

```

ARE RANDOM WALKS COMPLETED?

5 IF (E.LT.3.) GO TO 12

DETERMINATION OF FORCE TRANSMITTED BY EACH PARTICLE ON THE SURFACE

FORCE=FORCE/5

WRITE(6,105)((I,J,I=1,2),J=1,2)

105 FORMAT(1H ,5P110,1X,4(3HSS(,I1,1H,3HKXX,KZZ,,I1,1H),4X),5H5SUMZ1
J,1X,5H5SUMZ2,1X,5H5SUMZ3,1X,5H5SUMZ4,1X,5H5SUMZ5)

SUMMING ALL Z COMPONENTS OF FORCES CROSSING EVERY POSSIBLE SYSTEM
AND EQUATING TO INPUT FORCE IN ORDER TO NORMALISE

DO 6 KZZ=2,M,2

M3=M-2

M4=((LIMIT11-1)+2)-1

SUMZ1=0.

SUMZ5=0.

DO 6 KXX=1,LIMIT11

SUMZ2=0.

SUMZ3=0.

SUMZ4=0.

SUMMING Z FORCES ACTING AS SHEARING FORCES ON X BOUNDARIES

DO 10 J1=2,KZZ,2

SUMZ3=SUMZ3+SS(2,KXX,J1-1,1)

M1=KZZ

IF (M1.GT.M3) GO TO 10

DO 51 LEV1=M1,M3,2

SUMMING REENTRANT SHEARING FORCES ON X BOUNDARY

51 SUMZ4=SUMZ4+SS(2,KXX,J1-1,LEV1)

10 CONTINUE

SUMMING FORCES AT Z BOUNDARIES (PRESSURE FORCES)

SUMZ1=SUMZ1+SS(2,KXX,KZZ,1)

M2=(2*KXX)+1

IF (M2.GT.M4) GO TO 70

SUMMING REENTRANT PRESSURE FORCES

DO 52 LEV2=M2,M4,2

DO 52 KX=1,KXX

SUMZ2=SUMZ2+SS(2,KX,KZZ,LEV2)

52 CONTINUE

70 CONTINUE

LL=KZZ-1

SUMMING FORCES LEAVING AT THE TOP OF THE SYSTEM

DO 55 KZ=1,LL,2

55 SUMZ5=SUMZ5+SS(2,KXX,KZ,2)

TOTAL SUM OF Z FORCES AT THE PERIPHERY OF THE SYSTEM BEING CONSIDERED

SUMZ=SUMZ1+SUMZ3+SUMZ5-SUMZ2-SUMZ4

NORMALISATION FACTOR

60 RATIO=SUMZ/FORCE

IF (SJMZ) 111,111,112

111 WRITE(6,113)

113 FORMAT(1H ,10H5SUMZ IS NEGATIVE)

112 CONTINUE

X FORCES AT KXX BOUNDARY

SUM(1,KXX,KZZ-1,1)=SS(1,KXX,KZZ-1,1)

Z FORCES AT KXX BOUNDARY

SUM(2,KXX,KZZ-1,1)=SS(2,KXX,KZZ-1,1)

IF (M1.GT.M3) GO TO 71

SUBTRACTION OF REENTRANT FORCES

DO 54 LEV1=M1,M3,2

SUM(1,KXX,KZZ-1,1)=SUM(1,KXX,KZZ-1,1)-SS(1,KXX,KZZ-1,LEV1)

SUM(2,KXX,KZZ-1,1)=SUM(2,KXX,KZZ-1,1)-SS(2,KXX,KZZ-1,LEV1)

54 CONTINUE

71 CONTINUE

```

NORMALISATION WITH RESPECT TO INPUT FORCE
SUM(1,KXX,KZZ-1,1)=SUM(1,KXX,KZZ-1,1)/(2.*RATIO)
SUM(2,KXX,KZZ-1,1)=SUM(2,KXX,KZZ-1,1)/RATIO
FORCES AT Z BOUNDARY
SUM(1,KXX,KZZ-1,2)=SS(1,KXX,KZZ,1)
7 FORCES AT YZZ BOUNDARY
SUM(2,KXX,KZZ-1,2)=SS(2,KXX,KZZ,1)
IF(KZZ.GT.2)GO TO 72
ADDING FORCES LEAVING AT THE TOP
LL=M-1
DO 116 KZ=1,LL,2
SUM(1,KXX,KZZ-1,2)=SUM(1,KXX,KZZ-1,2)+SS(1,KXX,KZ,20)
SUM(2,KXX,KZZ-1,2)=SUM(2,KXX,KZZ-1,2)+SS(2,KXX,KZ,20)
116 CONTINUE
72 CONTINUE
IF(M2.GT.M4)GO TO 73
SUBTRACTION OF PENETRANT FORCES
DO 54 LEV2=M2,M4,2
SUM(1,KXX,KZZ-1,2)=SUM(1,KXX,KZZ-1,2)-SS(1,KXX,KZZ,LEV2)
SUM(2,KXX,KZZ-1,2)=SUM(2,KXX,KZZ-1,2)-SS(2,KXX,KZZ,LEV2)
54 CONTINUE
73 CONTINUE
NORMALISATION WITH RESPECT TO INPUT FORCE

SUM(1,KXX,KZZ-1,2)=SUM(1,KXX,KZZ-1,2)/(2.*RATIO)
SUM(2,KXX,KZZ-1,2)=SUM(2,KXX,KZZ-1,2)/RATIO
KKK=KZZ-1
WRITE(6,152)RATIO,((SUM(I,KXX,KKK,J),I=1,2),J=1,2),SUMZ1,SUMZ2,SUM
173,SJM74,SUM75
152 FORMAT(1H ,F3.0,4(E15.7,5X),5(F3.0,3X))
6 CONTINUE
DO 3005 KZZ=1,8
DO 3005 KXX=1,5
SS(1,KXX,KZZ,1)=0.
SS(2,KXX,KZZ,1)=0.
SS(1,KXX,KZZ,2)=0.
3005 SS(2,KXX,KZZ,2)=0.
DO 50 KZZ=1,11*112
DO 50 KXX=1,4
DO 50 I1=1,10
KKZZ=KZZ*2-1
SS(1,KXX,KZZ,1)=KS(KXX,I1,2)*SUM(1,I1,KKZZ,1)+SS(1,KXX,KZZ,1)
SS(2,KXX,KZZ,1)=KS(KXX,I1,1)*SUM(2,I1,KKZZ,1)+SS(2,KXX,KZZ,1)
SS(1,KXX,KZZ,2)=KS(KXX,I1,2)*SUM(1,I1,KKZZ,2)+SS(2,KXX,KZZ,2)
SS(2,KXX,KZZ,2)=KS(KXX,I1,1)*SUM(2,I1,KKZZ,2)+SS(2,KXX,KZZ,2)
50 CONTINUE
DO 150 KZZ=1,LIMIT2
DO 150 KXX=1,4
SS(1,KXX,KZZ,1)=SS(1,KXX,KZZ,1)/(PY*.01*FLOAT(KXX))
150 SS(2,KXX,KZZ,2)=SS(2,KXX,KZZ,2)/(PY*(2.*FLOAT(KXX)-1.)/100.)
WRITE(6,151)1,LIMIT2
151 FORMAT(1H ,2HPRESULTS FOR COMPACT ,I2,15HX10-1 INS. DIA.,2X,I2,19H
1X10-1 INS. IN DEPTH)
WRITE(6,8)((SS(I,J,K,L),J=1,5),K=1,6),I=1,2),L=1,2)
8 FORMAT(1H ,4HPRESSURE ON VERTICAL PLANES SPACED J.1 INS. APART/1H
1 ,8(/1H ,5(E15.7,1X))/1H ,5HSHEARING FORCES ON VERTICAL PLANES SP
2ACED J.1 INS. APART/1H ,8(/1H ,5(E15.7,1X))/1H ,52HPRESSURE ON HOR
3IZONTAL PLANES SPACED 0.05 INS. APART/1H ,8(/1H ,5(E15.7,1X))/1H ,
45HSHEARING FORCES ON HORIZONTAL PLANES SPACED 0.05 INS. APART/1H
5 ,8(/1H ,5(E15.7,1X)))
12 CONTINUE
RETURN
END

```

```

SUBROUTINE SMULT(N,M,S,KS)
  DIMENSION KS(5,10,2)
  COMMON E,RR,RAD,ITS,ZZ,X1,X2,NUMBER,LIMIT1,LIMIT2,G
  RAD1=0.2
C RADIUS OF PARTICLES ON THE SURFACE
  RAD2=RAD
C POROSITY OF SURFACE
  VOID=.52
C DISTANCE BETWEEN PARTICLE CENTRES
  G=(RAD2*2.)/(1.-VOID)
  S=C.
  K=1.
35 CONTINUE
  GO TO (30,31),K
30 NI=M
  GO TO 1
31 NI=1
C SUMMATION OF PARTICLES WITHIN RADIUS OF 10 PARTICLE DIAMETERS
C FOR POINTS IN SYSTEM SEPERATED BY A DISTANCE OF 0.1 INS.
  1 DO 100 KXX=1,NI
    IF(K.EQ.1)GO TO 11
    RAD1=FLOAT(LIMIT1)/20.
C SUMMATION OF ALL SURFACE PARTICLES
  11 DO 99 J=1,200
    IF(J.GT.(IFIX((RAD1/G)+1.E-5)+1))GO TO 100
    F=(G+FLOAT(J-1))*2
    FUNC=SQRT(RAD1*RAD1-F)
    NUM=IFIX((FUNC/G)+1.E-5)
    DO 98 I=1,100
      IF(I.GT.(NUM+1))GO TO 99
      IF(K.EQ.2)GO TO 30
      IF(J.NE.1)GO TO 2
      IF(I.NE.1)GO TO 3
      T1=1
      GO TO 4
  2 T1=IFIX((SQRT((G+FLOAT(I-1))*2+F)/.02)+.99)
      GO TO 4
  3 T1=IFIX(((G+FLOAT(I-1))/.(2)+.99)
  4 IF(I.NE.1)GO TO 5
      TEST=SQRT(F+(FLOAT(KXX)/10.))*2)+RAD2
      IF(TEST.GT.FLOAT(LIMIT1)/20.)GO TO 5
      IF(J.NE.1)GO TO 6
      KS(KXX,I1,1)=KS(KXX,T1,1)+1
      GO TO 98
  6 KS(KXX,I1,1)=KS(KXX,I1,1)+2
      GO TO 98
  5 TEST1=SQRT(F+(FLOAT(KXX)/10.)+G*(I-1))*2)+RAD2
      TEST2=SQRT(F+(FLOAT(KXX)/10.)-G*(I-1))*2)+RAD2
      IF(TEST1.GT.FLOAT(LIMIT1)/20.)GO TO 7
      IF(J.NE.1)GO TO 8
      KS(KXX,I1,1)=KS(KXX,T1,1)+2
      GO TO 98
  8 KS(KXX,I1,1)=KS(KXX,T1,1)+4
      GO TO 98
  7 IF(TEST2.GT.FLOAT(LIMIT1)/20.)GO TO 98
      IF(J.NE.1)GO TO 9
      KS(KXX,I1,1)=KS(KXX,T1,1)+1
      KS(KXX,I1,2)=KS(KXX,T1,2)+1
      GO TO 98
  9 KS(KXX,I1,1)=KS(KXX,T1,1)+2
      KS(KXX,I1,2)=KS(KXX,T1,2)+2
      GO TO 98

```

```

10 IF(I.NF.1)GO TO 21
   IF(J.NF.1)GO TO 22
   S=S+1
   GO TO 98
22 S=S+2
   GO TO 98
21 IF(J.NF.1)GO TO 23
   S=S+2
   GO TO 98
23 S=S+4
98 CONTINUE
99 CONTINUE
100 CONTINUE
   IF(K.EQ.1)GO TO 101
   WRITE(6,20)S
20  FORMAT(1H ,30HTOTAL NUMBER OF PARTICLES ON SURFACE = ,F4.0/)
   DO 105 I=1,5
   WRITE(6,40)I
40  FORMAT(1H ,48HDISTANCE OF GRID POINT FROM CENTRE OF SYSTEM =
     15H INS./1H ,64HDISTANCE OF PARTICLES CAPABLE OF INFLUENCE, F
     21S GRID POINT)
   WRITE(6,41)((I,J,K1,KS(I,J,K1),K1=1,2),J=1,10)
41  FORMAT(1H ,12(/1H ,2(3HK5(,I1,1H,,I2,1H,,I1,4H) = ,I2,5X)))
105 CONTINUE
101 K=K+1
   IF(K.EQ.2)GO TO 35

   RETURN
   END

```

TOTAL NUMBER OF PARTICLES ON SURFACE = 489.

DISTANCE OF GRID POINT FROM CENTRE OF SYSTEM = .1 INS.

DISTANCE OF PARTICLES CAPABLE OF INFLUENCE, FROM THIS GRID POINT

KS(1, 1,1) = 1	KS(1, 1,2) = 0
KS(1, 2,1) = 4	KS(1, 2,2) = 0
KS(1, 3,1) = 4	KS(1, 3,2) = 0
KS(1, 4,1) = 4	KS(1, 4,2) = 0
KS(1, 5,1) = 8	KS(1, 5,2) = 0
KS(1, 6,1) = 8	KS(1, 6,2) = 0
KS(1, 7,1) = 8	KS(1, 7,2) = 0
KS(1, 8,1) = 12	KS(1, 8,2) = 0
KS(1, 9,1) = 20	KS(1, 9,2) = 0
KS(1, 10,1) = 12	KS(1, 10,2) = 0

DISTANCE OF GRID POINT FROM CENTRE OF SYSTEM = .2 INS.

DISTANCE OF PARTICLES CAPABLE OF INFLUENCE, FROM THIS GRID POINT

KS(2, 1,1) = 1	KS(2, 1,2) = 0
KS(2, 2,1) = 4	KS(2, 2,2) = 0
KS(2, 3,1) = 4	KS(2, 3,2) = 0
KS(2, 4,1) = 4	KS(2, 4,2) = 0
KS(2, 5,1) = 8	KS(2, 5,2) = 0
KS(2, 6,1) = 8	KS(2, 6,2) = 0
KS(2, 7,1) = 8	KS(2, 7,2) = 0
KS(2, 8,1) = 12	KS(2, 8,2) = 0
KS(2, 9,1) = 20	KS(2, 9,2) = 0
KS(2, 10,1) = 12	KS(2, 10,2) = 0

DISTANCE OF GRID POINT FROM CENTRE OF SYSTEM = .3 INS.

DISTANCE OF PARTICLES CAPABLE OF INFLUENCE, FROM THIS GRID POINT

KS(3, 1,1) = 1	KS(3, 1,2) = 0
KS(3, 2,1) = 4	KS(3, 2,2) = 0
KS(3, 3,1) = 4	KS(3, 3,2) = 0
KS(3, 4,1) = 4	KS(3, 4,2) = 0
KS(3, 5,1) = 8	KS(3, 5,2) = 0
KS(3, 6,1) = 8	KS(3, 6,2) = 0
KS(3, 7,1) = 8	KS(3, 7,2) = 0
KS(3, 8,1) = 12	KS(3, 8,2) = 0
KS(3, 9,1) = 20	KS(3, 9,2) = 0
KS(3, 10,1) = 11	KS(3, 10,2) = 1

DISTANCE OF GRID POINT FROM CENTRE OF SYSTEM = .4 INS.

DISTANCE OF PARTICLES CAPABLE OF INFLUENCE, FROM THIS GRID POINT

KS(4, 1,1) = 1	KS(4, 1,2) = 0
KS(4, 2,1) = 4	KS(4, 2,2) = 0
KS(4, 3,1) = 4	KS(4, 3,2) = 0
KS(4, 4,1) = 4	KS(4, 4,2) = 0
KS(4, 5,1) = 8	KS(4, 5,2) = 0
KS(4, 6,1) = 7	KS(4, 6,2) = 1
KS(4, 7,1) = 6	KS(4, 7,2) = 2
KS(4, 8,1) = 7	KS(4, 8,2) = 5
KS(4, 9,1) = 12	KS(4, 9,2) = 8
KS(4, 10,1) = 7	KS(4, 10,2) = 5

DISTANCE OF GRID POINT FROM CENTRE OF SYSTEM = .5 INS.

DISTANCE OF PARTICLES CAPABLE OF INFLUENCE, FROM THIS GRID POINT

KS(5, 1,1) = 0	KS(5, 1,2) = 0
KS(5, 2,1) = 1	KS(5, 2,2) = 1
KS(5, 3,1) = 2	KS(5, 3,2) = 2
KS(5, 4,1) = 1	KS(5, 4,2) = 1
KS(5, 5,1) = 4	KS(5, 5,2) = 4
KS(5, 6,1) = 3	KS(5, 6,2) = 3
KS(5, 7,1) = 4	KS(5, 7,2) = 4
KS(5, 8,1) = 5	KS(5, 8,2) = 5
KS(5, 9,1) = 10	KS(5, 9,2) = 10
KS(5, 10,1) = 5	KS(5, 10,2) = 5

Nomenclature

C	Constants and coefficients
c	Constants and coefficients
D	Particle diameters, die diameters
d	Small particle diameters
d_f	Feret's diameter
d_m	Martin's diameter
F	Feret's diameter
h	Depth, height of a compact
k	Yield stress in shear
L	Length
l	Length of contact chords
P	Pressure, probability
p	Pressure, perimeter
R	Radius
r	Radius
s	Mean yield stress
V	Volume
X	Axis in Cartesian systems
x	Radii, filament lengths, diameters, coordinate in Cartesian systems
Y	Axis in Cartesian systems
y	Radii, filament lengths, diameters, coordinate in Cartesian systems
Z	Axis in Cartesian systems
z	Filament lengths, coordinate in Cartesian systems

Greek symbols

ω_0	Constant
α_j	Angle made by leading edge of a metallic junction in the Bowden and Tabor friction theory
α	Angle made by the chord of contact with the positive direction of the Z-axis
β	Axial to radial stress ratio The angle made by the projection on the particle's XY plane of the chord of contact, with the X-axis
θ	Angle made by the normal to the surface at the point of contact with the positive direction of the Z-axis of the particle

Nomenclature (continued)

- θ Angle made by the projection of the normal to the surface at the point of contact, on the particle's XY plane, with the positive direction of the particle's X-axis
- γ The angle made by the normal to the surface at a point of contact with the positive direction of the system's Z-axis
- ϕ The angle made by the projection of the normal at the point of contact, on the system XY plane, with the positive direction of the system X-axis
- ϵ Porosity, voidage
Cosines of angles in tensor analysis
- Δ Segregation coefficient
- μ_s Static coefficient of friction
- μ Coefficient of friction
- μ_i Internal coefficient of friction
- ρ Density
- Σ Summation sign
- \int Integration sign

BIBLIOGRAPHY

REFERENCES

1. R.Kamm, M.A.Steinberg and J.Wulff Metals Tech. A.I.M.E
T.P. 2133 Feb. 1947
2. " T.P. 2136 Aug. 1947
3. R.P.Seelig The Physics of Powder Metallurgy Ed W.E.Kingston
p344 New York 1950
4. D.Train and C.J.Lewis Trans.Inst.Chem.Eng. 40 p235, 1962
5. D.Train and J.A.Hersey Ind.Chem 38 p77 and 113, 1962
6. P.Duwez and L.Zwell J.Metals 1 p137-144, 1949
7. D.Train J.Pharm 8 p745-761, 1956
8. H.R.Gregory Trans.Inst.Chem.Eng 40 p241-251, 1962
9. C.Huffine and A.Bonilla A.I.Chem.E Jour. Sept. 1962
10. A.Duffield and P.Grootenhuis Iron and Steel Inst., London,
Symposium on Powder Metallurgy
Sp. Rep. 58, 1954
11. D.Train and J.A.Hersey See 5
12. D.Train and J.A.Hersey See 5
13. G.Bockstiegel Modern Developments in Powder Metallurgy
Vol. 1 Fundamentals and Methods Plenum Press
New York, 1966
14. W.M.Long Powder Metallurgy 6 p73, 1960
15. D.Train Trans.Inst.Chem.Eng 35 p258, 1957
16. R.Kamm, M.A.Steinberg and J.Wulff See 1 and 2
17. M.W.Pascoe and D.Tabor Proc.Roy.Soc. A235, p210, 1957
18. J.S.Courtney-Pratt and E.Eisner Proc.Roy.Soc A238, p529, 1957
19. D.Train and J.A.Hersey Powder Metallurgy 6 p20, 1960
20. W.J.M.Rankine Trans.Roy.Soc. 8 p9, 1856
21. H.G.Taylor Powder Metallurgy 6 p87-124, 1960
22. H.Silbereisen Planseeber Pulvermet. 7 p67, 1959
23. A.Squire Trans A.I.M.E 171 p474-505, 1947
24. A.Duffield Ph.D. London University 1953
25. R.K.McGeary J.Am.Cer.Soc. 44 p10, 1961
26. R.J.Adwick and Warmer Part.Size Analysis Conf., Loughborough
University 1966
27. H.H.Hausner Mats. and Methods. July, p98, 1946
28. W.M.Long Powder metallurgy 6 p52, 1960
29. V.S.Rakowski Fundamental Considerations in the Production
of Hard Alloys Moscow 1935

Contd.

- 30.H.Unckel Arch. Eisenhüttenw. 18 p125 and p161,1945
- 31.M.Y.Balshin The Theory of the Process of Pressing
Vestnik Metallopromishienosti 18 p124,1938
- 32.H.Rumpf and S.Debbas Chem.Eng.Sci. 21 p583-607,1966
- 33.L.R.Feret Assoc. internat.pour l' Essai des Mat.,Zurich
1931, Vol 2,Group D
- 34.H.Heywood A comparison of methods of measuring microscopic
particles. Inst of Min and Metall 1946
- 35.B.Scarlett and A.C.Todd Trans.A.I.M.E Jour.of Eng. for Ind.
1969
- 36.B.Scarlett and M.K.Bo To be published
- 37.D.Chorafas Statistical Processes and Reliability Engineering
Van Nostrand. N.J. p202,1960
- 38.F.P.Bowden and G.W.Rowe Proc.Roy.Soc.,A, 233(1195)p429,1955
- 39.F.P.Bowden and D.Tabor Friction and Lubrication,Oxford,1950
- 40.F.P.Bowden Sci.News 4-6 p139,1947/8
- 41.Johnson and Adams Z.Anorg.Chemie 30 p299,1913
- 42.A.P.Green Proc.Roy.Soc.,A,228 p191,1954
- 43.J.A.Greenwood and D.Tabor Proc Phys.Soc. 68,9(B) p609,1955
- 44.
- 45.D.Tabor The Hardness of Metals,Clarendon,1951
- 46.J.S.McFarlane and D.Tabor Proc.Roy.Soc.,A,202 p244,1950
- 47.S.J.Dokos Trans.A.S.M.E. 68 pA148,1946
- 48.
- 49.G.Franklin Can.Mach. and Metalworking 79(2) p72,1968
- 50.Goetzel Treatise on Powder Metallurgy Vols 1-4
- 51.P.M.Leopold and R.C.Nelson Int.Jour. of Powder Metallurgy
1(3) p37,1965
52. " 1(4) p37,1965
- 53.Heywood Jour.Imp.Coll.Eng.Soc. 2,1946
- 54.White and Walton J.AM.Ceram Soc. 20 p155,1937
- 55.R.K.Mcgeary " 44 p10,1961.
- 56.Graton and Fraser J.Geology 43 p785,1935
- 57.K.Ridgway and R.Tarbutck J.Pharm.Pharmacol. 18 p168s,1967
- 58.W.A.Gray Ph.D University of Leeds 1959
- 59.Smith,Foote and Busang Phys.Rev. Nov p34,1929

Contd.

87. J. Priemer Fortschritt-Berichte VDJ-Zeitschrift Reihe 3, no. 8
Dusseldorf 1965
88. Van der Ohe Chemie-Ing-Technik 39(516) p357, 1967
89. A. E. Scheidegger Flow Through Porous Media ,Toronto,
90. H. H. Hausner and I. Sheinhart Proc Met. Powd. Assoc. 1 p6-27, 1954

